

Adhesion of adhesive resin cements to dental zirconia ceramic and human dentin

Dissertation

zur Erlangung des akademischen Grades
Doktor der Ingenieurwissenschaften
(Dr.-Ing.)
der Technischen Fakultät
der Christian-Albrechts-Universität zu Kiel

Bin Yang

Kiel

2008

For Siyu and Qingshan

1. Gutachter

Prof. Dr. R. Adlung

2. Gutachter

Prof. Dr. V. Abetz

Datum der mündlichen Prüfung

16 .06.2008

Contents

Abbreviations	I
1 General Introduction	1
Part I. Adhesion of adhesive resin cements to dental zirconia ceramic.....	3
2 Background introduction.....	3
2.1 Factors that influence the adhesion	3
2.1.1 Wetting of the surface.....	3
2.1.2 Surface pretreatment.....	5
2.1.3 Structure of the materials to be bonded	6
2.2 Resin bonding to zirconia ceramic.....	6
2.2.1 Adhesive resin cements	7
2.2.2 Zirconia ceramics	8
2.2.3 Surface pretreatment of zirconia ceramic.....	9
2.3 Summary.....	10
3 Effect of surface pretreatment on durability of adhesive resin cements bond to zirconia ceramic	12
3.1 Introduction.....	12
3.2 Materials used in this study.	12
3.3 Study design for XPS examination and tensile bond strength testing.....	13
3.4 X-ray photoelectron spectroscopy (XPS)	13
3.5 Specimen preparation for bonding with resin cements	14
3.6 Bonding with resin cements and tensile bond strength (TBS) testing.....	14
3.7 SEM examination	15
3.8 XPS examination	15
3.9 Tensile bond strength and SEM observation.....	16
3.10 Effect of surface pretreatment on bonding durability of adhesive resin cements to zirconia ceramic.....	23
3.11 Summary and Outlook.....	27
3.10 Author's Related Publications	28
4 Influence of contaminations on resin bonding durability to zirconia ceramic	29
4.1 Introduction.....	29
4.2 Study design and specimen preparation	30
4.3 XPS examination	31
4.4 Tensile bond strength (TBS) testing.....	31
4.5 SEM examination	32
4.6 XPS results.....	32
4.7 TBS results.....	33
4.8 SEM observation and fractographic analysis.....	34
4.9 Influence of contamination on zirconia ceramic bonding.....	36

4.10	Summary and Outlook.....	37
4.11	Author's Related Publications	38
Part II. Adhesion of adhesive resin cements to human dentin.....		39
5	Background introduction.....	39
5.1	Dentin-resin bonding.....	39
6	Micro-tensile bond strength of three resin cements to human regional dentin	42
6.1	Introduction.....	42
6.2	Tooth preparation	43
6.3	Micro-tensile bond strength (μ TBS) testing.....	45
6.4	SEM examination and Fractographic analysis	46
6.5	TEM examination.....	46
6.6	μ TBS of the test groups to human regional dentin	47
6.7	Micro-tensile bond strength of there resin cements to human regional dentin.....	53
6.8	Summary and Outlook.....	55
6.9	Author's Related Publications	56
7	Effect of structural change of collagen fibrils on the durability of dentin bonding..	57
7.1	Introduction.....	57
7.2	Tooth preparation	58
7.3	Tapping mode AFM study.....	58
7.4	Micro-tensile bond strength (μ TBS) testing.....	59
7.5	SEM and TEM examination	59
7.6	Tapping mode AFM result.....	60
7.7	Structural change of intact collagen fibrils during acidic condition	62
7.8	Micro-tensile bond strength (μ TBS) testing.....	63
7.9	SEM and TEM results.....	64
7.10	Effect of thermal cycling on the durability of μ TBS	67
7.11	Effect of denatured collagen fibrils in the smear layer on the durability of μ TBS ...	69
7.12	Effect of structural changes of intact collagen fibrils on the durability of μ TBS.....	69
7.13	Schematic drawing of bonding procedures and fractographic analysis during tensile testing – Investigation of resin-dentin bonding mechanism	70
7.14	Summary and outlook.....	72
7.15	Author's Related Publications	74
8	General Conclusions and Outlook	75
Bibliography.....		79
List of Figures.....		85
List of Tables.....		91
Acknowledgments		92
Curriculum Vitae.....		93

Abbreviations

AFM: Atomic force microscopy

Bis-GMA: bisphenol A diglycidyl methacrylate

BPEDMA: Bisphenol-A-polyethoxy dimethacrylate

CCP: Clearfil™ ceramic primer

CH: Chemiace II

CE: Clearfil™ Esthetic cement

DMA: Aliphatic dimethacrylate

HL: Hybrid layer

10-MDP: 10-methacryloyloxydecyl dihydrogenphosphate

4-META: 4-methacryloxyethyl trimellitate anhydride

MZP: Metal/Zirconia primer

MMA: Methyl methacrylate

PF: Panavia F 2.0 luting composite resin

MS: Monobond S:

PMMA: Polymethyl methacrylate

PLM: Porcelain Liner M

RU: RelyX Unicem

SB: Super-Bond C&B resin cement

SEM: Scanning electron microscopy

10-3 solution: 10% citric acid with 3% ferric chloride

TBB: Partially oxidized tri-N-butyl borane

TBS: Tensile bond strength

TC: Thermal cycling

TEGDMA: triethylene glycol dimethacrylate

TEM: Transmission electron microscopy

UDMA: urethane dimethacrylate or 1,6-di(methacryloyloxyethylcarbamoyl)-3,30,5-trimethylhexaan

XPS: x-ray photoelectron spectroscopy

μTBS: Micro-tensile bond strength

μTS: Micro-tensile strength

1 General Introduction

Indirect dental ceramic restorations such as veneers, inlays, crowns and bridges have been encouraged by the development of adhesive resin cements and techniques. Adhesive techniques are able to allow the brittle and "fragile" ceramic restoration and the underlying tooth preparation to become a reliable tooth-restoration system with an adequate stress distribution from ceramic restoration to the underlying tooth hard structure. Therefore, the adhesion of indirect ceramic restorations to tooth preparation with adhesive resin cements can be considered to include the adhesive bonding of adhesive resin cement to the indirect ceramic restorations and the adhesion of adhesive resin cements to tooth hard tissues like enamel, or mostly dentin.

The introduction of high strength zirconia ceramic materials to the dental field opened the design and application limits of all-ceramic restorations. Combined with CAD/CAM technology, the fabrication of extensive zirconia restorations became a simple and an accurate procedure. However, due to the chemical inertness, zirconia are proved to be difficult to establish a chemical bonding with adhesive resins by means of common bonding methods used with other glass containing ceramics such as acid etching and silanization. Recently the rapidly increasing popularity of high strength zirconia ceramic restoration systems require further investigation of adhesive bonding mechanism of resin cements to the zirconia ceramic surface. Limited available literature and failures related to debonding and difficulties in achieving durable adhesion have initiated this PhD research program in order to understand the bonding mechanisms of adhesive resins to zirconia ceramic (part I) and human dentin (part II).

In Part I of this thesis, the adhesive bonding mechanism of adhesive resin cement to zirconia ceramic and the influence of contamination in clinic on the bonding durability of the adhesive resin cement to the zirconia ceramic are investigated. Therefore, in chapter 3 the influence of surface pretreatment on the bonding durability of the resin composite to zirconia ceramic is studied. Most importantly, the influence of chemical reaction of functional monomers in primer on the resin bonding is investigated. Chapter 4 demonstrate the influence of contaminations including saliva and silicone related with "Fit Checker" on the resin bonding durability to zirconia ceramic was investigated.

An ideal adhesive resin should provide a long-term reliable bond to the indirect restoration and tooth hard tissue. However, compared to the bonding of new composite adhesive resins to hydrophobic enamel, dentin bonding of adhesive resins still remains problematic, such as lower long-term bonding strength, since dentin is a hydrated composite material composed of the collagen-based organic matrix and mineral reinforcement, varying with the anatomical location. Therefore, understanding the degradation mechanism of dentin bonding is of significant importance for improving the

long-term dentin bonding of adhesive resins, which influences the reinforcement of brittle restorations and so the longevity of bonded restorations.

In Part II of this thesis, the adhesive bonding mechanism of adhesive resin cement to human dentin is investigated. In chapter 6, micro-tensile bond strength (μ TBS) was used to evaluate the bonds of three resin cements with different chemical compositions and application techniques to different regions of dentin. SEM and TEM were used to investigate the resin-dentin bonding interface and fractographic analysis after μ TBS testing. In chapter 7, a total etching bonding system and a self-etching bonding system were utilised to evaluate the μ TBS to regional dentin, to further identify the difference in their bonding mechanisms and the influence of the structural changes of dentin collagen fibrils on the durability of dentin bonding.

In the last chapter the results of this work on the adhesion of resin composites to ceramic and dentin are summed up, finally general conclusions and an outlook are provided.

Part I. Adhesion of adhesive resin cements to dental zirconia ceramic

2 Background introduction

2.1 Factors that influence the adhesion

The bonding of an adhesive to an object or a surface is the sum of a number of mechanical, physical, and chemical forces that overlap and influence one another. As it is not possible to separate these forces from one another, we distinguish between mechanical interlocking, caused by the mechanical anchoring of the adhesive in the pores and the uneven parts of the surface, electrostatic forces, and the other adhesion mechanisms dealing with intermolecular and chemical bonding forces that occur at the interfaces of heterogeneous systems.

The stronger adhesion of bonds between mechanically or chemically roughened surfaces is based on the enlargement of the effective surface (contact surface between the adhesive and the substrate), and an increase in the number of active centers, e. g., edges, corners, and faulty parts which, as in the heterogeneous catalysis, increase the interactive forces in the interface adhesive/surface. The following factors have a predominant importance in the adhesion process:

- Wetting of the surface
- Surface pretreatment
- Structure of the materials to be bonded (incl. Adhesives and substrates)

2.1.1 Wetting of the surface

To enable the adhesive bonds between the adhesive and the surface, intimate contact must be reached such that van der Waals interaction or the acid-base interaction or both take place; hence good wetting is essential. Wetting is the contact between a liquid and a solid surface, resulting from intermolecular interactions when the two are brought together. The amount of wetting depends on the energies (or surface tensions) of the interfaces involved such that the total energy is minimized. The degree of wetting is described by the contact angle, the angle of contact that forms between a drop of liquid and a smooth, plain solid surface if a liquid droplet is placed on a solid surface. If the wetting is very favorable, the contact angle will be low, and the fluid will

spread to cover a larger area of the surface. If the wetting is unfavorable, the fluid will form a compact droplet on the surface.

The wettability can be observed if a liquid droplet is placed on a solid surface, see figure 2.1. According to Young's equation, the surface tensions at the three phase contacts are related to the equilibrium contact angle θ through:

$$\gamma_{SG} = \gamma_{SL} + \gamma_{LG} \cos \theta$$

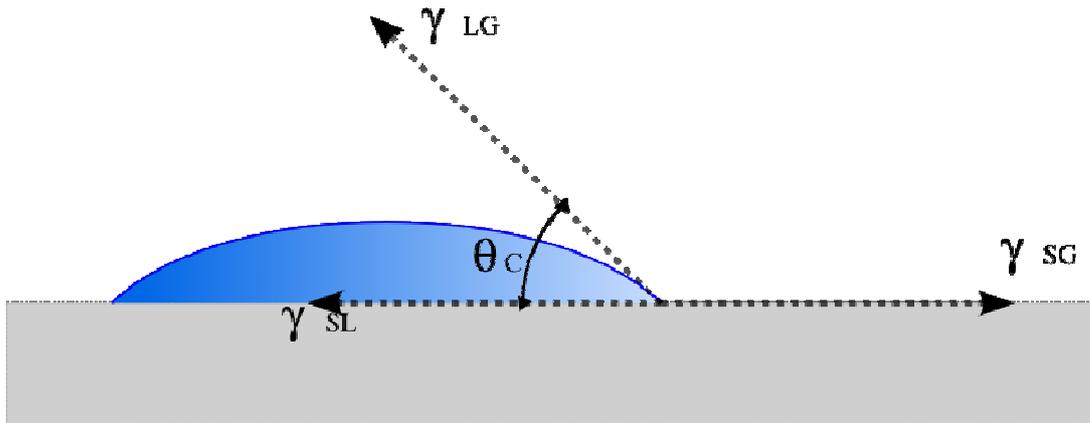


Figure 2.1 Angle of contact of a drop of liquid with the surface of a solid object (published by Wikimedia foundation, San Francisco, California, U.S.A.)

A good wetting occurs when the angle of contact between the adhesive and the substrate is inferior to 90° . Complete wetting occurs when the molecular attraction between the liquid and solid molecules is greater than that between similar liquid molecules. Whether or not a given liquid will wet a solid depends on the surface tension of both substances, e.g., luting agent and substrate.

The contact surface formed during wetting depends on the surface tension and the viscosity of the adhesive, and also on the structure (shape and size of the pores) of the surface. The viscosity of the adhesive is critical to wetting, e.g.,: the lower the viscosity, the faster it will wet the substrate. The size of the effective surface is generally smaller than the true surface of the substrate, because the pores and uneven parts of the surface are not completely filled by the adhesive. Pressure may also help enhance the adhesion. Generally, bonds that have been set under pressure have higher adhesive strength. Pressure imparts better wetting and consequently a more complete interfacial contact. It is obvious to say that the rheological properties of the adhesive must be adapted to the application conditions (substrate's surface, curing time, pressure, temperature).

2.1.2 Surface pretreatment

To ensure a good adhesion it is sometimes necessary to carry out, particularly on metals or ceramics, mechanical and/or chemical pretreatment (e.g., sandblasting and pickling) ¹⁾. In principle, these processes serve to form active centers and polar, reactive groups, which favour the wettability and the chemisorption of suitably pretreated surfaces.

The mechanical interlocking theory of adhesion states that good mechanical adhesion occurs only when an adhesive penetrates into the pores, holes and crevices and other irregularities of the adhered surface of a substrate, and locks mechanically to the substrate. The adhesive must not only wet the substrate, but also have the right rheological properties to penetrate pores and openings in a reasonable time. Since good adhesion can occur between smooth adherend surfaces as well, it is clear that while interlocking helps to promote adhesion, it is not really a generally applicable adhesion mechanism.

These pretreatments (especially plastic surface treatments) result in micro-roughness on the adherend surface, which can improve bond strength and durability by providing mechanical interlocking. Beyond mechanical interlocking, the enhancement of the adhesive joint strength due to the roughing of the adherend surface may also result from other factors such as formation of a larger surface, improved kinetics of wetting and increased plastic deformation of the adhesive ^{2,3)}. The chemical bonding mechanism suggests that primary chemical bonds may form across the interface. Chemical bonds are strong and make a significant contribution to the intrinsic adhesion in some cases. For example, primary chemical forces have energies ranging between 60-1100 kJ/mol, which are considerably higher than the bond energies secondary forces have (0.08-5 kJ/mol) ⁴⁾. The coupling agents and adhesion promoters are often used to help in fixing the adhesive at the surface by chemical reaction ⁵⁾.

The quality of the parts being joined is paramount for the quality of the bonded joint and, in particular, its resistance to ageing. The surface must therefore be suitably treated before the adhesive is applied. In this part, we should also mention coupling agents or adhesion promoters. These are in most cases bifunctional, low-molecular substances, e. g., titanates, chlorosilanes, and chromium complexes of unsaturated carboxylic acids, which fix the adhesive on the surface by chemical reactions. The mode of action of these adhesion promoters is based on their bifunctionality. One group reacts with reactive groups of the adherends, while the second group reacts with the adhesive. It is advisable, therefore, to use adhesion promoters whose groups react differently or according to different types of reaction, e. g., by substitution or radical reaction.

Surface contamination is difficult to avoid during the manufacturing process. Surface contamination is a major cause of poor bond strength and adhesion to the bonding substrate. Therefore, in every case contaminant such as oil, grease, drawing and releasing agents, plasticizers, etc. must be removed with suitable cleaning agents.

2.1.3 Structure of the materials to be bonded

Besides the surface condition, the microstructure and composition of the materials to be bonded is also of decisive importance. Porous materials absorb low viscosity adhesives. The results of this adhesive's penetration are thin, uneven joints which often impair the strength of the bond. On another hand, the more volatile, i. e. low molecular substance, are absorbed by the capillaries preferably.

This process results in a rapid adhesion, but it can have a negative influence on the distribution of the polymer in the glue line owing to the simultaneous separation of oligomers. In addition, the solvent molecules compete with the adhesive molecules in regard to the adsorption. The adhesive molecules are first adsorbed out of the adhesive solution through contact points separated by loops with progressing evaporation of the solvent, the adhesive molecules are then adsorbed mainly at the surface.

The molecular structure of the adhesive is decisive for the cohesion, i. e. the state in which the particles of a single substance are held together, and in connection with the surface condition described above, for the adhesion. The principal molecular influencing factors are: the molecular weight or the distribution of the molecular weight, the number and size of the side-groups, and the polarity. The higher the molecular weight is, the higher the tensile strength of linear polymers is.

2.2 Resin bonding to zirconia ceramic

The introduction of zirconia based materials to the dental field opened the design and application limits of all-ceramics restorations. With the unique mechanical properties of zirconia framework materials, three or four fixed partial dentures are no longer the safe limit for the construction of all-ceramic restorations. Combined with CAD/CAM technology, the fabrication of extensive zirconia restorations became a simple and an accurate procedure.

A strong, durable resin bond provides high retention ⁶⁾ improves marginal adaptation and prevents microleakage ⁷⁾ and increases fracture resistance of the restored tooth and the restoration ⁸⁾. Bonding to traditional silica-based ceramics is a predictable procedure yielding durable results when certain guidelines are followed. ⁹⁻¹²⁾ However, the composition and physical properties of high-strength ceramic materials, such as

aluminum oxide- based (Al_2O_3) and zirconium oxide-based (ZrO_2) ceramics ¹²⁾, differ substantially from silica-based ceramics, and require alternative bonding techniques to achieve a strong, long-term, durable resin bond ¹²⁾.

2.2.1 Adhesive resin cements

Adhesive resin cements are increasingly used for luting all-ceramic, metal or composite indirect restorations due to advantages such as excellent mechanical properties, better bond strengths and improved aesthetics when compared to conventional cements ¹³⁾. Therefore, resin-based luting composites are the material of choice for the adhesive luting of ceramic restorations ¹⁴⁾. Composite cements have compositions and characteristics similar to conventional restorative composites and consist of inorganic fillers embedded in an organic matrix (for example: Bis-GMA, TEGDMA, UDMA). Composite cements can be classified according to their initiation mode as autopolymerizing (chemically activated), photoactivated, or dual-activated materials ¹⁴⁾. Photoactivated composites offer wide varieties of shades, consistencies, and compositions. Clinical application is simplified through long handling times before and rapid hardening after exposure to light. Shade, thickness, and transmission coefficient of the bonded ceramic restoration and the composite itself influence the conversion rate of the photo-activated material and limit its application to thin silica-based ceramics. Dual-activated composites offer extended working times and controlled polymerization ¹⁴⁾, although chemical activators ensure a high degree of polymerization. Most dual-activated resin cements still require photopolymerization and demonstrated inferior hardness when light polymerization was omitted. Autopolymerizing resin cements have fixed setting times and are generally indicated for resin bonding metal-based or opaque, high-strength ceramic restorations.

Resin cements with reduced filler contents offer improved flow, increased surface wettability, and optimal positioning of the restoration ¹⁵⁾. However, filler-containing composite cements revealed higher bond strengths than resins without fillers ¹⁶⁾ and hybrid composites showed better results than microfilled composites. Highly filled resin cements may improve abrasion resistance at the marginal area, reduce polymerization shrinkage, and facilitate removal of excess cement ¹⁴⁾. Wear and substance loss of composite cements after final insertion have been extensively studied in laboratory and clinical investigations that demonstrated a correlation of marginal gap width and depth of wear ¹⁷⁾. However, the effect of wear resistance of resin cements on the clinical long-term success of bonded restorations remains to be determined. Other properties of these materials need to be investigated before they can be recommended for bonding of ceramic high viscosity materials may be pulled out of the luting gap during cleaning restorations without reservation.

2.2.2 Zirconia ceramics

Zirconium, a high-strength ceramic was recently introduced for dental use as a core material for conventional and resin-bonded FPDs and complete coverage crowns. A number of zirconium-oxide ceramic systems have been recently introduced, such as Cercon (Dentsply, Amherst, N.Y.), DCS system (DCS Dental AG, Allschwil, Switzerland), LAVA (3M ESPE) and Procera AllZirkon (NobelBiocare). Following the clinical success of CAD/CAM-fabricated densely sintered high-purity aluminum-oxide ceramic restorations (Procera AllCeram; Nobel Biocare, Goteborg, Sweden), a new material, densely sintered high-purity zirconium-oxide ceramic (Procera All- Zirkon), was added to this line of CAD/CAM products. The clinical use of zirconium oxide (ZrO_2) as a core material has advantages, including favorable optical properties and a high flexural strength of over 1000 MPa. Polycrystalline ZrO_2 is typically used in a tetragonal crystalline phase, partially stabilized with yttrium oxide. A unique property is the so-called “transformation toughening,” where a partially stabilized zirconium oxide can actively resist crack propagation through a transformation from a tetragonal to monoclinic phase at the tip of a crack, which is accompanied by a volume increase ¹⁸⁾.

Zirconium-oxide ceramic is indicated for conventional and resin-bonded fixed partial dentures (FPDs), full-coverage crowns, implant abutments, and endodontic posts. In CAD/CAM fabricated restorations, zirconium-oxide is used as a core material for complete coverage crowns and FPDs. The use of the zirconium-oxide all-ceramic material provides several advantages, including a high flexural strength and desirable optical properties, such as shading adaptation to the basic shades and a reduction in the layer thickness (compared to conventional ceramics) of the veneer ceramic required to achieve the desired color ¹⁹⁻²¹⁾.

Along with the strength of the zirconia ceramics, the cementation technique is also important to the clinical success of a restoration ²¹⁾. Due to their high fracture resistance, zirconium-oxide crowns and FPDs can be cemented using conventional methods recommended by the manufacturers. However, a sufficient resin bond has the aforementioned advantages and may become necessary in some clinical situations, such as compromised retention and short abutment teeth ²²⁾. It has been suggested that even if the clinical success of a restoration does not rely on the resin bond to the tooth, successful resin bonding can improve retention ²³⁾ marginal adaptation, ²⁴⁾ and fracture resistance of the restoration and the abutment tooth ⁸⁾. Some authors concluded that, based on the current evidence, adhesive cementation procedures are necessary to support all-ceramic materials. In vitro studies may provide insight enabling the restorative team to isolate cementation methods and bonding materials that have favorable potential prior to clinical implementation.

2.2.3 Surface pretreatment of zirconia ceramic

Successful ceramic-resin bonding is achieved by the formation of chemical bonds and micromechanical interlocking at the resin-ceramic interface ^{12, 25)}. With conventional silica-based ceramics, acid etching and application of a silane coupling agent create a rough surface of increased wettability for successful ceramic-resin bonds ¹²⁾. High-strength aluminum-oxide and zirconium-oxide ceramics are not silica based and present a unique challenge for predictable resin bonding since chemical silica-silane bonds can not be established ^{12, 26)}. Also, the application of acidic agents, such as phosphoric acid and hydrofluoric acid, to high-strength ceramics will not create a sufficiently roughened surface for enhanced micromechanical retention ²⁷⁾.

Pretreatment methods applied on ceramic surfaces can enhance resin adhesion. A strong resin bond relies on micromechanical interlocking and chemical bonding to the ceramic surface, which requires roughening and cleaning for adequate surface activation ^{12, 25, 28)}. Common treatment options include grinding with diamond rotary instruments, airborne particle abrasion with aluminum oxide, acid etching, and combinations of any of these methods.

Acid etching increases the surface area and the wettability of silicate-based ceramics, changing their surface energy and the bonding potential of this kind of ceramic to resin ²⁹⁾. However, the microstructure of the zirconia ceramic system is composed of acid-resistant zirconium oxide ³⁰⁾. Thus, the acid etching does not produce significant topographic alterations in ceramics with high crystalline content, reducing the bond with the resin cement ³¹⁾.

Airborne particle abrasion with Al_2O_3 abrasive particles is a surface treatment option that produces irregularities in acid-resistant high-strength ceramics. This method has proven to be effective both for aluminum-oxide and zirconium-oxide ceramics ^{12, 25, 28, 32-35)}. However, some studies reported that sandblasting the high-strength ceramics may be effective for the initial bond to some luting agents, yet it is not stable, since it presents failure when specimens are stored for extended periods in artificial saliva and submitted to thermocycling in water ³⁶⁾. This may be due to the fact that this treatment creates surface irregularities without micromechanical retention.

Application of a silica coating on ceramics with high crystalline (low silica) content, as In-Ceram, has been used as an experimental surface treatment method. This technology was initially developed for metals to increase bonding to resins. The silica coating systems include the Rocatec and Cojet from ESPE (Germany) and the Silicoater MD from Heraeus Kulzer (Germany). Cojet is an in-office silica coating system that uses 30- μm silica-modified Al_2O_3 particles (Cojet-Sand) blasted to the surface, followed by the application of a silane agent (ESPE-Sil) ³⁷⁾ These silica coating systems

have showed adequate bond strength values in several studies.^{38),39, 40)} Kern, Thompson³⁵⁾ analyzed the composition and morphology of In-Ceram ceramic submitted to different treatments and observed an effective increase in the silica content after using the Rocatec system compared to Silicoater MD and sandblasting with aluminum oxide, favoring the action of silane on resin bonding. A similar study evaluated these alternative adhesive methods, investigating the stability of bonding by storage in artificial saliva and thermocycling, which also revealed the highest bond strengths for the Rocatec system, which also presented stable bond strength, whereas the bond strength values for Silicoater MD were drastically reduced after 150-day storage³⁶⁾.

A few studies evaluated different methods and materials to bond to zirconia ceramics and also tested durability after long-term water storage and thermal cycling. Kern and Wegner²⁶⁾ reported that airborne-particle abrasion, silane application, and conventional Bis-GMA resin luting agents failed after simulated aging. Only airborne-particle abrasion and use of a modified Bis-GMA resin luting agent (Panavia 21, Kuraray, Tokyo, Japan), containing the adhesive phosphate monomer 10-methacryloyloxydecyl dihydrogen phosphate (MDP), provided a long-term durable resin bond to zirconium-oxide ceramic^{12, 26, 33, 41, 42)}. Some studies suggest the use of Panavia without a silane or a bonding agent to bond to high-strength ceramics. However, application of a MDP containing resin bonding/silane coupling agent mixture (Clearfil New Bond and Clearfil Porcelain Bond Activator, Kuraray) significantly increased bond strength to airborne-particle-abraded intaglio surfaces of alumina restorations¹²⁾. The bonding/silane agent possibly improves wettability of the rough intaglio surface.

2.3 Summary

Adhesive cementation may not be required for final insertion of high-strength all-ceramic restorations with proper mechanical retention. However, some clinical situations and restorative treatment options mandate resin bonding and adequate ceramic-surface conditioning. Preferred treatments for glass-infiltrated aluminum-oxide ceramic are either airborne particle abrasion with Al_2O_3 (50 to 110 μm at 2.5 bar) and use of a phosphate-modified resin cement (Panavia 21) or tribochemical surface treatment (Rocatec System) in combination with conventional Bis-GMA resin cement. The small number of long-term in vitro studies on the bond strength to densely-sintered aluminum-oxide ceramic does not allow for clinical recommendations. The few available studies on resin bonding to zirconium oxide ceramics suggest the use of resin cements that contain special adhesive monomers. Compared with silica-based ceramics, the number of in vitro studies on the resin bond to high-strength zirconia ceramics is small. The rapidly increasing popularity of all-ceramic systems requires further investigation of resin-zirconia ceramic bonding.

A strong durable resin-ceramic bonding can be achieved through surface pretreatments in strictly controlled clean *in vitro* tests. However, during clinical try-in procedures, the contaminations on luting surfaces of ceramic restorations by saliva, blood or silicone indicators cannot be avoided, which may lead to a significantly reduced bond strength in clinical situations. The influences of contaminations on resin bonding durability of zirconia ceramic are not reported until now. Therefore, in order to promise a strong durable resin-ceramic bonding durability in clinical situations approaching to the result achieved in labor study, it is required to further investigate the influences of contaminations and cleaning methods on resin-ceramic bonding durability.

3 Effect of surface pretreatment on durability of adhesive resin cements bond to zirconia ceramic

3.1 Introduction

A strong, durable resin-ceramic bonding provides high strength ceramic restorations such as zirconia ceramic with high retention, improved marginal adaptation and increased fracture resistance of the restored teeth and the restorations ²¹⁾, although conventional cements (zinc phosphate and glass ionomer cements) can be also used for luting zirconia ceramic restorations in most cases ¹²⁾. Available literatures reported that the adhesive composite resin cements revealed different bonding performances due to the difference in their chemical composition and physical properties. Derand ³⁹⁾ pointed out that a 4-META containing adhesive resin (Superbond C&B) had a bond strength superior to Panavia 21 regardless of the surface treatments. However, 10-MDP -containing luting composite resins, e.g. Panavia 21 and Panavia F, showed a long-term durable bond to airborne-particle abraded zirconia ceramic after water storage for 150 days ^{26) 33)} and 2 years ⁴¹⁾ with repeated thermal cycling. The rapidly increasing popularity of high strength all-ceramic restoration systems require further investigation of adhesive bonding mechanism of resin cements to ceramic surface.

In order to obtain a durable adhesion between resin cements and zirconia ceramic surface, the surface pretreatments ¹²⁾ with primers containing functional primers such as 4-META, MDP, and other adhesive phosphate monomers are often used to improve the wettability of adhesive resins to the ceramic bonding substrate. This pretreatment was thought to produce chemical bonding between resin cement and ceramic surface. Up to date, little information is available about the chemical reaction between resin cement and zirconia ceramic and the effect of pretreatment with primers on the bonding durability of adhesive resin cement to zirconia ceramics.

Therefore, in this chapter, the aim of this study is to evaluate the bonding durability of three resin cements to zirconia ceramic with different priming after long-term water storage with thermal cycling. The influence of pretreatment with primers on the bonding durability of zirconia ceramic was investigated with x-ray photoelectron spectroscopy (XPS), tensile bond strength (TBS) and SEM.

3.2 Materials used in this study.

Table 3.1 Compositions and application of the test adhesive resin cements and primers.

Adhesive resin cements	Main composition	Primer	Main composition
		Monobond S (MS)	Silane, Solvent
		Metal/Zirconia primer (MZP)	Solvent Phosphoric acid acrylate Ethoxylated Bis-GMA Initiators and Stabilizers
Superbond C&B (SB) <i>Self-curing unfilled adhesive resin cement</i> Sun Medical Co. Ltd., Shiga, Japan	Methyl methacrylate (MMA), 4-META, Polymethyl methacrylate (PMMA), Partially oxidized tri-N-butyl borane (TBB); radiopaque pigments, acetone	Porcelain Liner M (PLM)	Silane, 4-META, MMA
Chemiace II (CH) <i>Self-curing adhesive resin cement composite</i> Sun Medical Co. Ltd., Shiga, Japan	Zirconia (ZrO ₂), silica (SiO ₂), TMPT filler, Aromatic Amine 2-hydroxyethyl methacrylate (HEMA), 4-META, di(meth)acrylates, Benzoyperoxide	Porcelain Liner M (PLM)	Silane, 4-META, MMA
Clearfil™ Esthetic Cement (CE) <i>Dual curing adhesive resin cement composite</i> Kuraray Medical nc., Osaka, Japan	BPEDMA/MDP/DMA, Ba-B-Si-glass, chemical and photoinitiators	Clearfil™ ceramic primer (CCP)	Silane, MDP, Solvent

3.3 Study design for XPS examination and tensile bond strength testing

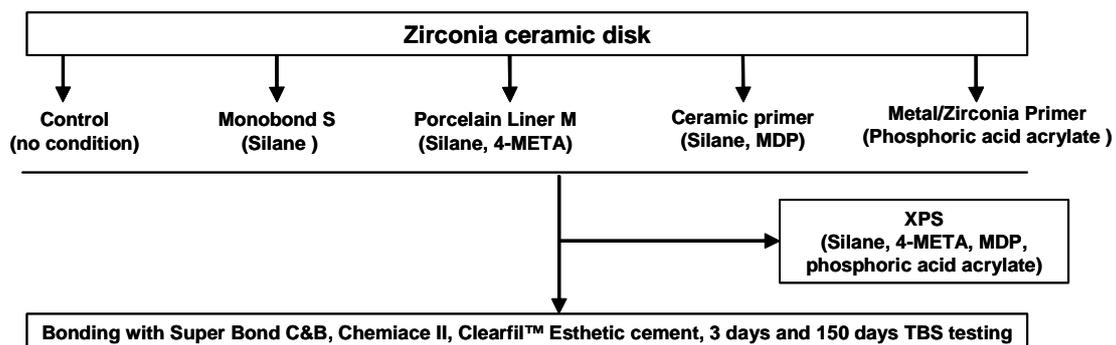


Figure 3.1 Study design for XPS examination and TBS testing.

3.4 X-ray photoelectron spectroscopy (XPS)

For chemical analysis with XPS (Vacuum Generators, England), specimens of the above test groups were highly wet polished until 4000 grit silicon carbide paper to

reduce the negative influence of irregular surface texture on the chemical analysis and followed by ultrasonic cleaning for two times with 10 minutes each. Then the highly polished specimens were air-dried and pre-treated with each of four primers according to the manufacturers' priming instructions, followed by ultrasonic rinsing in 96% ethanol for 10 minutes prior to XPS analysis to remove the solvents contained in primers. Clearfil™ ceramic primer (CCP), Monobond S (MS), Metal/Zirconia primer (MZP), or Porcelain Liner M (PLM) were used in this study (Table 3.1). The specimens without priming pretreatment were used as control. XPS was used to further identify the chemical bonding of functional monomer on the ceramic surface. All measurements were done using a XPS system with an x-ray source providing Al K α x-rays and kinetic energy of 1486.6 eV. A hemispherical analysis with five channeltrons was used for detection of the photoelectrons. A pass energy setting of 100 allowed adequate quantitative analysis. In order to examine the surface composition of the test specimens high resolution scans of the carbon (C1s), oxygen (O1s), zirconium (Zr3-d) nitrogen (N1s) and phosphoric (P2s and P2p) peaks were taken.

3.5 Specimen preparation for bonding with resin cements

Densely-sintered partially-stabilized zirconia ceramic disk-like specimens (Cercon, DeguDent, Hanau, Germany) were used in this study. The specimen surfaces were wet polished with 600 grit silicon carbide paper and then airborne-particle abraded with 50 μm Al₂O₃ at 2.5 bar pressure for 15 s at a distance of 10 mm. Afterwards the specimen surfaces were air-cleaned for 20 s with the Rocatector delta device (3M ESPE, Seefeld, Germany). Air-born abraded ceramic specimens were pre-treated with one of the following four primers according to manufacturers' instructions. The specimens without treatment were served as control subgroups. Superbond C&B (SB), Chemiace II (CH), and Clearfil™ Esthetic cement (CE) were used in this study (Table 3.1).

3.6 Bonding with resin cements and tensile bond strength (TBS) testing

Plexiglas tubes filled with composite resin were bonded to the experimental ceramic specimens using Super Bond C&B, Chemiace II (CH), or Clearfil™ Esthetic cement (CE) using an alignment apparatus under a load of 750 g according to the manufacturers' instructions. For groups SB, the ceramic specimens were bonded with resin cements at self-curing mode for 7 minutes. For groups CH and CE, the specimens bonded with resin cements were light-cured for 20 s from two opposite sides with a dental curing light (Optilux 500, Kerr, Danbury, USA). Afterwards, the bonded specimens were placed at room temperature for 20 min, then stored in 37 °C water for 3 days or 150 days with 37,500 thermal cycles between 5 °C and 55 °C. After the different storage conditions,

tensile bond strength (TBS) was tested with a universal testing apparatus (Zwick Z010/TN2A, Germany) at a crosshead speed of 2 mm/min. Statistical analysis was performed with the Wilcoxon rank sum test adjusted according to Bonferroni-Holm for multiple testing at $\alpha = 5\%$.

3.7 SEM examination

A scanning electron microscope (SEM, XL 30 CP, Philips, Kassel, Germany) operating at 10 to 25 KV was used to observe the failure modes of the debonded ceramic specimens after tensile testing. Failure modes were classified into one of the following modes: A: Adhesive failure at ceramic surface; C: Cohesive failure in the luting composite resin or in the tube filling composite resin; TL: Cohesive failure in the thin layer of adhesive resin cement or primer at ceramic surface.

3.8 XPS examination

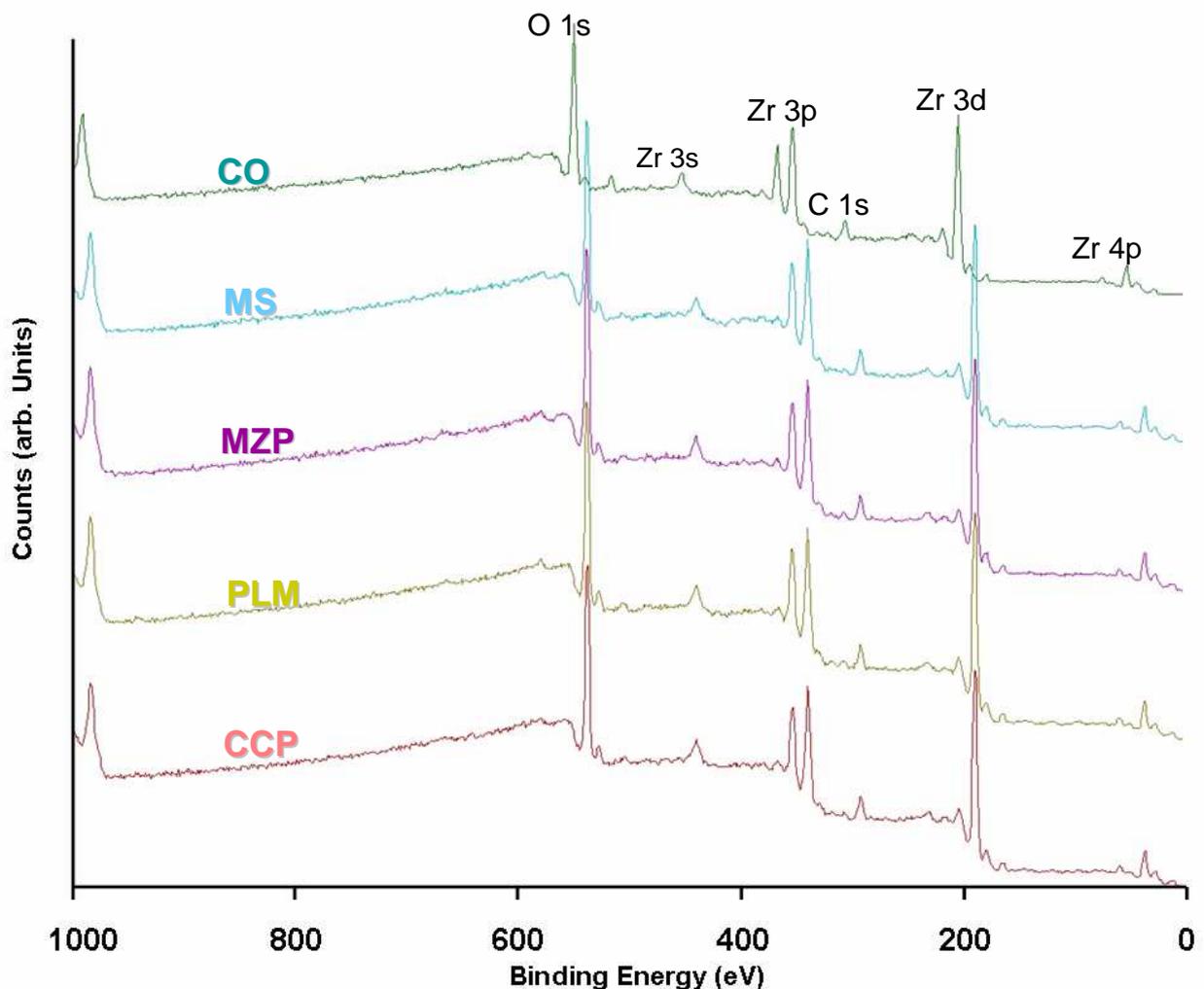


Figure 3.2 XPS wide-scan spectra of untreated zirconia ceramic surface, and treated surface with Monobond S (MS), Metal/Zirconia primer (MZP), Porcelain Liner M (PLM) or Clearfil™ ceramic primer (CCP).

XPS wide-scan spectra of untreated zirconia ceramic revealed besides Zr and O that originated from zirconium oxide, also partially O and C that should be attributed to common organic contamination adsorbed to the specimen surface (Fig. 3.2). When zirconia ceramic surface was treated with Monobond S (MS), Metal/Zirconia primer (MZP), Porcelain Liner M (PLM) or Clearfil™ ceramic primer (CCP) followed by ultrasonic rinsing in 96% ethanol for 10 minutes, a XPS wide-scan spectrum similar to control group was obtained, without different element such as P detected originating from primers.

3.9 Tensile bond strength and SEM observation

Table 3.2 Tensile bond strength and the percentage of failure mode for Super Bond C&B to zirconia ceramic after different surface pretreatment. Means, standard deviations (SD) and medians in MPa (n = 8).

Groups	Super Bond C&B ⁴³⁾					
	3-d			150-d / 37,500TC		
	Means (SD)	Medians	Failure percentage (%)	Means (SD)	Medians	Failure percentage (%)
Control (CO)	51.6 (5.0)	51.7 ^A _α	A: 3% B: 95% TL: 2%	27.5 (6.4)	23.3 ^B _β	A: 2% B: 5% TL: 93%
Monobond S (MS)	52.8 (10.0)	55.8 ^A _α	A: 2% B: 98%	33.6 (5.5)	33.5 ^{CB} _β	A: 3% B: 29% TL: 68%
Metal/Zirconia Primer (MZP)	37.7 (4.5)	36.7 ^B _α	A: 3% B: 85% TL: 2%	32.0 (6.8)	29.5 ^A _α	A: 4% B: 40% TL: 56%
Porcelain Liner M (PLM)	43.0 (9.9)	41.3 ^A _α	A: 3% B: 96% TL: 2%	33.2 (8.3)	35.5 ^{CB} _α	A: 5% B: 38% TL: 57%
Clearfil™ ceramic primer (CCP)	50.0 (9.3)	51.4 ^A _α	A: 3% B: 97% TL: 2%	42.3 (8.2)	41.1 ^B _α	A: 3% B: 52% TL: 45%

All specimens in this group debonded spontaneously during water storage with thermal cycling. TC = thermal cycles. A: adhesive failure at ceramic surface; B: cohesive failure in bulk adhesive resin cement or filling composite resin; TL: cohesive failure in thin layer of adhesive resin cement at the bonding interface. Within the same column, medians with the same superscript letter are not statistically different ($p > 0.05$), within the same row, medians with the same Greek subscript letter are not statistically different ($p > 0.05$). Statistical analysis was performed with the Wilcoxon rank sum test adjusted according to Bonferroni-Holm for multiple testing at $\alpha = 5\%$.

For SB, the 3-d TBS of control group is 51.6, and 150-d water storage with thermal cycling decreased the TBS (27.5 MPa) significantly. In contrast, the pretreatment in groups CCP, MZP, and PLM significantly improved the bonding durability of SB to zirconia ceramics compared to the control group, and there are no statistical difference detected between the TBS of groups 3-d (CCP: 50.0 MPa, MZP: 37.7 MPa and PLM: 43.0 MPa) and 150-d (CCP: 42.3 MPa, MZP: 32.0 MPa, PLM: 33.2 MPa). Although the initial TBS of group MS (52.8 MPa) is the highest in test groups, 150-d water storage with thermal cycling decreased the TBS (33.6 MPa) significantly (Fig. 3.3).

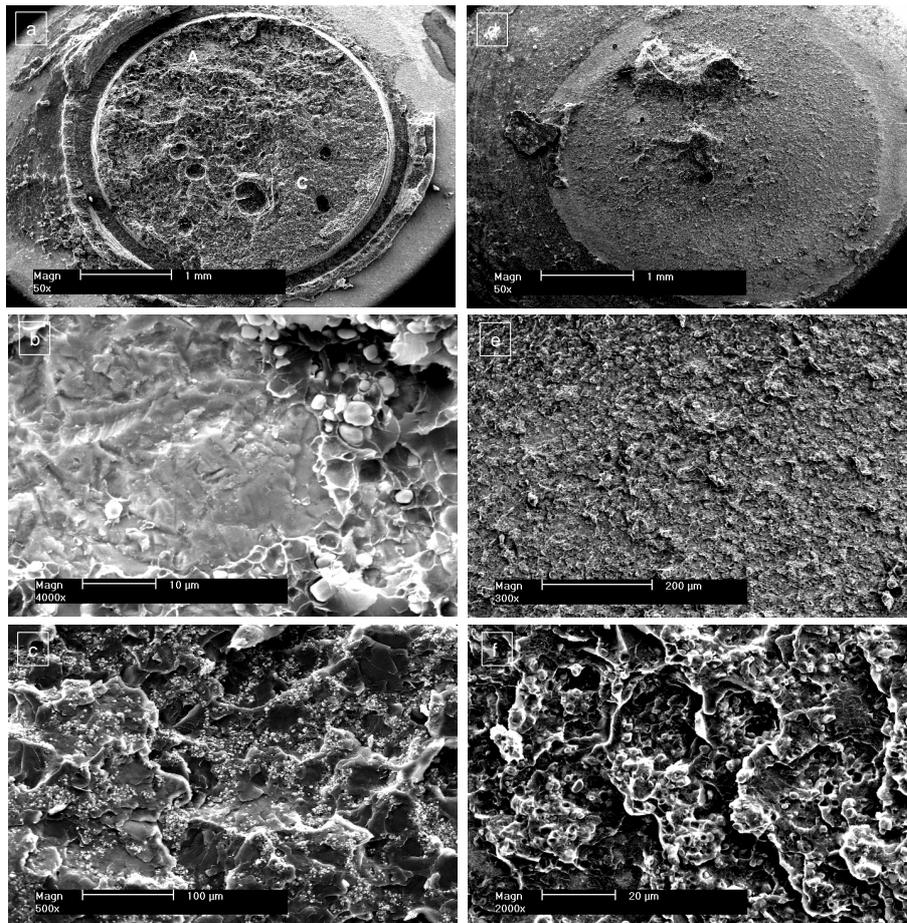


Figure 3.3 (a) One representative debonded ceramic surface in group Super-Bond C&B⁴³⁾-control after 3-d showed small area of adhesive failure from ceramic surface (A) and big area of cohesive failure in luting cement (C) at low magnification. (b) Cohesive failure in luting cement at high magnification. (c) Adhesive failure at high magnification. (d) One representative debonded ceramic surface in group SB after 150d and 37,500 thermal cycling showed big area of cohesive failure with a very thin layer of SB adhesive resin cement remaining on the ceramic surface and small area of cohesive failure in luting cement at low magnification. (e) and (f) Cohesive failure in luting cement (a) at high magnification (b).

Table 3.3 Tensile bond strength and the percentage of failure mode for Chemiac II to zirconia ceramic after different surface treatment. Means, standard deviations (SD) and medians in MPa (n = 8).

Groups	Chemiac II (CH)					
	3 d			150-d / 37,500TC		
	Means (SD)	Medians	Failure percentage (%)	Means (SD)	Medians	Failure percentage (%)
Control (CO)	32.7 (6.3)	34.4 ^A _α	A: 10% C: 50% TL: 40%	0*	0 ^A _β	A: 2% C: 5% TL: 93%
Monobond S (MS)	48.3 (9.2)	49.7 ^B _{αα}	A: 2% C: 98%	0*	0 ^A _β	A: 3% C: 29% TL: 68%
Metal/Zirconia Primer (MZP)	34.6 (6.9)	35.7 ^A _α	A: 3% C: 85% TL: 2%	0*	0 ^A _β	A: 4% C: 40% TL: 56%
Porcelain Liner M (PLM)	39.4 (10.0)	35.5 ^A _α	A: 3% C: 96% TL: 2%	4.6 (2.3)	5.6 ^B _β	A: 5% C: 38% TL: 57%
Clearfil™ ceramic primer (CCP)	42.4 (6.8)	40.5 ^B _α	A: 3% C: 97% TL: 2%	4.8 (1.3)	5.0 ^B _β	A: 3% C: 52% TL: 45%

All specimens in this group debonded spontaneously during water storage with thermal cycling. TC = thermal cycles. A: adhesive failure at ceramic surface; C: cohesive failure in bulk adhesive resin cement or filling composite resin; TL: cohesive failure in thin layer of adhesive resin cement at the bonding interface. Within the same column, medians with the same superscript letter are not statistically different ($p > 0.05$), within the same row, medians with the same Greek subscript letter are not statistically different ($p > 0.05$). Statistical analysis was performed with the Wilcoxon rank sum test adjusted according to Bonferroni-Holm for multiple testing at $\alpha = 5\%$.

For CH, the initial TBS of groups SCP (42.4 MPa) and MS (48.3 MPa) were higher than those of groups CO (32.7 MPa), MZP (34.6 MPa) and PLM (39.4 MPa). However after 150-d long-term water storage with thermal cycling all specimens in groups CO (0 MPa), MS (0 MPa) and MZP (0 MPa) debonded spontaneously, and TBS of groups SCP (4.8 MPa) and PLM (4.6 MPa) decreased significantly to very low values. For CH, the pretreatments with MS or MZP seem not to contribute to the long-term TBS (Fig. 3.4).

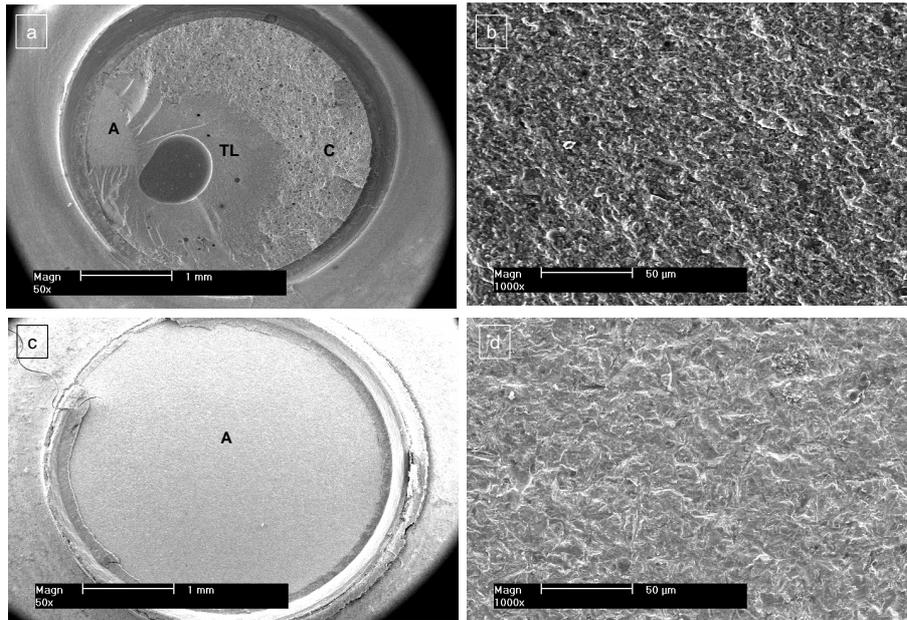


Figure 3.4 (a) One representative debonded ceramic surface in group Chemiace II (CH) -control after 3-d showing small area of adhesive failure from ceramic surface (A), cohesive failure in thin layer of adhesive resin cement and big area of cohesive failure in luting cement or filling resin (C) at low magnification. (b) Adhesive failure at ceramic surface at high magnification. (c) One representative debonded ceramic surface in group SB-control after 150d and 37,500 thermal cycling showing completely adhesive failure at ceramic surface at low magnification. (d) Adhesive failure at ceramic surface at high magnification.

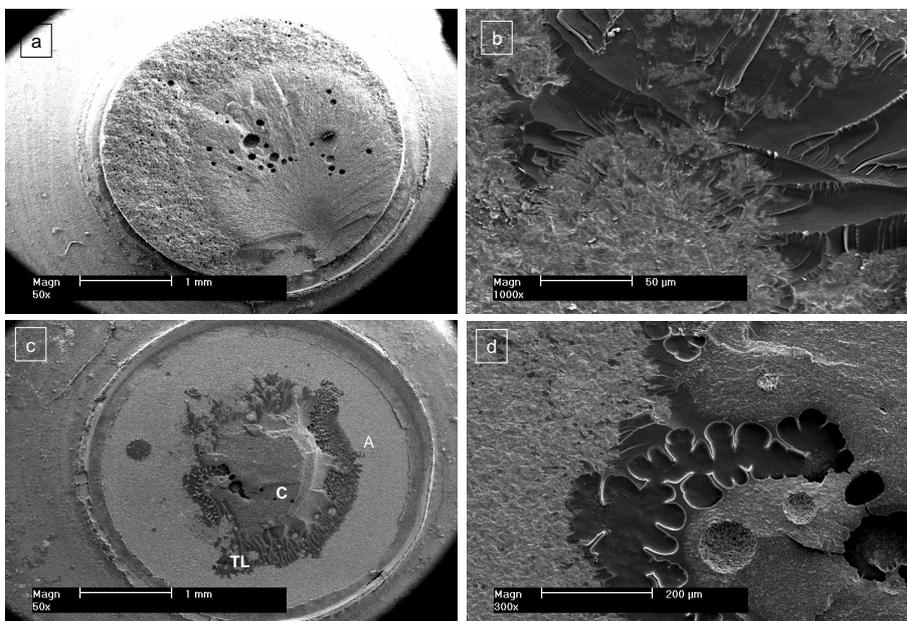


Figure 3.5 (a) One representative debonded ceramic surface in group Chemiace II (CH)- Pocerlain Liner M (PLM) after 3-d showing primarily cohesive failure in bulk adhesive resin cement or filling composite resin and big area of cohesive failure in luting cement or filling resin at low magnification. (b) Adhesive failure at ceramic surface with PLM primer infiltrating in ceramic surface at high magnification. (c) One

representative debonded ceramic surface in group CH-PLM after 150d and 37,500 thermal cycling showing mostly adhesive failure at ceramic surface (A) and small area of adhesive failure at the bonding interface between adhesive resin cement and PLM primer at low magnification. (d) Cohesive failure in adhesive resin cement or adhesive failure at the bonding interface between adhesive resin cement and PLM primer at high magnification.

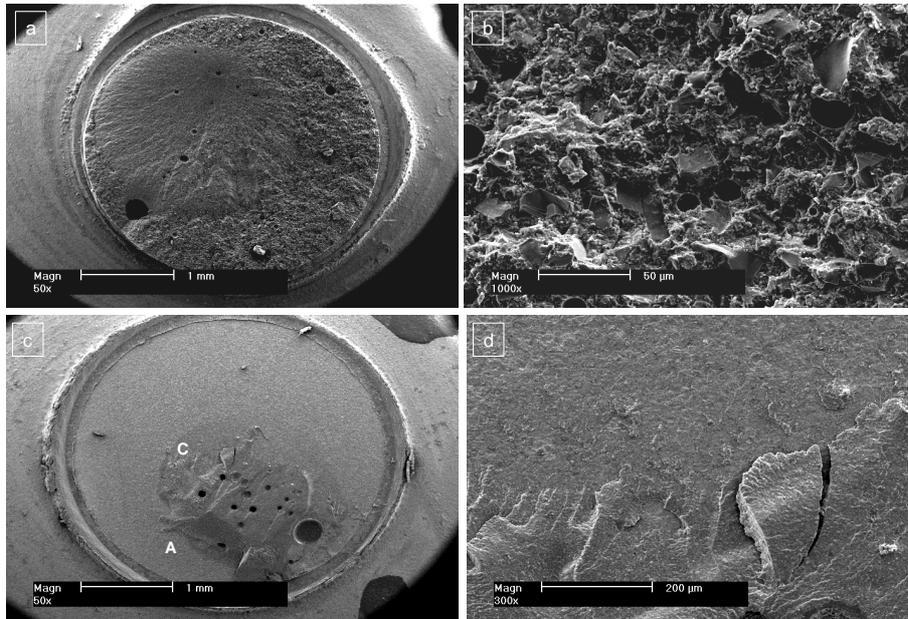


Figure 3.6 (a) One representative debonded ceramic surface in group Chemiace II (CH)- Clearfil™ ceramic primer (CCP) after 3-d showing primarily cohesive failure in bulk adhesive resin cement or filling composite resin and big area of cohesive failure in luting cement or filling resin at low magnification. (b) Cohesive failure in bulk adhesive resin cement at high magnification. (c) One representative debonded ceramic surface in group CH-CCP after 150d and 37,500 thermal cycling showing mostly adhesive failure at ceramic surface (A) and small area of cohesive failure in adhesive resin cement at low magnification. (d) Cohesive failure with adhesive resin cement remaining at ceramic surface at high magnification.

Table 3.4 Tensile bond strength and the percentage of failure mode for Clearfil™ Esthetic cement to zirconia ceramic after different surface treatment. Means, standard deviations (SD) and medians in MPa (n = 8).

Clearfil™ Esthetic cement (CE)						
Groups	3-d			150-d / 37,500TC		
	Means (SD)	Medians	Failure percentage (%)	Means (SD)	Medians	Failure percentage (%)
Control (CO)	9.7 (2.2)	10.0 ^A _α	A: 100%	0*	0 ^A _β	A:100%
Monobond S (MS)	54.8 (13.5)	54.6 ^C _α	A: 5% C: 75% TL: 20%	40.0 (6.5)	41.7 ^B _β	A: 10% C:65% TL: 25%
Metal/Zirconia Primer (MZP)	44.6 (6.2)	44.0 ^B _α	A: 8% C:70% TL:22%	39.0 (15.2)	40.0 ^B _α	A: 18% C: 60% TL:32%
Porcelain Liner M (PLM)	34.8 (8.9)	33.5 ^D _α	A: 8% C: 80% TL: 12%	35.8 (12.3)	38.4 ^B _α	A: 12% C: 77% TL: 11%
Clearfil™ ceramic primer (CCP)	43.2 (5.3)	44.1 ^B _α	A: 3% C: 85% TL: 12%	41.7 (10.4)	43.7 ^B _α	A: 5% C: 80% TL:15%

All specimens in this group debonded spontaneously during water storage with thermal cycling. TC = thermal cycles. A: adhesive failure at ceramic surface; C: cohesive failure in bulk adhesive resin cement or filling composite resin; TL: cohesive failure in thin layer of adhesive resin cement at the bonding interface. Within the same column, medians with the same superscript letter are not statistically different ($p > 0.05$), within the same row, medians with the same Greek subscript letter are not statistically different ($p > 0.05$). Statistical analysis was performed with the Wilcoxon rank sum test adjusted according to Bonferroni-Holm for multiple testing at $\alpha = 5\%$.

For CEC, the initial TBS (10 MPa) of control group was significantly lower than other treatment groups, and all specimens debonded spontaneously during storage. Although the initial TBS of group MS (54.6 MPa) is the highest in test groups, 150-d water storage with thermal cycling decreased the TBS (40.0 MPa) significantly. There are no statistical difference between the initial TBS of groups SCP (44.1 MPa), MZP (44.0 MPa) and PLM (33.5 MPa) and the pretreatment with SCP, MZP and PLM primers showed improved stable long-term TBS (SCP: 43.7 MPa, MZP: 40.0 MPa, PLM: 38.4 MPa) (Fig. 3.7).

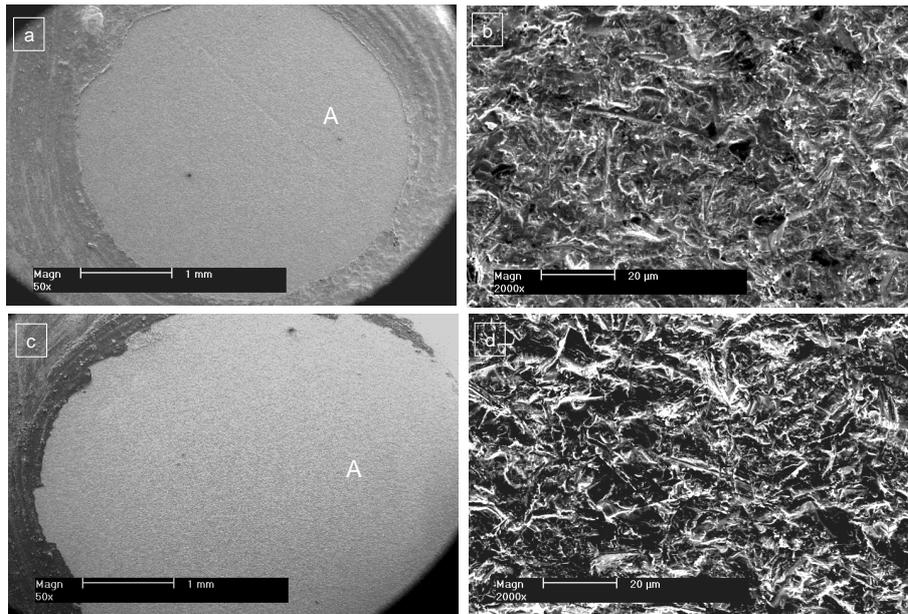


Figure 3.7 (a) One representative debonded ceramic surface in group Clearfil™ Esthetic cement (CE) - control after 3-d showing completely adhesive failure from ceramic surface (A) at low magnification. (b) Adhesive failure without any adhesive resin cement on ceramic surface at high magnification. (c) One representative debonded ceramic surface in group Clearfil™ Esthetic cement (CE) - control group after 150d and 37,500 thermal cycling showing completely adhesive failure at ceramic surface at low magnification. (d) Adhesive failure without any adhesive resin cement on ceramic surface at high magnification.

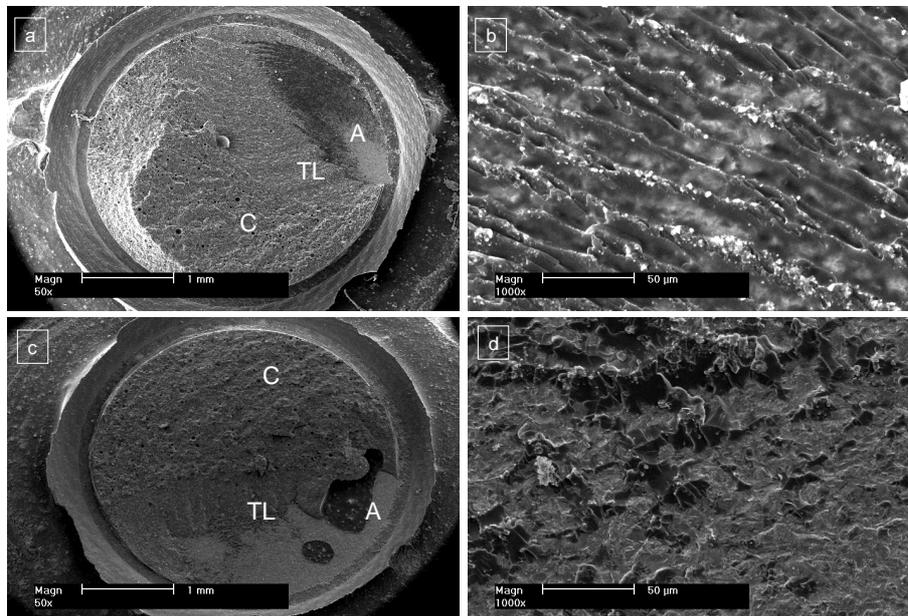


Figure 3.8 (a) One representative debonded ceramic surface in group Clearfil™ Esthetic cement – Pocerlain Liner M (PLM) after 3-d showing primarily cohesive failure in bulk resin cement (C) at low magnification. (b) Adhesive failure with primer on ceramic surface at high magnification. (c) One representative debonded ceramic surface in group Clearfil™ Esthetic cement (CE) - Pocerlain Liner M (PLM) after 150d and 37,500 thermal cycling showing primarily cohesive failure in bulk resin cement (C) with increasing adhesive failure at ceramic surface at low magnification. (d) Adhesive failure with primer on ceramic surface at high magnification.

3.10 Effect of surface pretreatment on bonding durability of adhesive resin cements to zirconia ceramic

Differences in pretreatment of ceramic surface, the chemistry and physical properties of luting agents, and storage condition will significantly influence the nature of the bonding mechanism and resin-bonding durability to zirconia^{12, 26, 33, 44}). Long-term storage and thermal cycling are often used as the artificial aging methods *in vitro* bonding testing^{41, 42, 44-47}). The combination of these two important parameters to simulate oral conditions can have effects on the durability of the resin bond strength to zirconium. However, in many studies, only short-term bond strength and/or after short-term thermal cycling are used to investigate the effects of various pretreatment and adhesive resins on the bond to ceramic^{44, 48}). The *in vitro* bonding testing after long-term oral simulation is necessary to be performed before clinical recommendations can be provided. Therefore, in this study, the effects of thermal cycling and long-term storage on the bond durability of three adhesive resins to zirconia ceramic were evaluated. In this study, water storage and thermal cycling decreased the bonding durability of control groups (without pretreatment) for all three adhesive resin cements to zirconia ceramic significantly. For groups SB, CH and CE, the pretreatment with Monobond S seems not to contribute to a durable long-term resin bond after long term water storage and thermal cycling although the initial bond strength are rather high.

The adhesive bonding mechanism of resin cements to the bonding substrate surface is the sum of micromechanical interlocking and chemical bonding forces. The mechanical interlocking can be caused by the mechanical anchoring of the adhesive cements in the pores and the uneven parts of the ceramic surface. The mechanical interlocking theory of adhesion states that good adhesion occurs only when an adhesive penetrates into the pores, holes and other irregularities of the adhered surface of a substrate, and locks mechanically to the substrate¹). The adhesive must not only wet the substrate, but also have the right rheological properties to penetrate pores and openings in a reasonable time. In this study, airborne-particle abrasion was used to pretreat ceramic surface of all specimens in order to form a certain surface texture with a certain roughness, promoting the micromechanical interlocking of resin composite on ceramic surface^{12, 30, 49}). This method can significantly improve bond strength and durability by providing mechanical interlocking⁵⁰). Beyond mechanical interlocking, the enhancement of the adhesive resin cement joint strength due to the roughing of the adherend surface may also result from other factors such as formation of a larger surface, improved kinetics of wetting and increased plastic deformation of the adhesive.

The chemical bonding forces that occur at the interfaces of heterogeneous systems is believed to occur between functional monomers and metal ion on ceramic surface^{12, 51}).

Therefore, in order to obtain a durable adhesion between resin cements and ceramic surface, the surface pretreatment with primers containing functional primers such as 4-META, MDP, and other adhesive phosphate monomers are often recommended to improve the wettability of adhesive agents to the ceramic bonding substrate and produce chemical bonding between resin cements and ceramic surface^{12, 51-53}. Silane agent used for silanization also contributes to the bond strength by increasing surface energy and improving the surface wettability to resin although the chemical reaction of silane is not possible for zirconia ceramic^{39, 41, 54}.

In nature, Zirconia ceramic is a kind of metal oxide. MDP contained in Clearfil™ Ceramic primer, phosphoric acid acrylate contained Metal/Zirconia primer and 4-META contained in Porcelain Liner M are believed to have the ability to form chemical bond with metal oxide, contributing to the bonding durability of resin-ceramic, supported by technical information from companies. The chemical bonding mechanism suggests that primary chemical bonds may form across the interface. Chemical bonds are strong and make a significant contribution to the intrinsic adhesion in some cases. For example, primary chemical forces have energies ranging between 60-1100 kJ/mol, which are considerably higher than the bond energies secondary forces have (0.08-5 kJ/mol)⁴. Therefore, the coupling agents like silane and adhesion primers are recommended to help in fixing the adhesive at the surface by chemical reaction^{5, 55}. However, in this study, our XPS result showed that there is no P 2s or P 2p was remained on ceramic surface after ethanol ultrasonic cleaning. It indicates that the four primers have no chemical reaction to the zirconia ceramic. At least no primary chemical bonds formed between the primers and zirconium oxide.

According to adhesion theory - adsorption theory, the most common surface forces that form at the adhesive-adherend interface are van der Waals forces. In addition, acid-base interactions and hydrogen bonds, generally considered a type of acid-base interaction, may also contribute to intrinsic adhesion forces⁵⁶. In the present study, in order to obtain the intimate contact between adhesive resin cements and ceramic surface and good adsorption, silane agent is mostly involved in primers to increase surface energy and improve the surface wettability although the chemical reaction of silane is not possible for zirconia ceramic^{39, 41, 54}. In addition, 750 g pressure was also applied to improve the wettability of adhesive resin cement to ceramic surface. Under such condition the intimate contact between adhesive resin cement and ceramic surface is reached, van der Waals interaction, or hydrogen bonds form between zirconium oxide and functional monomer such as MDP contained in CCP, phosphoric acid acrylate contained in MZP, or 4-META contained in PLM should take place. Research^{57, 58} has experimentally demonstrated that the mechanism of adhesion in many adhesive joints only involves interfacial secondary forces. These interfacial secondary forces are very

essential for resin-ceramic bonding. Therefore, the primers containing both silane and functional monomers - MZP, PLM, and CCP- contribute to the stable bonding durability of SB and CE. Whileas for groups SB, CH and CE, the pretreatment with Monobond S containing only silane did not provide a durable long-term resin bond after long term water storage and thermal cycling although the initial bond strength are rather high. However, this kind of secondary force may be removed easily by ethanol ultrasonic cleaning, showing no obvious chemical element change in XPS wide-scan spectra.

MDP is an acidic monomer used in specific dental adhesive materials and is an ester originating from the reaction of a bivalent alcohol with methacrylic acid and phosphoric acid derivatives. In one previous study, XPS result show that MDP has chemical reaction with titanium with a P 2s and P 2p peak appearing in XPS wide-scan spectra. In that study, titanium was immersed in a 15w/w% 10-MDP solution for 2 h, followed by ultrasonic rinsing twice in 52.9w/w% ethanol for 20 min. However, in this study, since the commercially available original primers were used according to the manufacturers' instructions to pre-treat zirconium oxide which is more inert than titanium, the concentration of functional monomers in primers are rather low, about 5% or even lower, and the pretreatment time is only 3 minutes. Due to the high concentration of solvent (90% to 99%) in the used primers, 96% ethanol ultrasonic cleaning was used to remove the remained solvent after evaporation of primers. Obviously, the difference of XPS results in two studies might be explained with the above differences in pretreatment conditions and chemical element.

In this study, for groups SB and CE, the pretreatments with primers except MS can improve the bonding durability to zirconia ceramic while for CE all of specimens in non-pretreatment subgroups debonded spontaneously during storage and thermal cycling ($p \leq 0.05$) with complete adhesive failure from ceramic surface. These results indicate that for the adhesive resin cements containing no MDP or phosphoric acid modified monomers, pretreatment with functional monomers-containing bonding/silane coupling primers are necessary for the resin-ceramic bonding durability, in agreement with one previous study¹²).

For one conventional PMMA based-adhesive resin – SB, no significant difference in initial TBS to zirconia ceramic surfaces was found between both groups non-pretreatment (51.6 MPa) and pretreatment with PLM (43.0 MPa). However, the bonding durability of both subgroups non-pretreatment and pretreatment with PLM significantly reduced to 27.5 MPa and 33.2 MPa separately although TBS of group pretreatment is slightly higher than that of group non-pretreatment. After long-term storage, the cohesive failure in bulk SB observed in subgroup 3-d changed to cohesive failure with a very thin layer of SB remaining on the ceramic surface. SEM observation and the reduction of TBS results might be explained by water absorption of PMMA during

storage and TC, which seems to weaken the cohesive strength of SB cement and decrease the bonding durability of SB to zirconia ceramic.

Compared to the pretreatment with other primers containing functional monomers, such as MZP and CCP, no statistical difference between 3-d and 150-d combined with increasing percentage of cohesive failure in bulk adhesive resin cement indicated that MZP and CCP has good bond with SB adhesive resin cement, reinforce the interfacial bonding between adhesive resin cement and ceramic, contributing to a stable adhesive resin cement-ceramic bonding durability.

For another 4 META/MMA filled adhesive adhesive resin cement-CH, the initial TBS of CH in control group and pretreatment groups are rather high with high percentage of cohesive failure in bulk adhesive resin cement. However, for control group without pretreatment and pretreatment with MS, all specimens debonded spontaneously during storage with complete adhesive failure from ceramic surface. The bonding durability of CH to zirconia ceramic for groups pretreatment with PLM and CCP reduced to also too low to be used at clinic since 10-13 Mpa is the minimum strength needed for clinical bonding⁵⁹⁾. SEM result showed that there is some adhesive resin cement remaining at the middle of ceramic surface, indicating the bonding of PLM to zirconia ceramic is stronger than the bonding between PLM and CH adhesive resin cement. It is obvious that besides the surface pretreatment with primers, the composition and micro-structure of adhesive adhesive resin cement are also of decisive importance to resin bonding.

The molecular structure of the adhesive is decisive for the cohesion, i. e. the state in which the particles of a single substance are held together, and in connection with the surface condition described above for the adhesion. As one main component of liquid part of CH, HEMA is an often used adhesion-promoting monomer to improve the wettability of adhesive resin cement agents due to its hydrophilicity. However, both in uncured and cured state, HEMA will readily absorb water. HEMA fixed in a polymer chain after polymerizing will still exhibit hydrophilic properties and will lead to water uptake with consequent swelling and discoloration⁶⁰⁾. Apart from the water uptake, which adversely influences the mechanical strength of CH, high amounts of HEMA will result in flexible polymers with inferior qualities⁶¹⁾. PolyHEMA is basically a flexible porous polymer ('gel')⁶²⁾. As such, high concentrations of HEMA in an adhesive may have deteriorating effects on the mechanical properties of the resulting polymer. The high amount of HEMA in CH might lead to the decreased cohesion strength and long-term bonding durability of CH to ceramic and complete adhesive failure from ceramic surface.

One previous study reported³⁴⁾ that after water storage and thermal cycling, bonding strength of Panavia F 2.0 to zirconia ceramic is not stable. One possible reason

for this result is the hydrolytic instability of resin cement due to the hydrophilic property of Panavia F 2.0 resin cement as well as its component – MDP which may easily decompose during water storage. Therefore, the late product after Panavia F 2.0 is CE. Comparing to Panavia F 2.0, there is no MDP in the CE resin cement and there is a low amount of MDP and no water in the primer in order to extend the storage time of MDP. During priming process, through ethanol evaporation more concentrated MDP is left on ceramic surface to function with zirconia ceramic. In this study, for CE with pretreatment of CCP, the high initial TBS remained statistically stable over 150 days water storage with thermal cycling, and no significant difference was detected among the groups, in agreement with previous reports^{12, 42, 46}). It also confirms that a MDP-containing resin luting agent or an MDP-containing bonding/silane coupling agent mixture provided a strong resin bond to airborne-particle-abraded zirconia ceramic restorations¹²). In addition, the pretreatment of PLM and MZP also help CE to get durable bonding strength although there is debond between PLM and CE adhesive resin cement.

3.11 Summary and Outlook

Within the limitation of this study, priming pretreatment with primers can increase the bonding durability of three resin cements to airborne-particle abraded zirconia ceramic. MS containing only silane is important for the initial resin-ceramic bonding, but are not able to produce a strong durable resin-ceramic bonding.

The pretreatment with MDP or 4-META - containing primers make SB and CE to produce a durable bond to airborne-particle abraded zirconia ceramic. Due to the decomposition of CH resin cement, the bonding durability of CH without pretreatment and with pretreatment with MS and MZP are not testable due to the spontaneous debond during storage. However the pretreatment with PLM and CCP help CH produce a low bonding strength after long-term water storage and thermal cycling. Without surface priming pretreatment, only SB showed superior long-term bond strength to airborne-particle abraded zirconia ceramic. These conclusions can be supported by the combination of XPS, TBS and SEM results.

A strong durable resin-ceramic bonding can be achieved through surface pretreatments in strictly controlled clean *in vitro* tests. However, during clinical try-in procedures, the contaminations on luting surfaces of ceramic restorations by saliva, blood or silicone indicators cannot be avoided, which may lead to a significantly reduced bond strength in clinical situations. The influences of contaminations on resin bonding durability of zirconia ceramic are not reported until now. Therefore, in order to promise a strong durable resin-ceramic bonding durability in clinical situations approaching to the

result achieved in labor study, it is required to further investigate the influences of contaminations and cleaning methods on resin-ceramic bonding durability.

3.10 Author's Related Publications

[1] Effect of surface pretreatment on durability of resin-based cements bonded to zirconia ceramic. Bin Yang, Michael Scharnberg, Rainer Adelung, Matthias Kern. [In preparation].

4 Influence of contaminations on resin bonding durability to zirconia ceramic

4.1 Introduction

A strong, durable resin-ceramic bonding provides all-ceramic restorations with high retention, improved marginal adaptation and increased fracture resistance of the restored teeth and the restorations, although conventional cements can also be used for luting zirconia ceramic restorations in most cases ¹²⁾. Especially, 10-MDP - containing composite resins showed a long-term durable bond to zirconia ceramic after airborne particle abrasion ^{12, 32, 41)}.

However, a strong resin-ceramic bonding achieved in strictly controlled clean *in vitro* tests might be compromised in clinical situations, leading to significantly reduced bond strength. During clinical try-in procedures contaminations of restorative luting surfaces by saliva, blood or silicone indicators cannot be avoided ⁶³⁾. Saliva contamination is frequently one main reason for a reduced resin bond strength ⁶³⁻⁶⁷⁾. In dental textbooks, organic solutions are recommended for removing saliva contamination on luting surfaces of restorations before cementation ⁶⁸⁾. In the instructions of modern adhesive composite resins, phosphoric acid gel is sometimes recommended to remove contaminants.

Due to chemical stability of set silicone, it is believed that a clean, residue-free fitting surface remains after removal of a set silicone indicator film after try-in procedure (technical instructions of Fit checker, GC Co., Tokyo, Japan). However, the silicone disclosing procedure may leave one thin layer of residual unpolymerized organic film on the bonding surfaces of the restorations, leading to compromised resin bonding ^{7, 69, 70)}. Some investigators presumed that chemical reactions ^{7, 71)} and covalent bonds ⁷⁰⁾ might occur between silicone indicator films and restorations, leading to a stable adherence of silicone to bonding substrate and therefore reducing resin bonding.

MDP-containing composite resins, e.g. Panavia 21 and Panavia F, showed a long-term durable bond to airborne-particle abraded zirconia ceramic after water storage for 150 days ^{26, 33)} and 2 years ⁴¹⁾ with repeated thermal cycling. However, after saliva and silicone contaminations and different cleaning methods simulating clinical conditions the long-term bond to zirconia ceramic with Panavia F 2.0 was not stable ⁷²⁾. In this previous study, the presence of contaminants and the effectiveness of cleaning methods have not been identified with chemical analysis. Therefore in this

study, XPS, a highly surface sensitive technique for determining the chemical composition of multiphase compounds and for detecting surface contaminants ⁷³⁾, was used to identify the existence of saliva and silicone contamination on zirconia ceramic surface after try-in simulation. In addition, the influence of long-term water storage with thermal cycling on bonding durability of MDP-containing composite resins to ceramic after contamination and cleaning was investigated.

4.2 Study design and specimen preparation

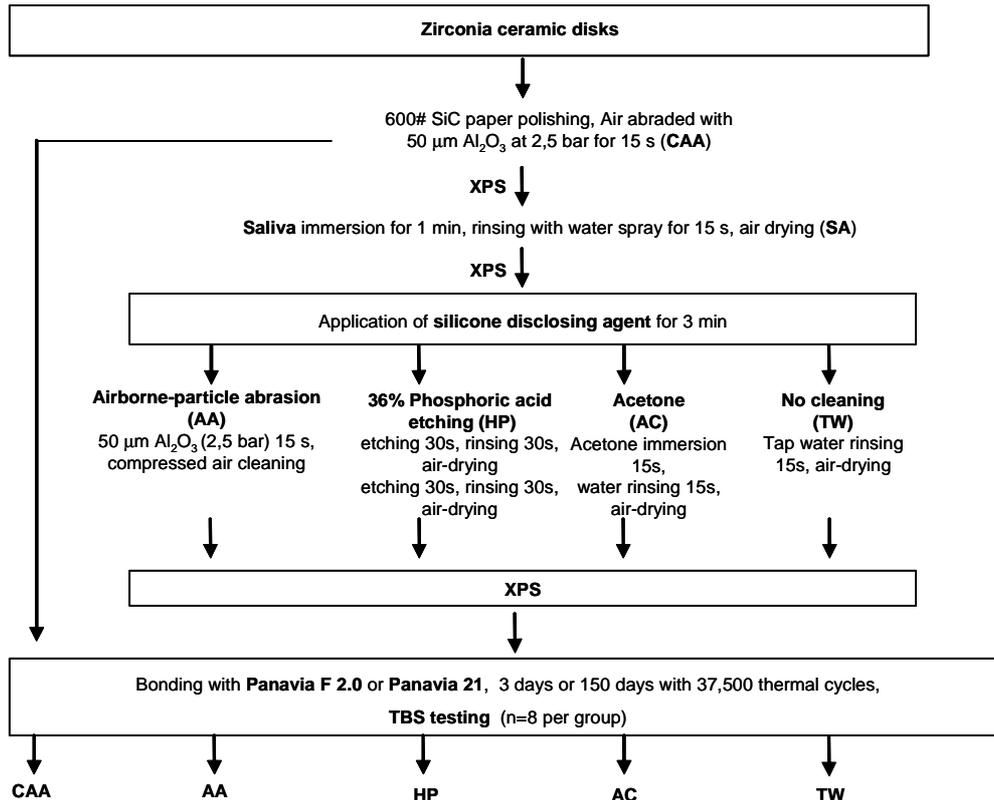


Figure 4.1 Study design for XPS examination and TBS testing

Densely-sintered partially-stabilized zirconia ceramic disk-like specimens (Cercon, DeguDent, Hanau, Germany) were used in this study (Fig. 4.1). The specimen surfaces were wet polished with 600 grit silicon carbide paper and then airborne-particle abraded with 50 μm Al_2O_3 at 2.5 bar pressure for 15 s at a distance of 10 mm. Afterwards the surfaces were air-cleaned for 20 s with the Rocatector delta device (3M ESPE, Seefeld, Germany). For XPS examination specimens were cleaned ultrasonically in distilled water bath for 10 min. Then, the cleaned specimens were immersed in saliva for 1 min. Saliva was collected from one healthy female donor who had refrained from eating and drinking 1.5 h prior to the collection procedure, which was approved by ethics committee of Christian-Albrechts University at Kiel. All experiments were performed using fresh saliva collected at the same occasion. After

saliva immersion, the specimens were rinsed with tap water for 15 s and air-dried for 15 s. Then the specimens were pressed into the freshly mixed silicone indicator (Fit Checker black, GC Corporation, Tokyo, Japan) with finger pressure for 3 min. For XPS examination and TBS testing, the specimens were classified into five test groups, i.e. using four cleaning methods generally available in dental offices and one control group (Fig. 4.1):

(AC) immersed in acetone for 15 s and then rinsed with tap water for 15 s;

(HP) etched with 36% phosphoric acid gel (Conditioner 36, Dentsply DeTrey, Constance, Germany) for 30 s two times and then rinsed with tap water for 30 s;

(AA) airborne-particle abraded with 50 μm Al_2O_3 at 2.5 bars pressure for 15 s at a distance of 10 mm and then cleaned with compressed air;

(TW) rinsed only with tap water;

(CAA) clean airborne-particle abraded specimens without contaminations as control group.

4.3 XPS examination

Specimens of the above test groups and additionally only saliva-immersed specimens (SA) were examined with XPS (Vacuum Generators, England) to identify the contaminations chemically and to evaluate the effectiveness of the cleaning methods (Fig. 4.1). All measurements were done using a XPS with an x-ray source providing Al $K\alpha$ x-rays. A pass energy setting of 100 eV allowed adequate quantitative analysis enabling high resolution scans of the carbon (C1s), oxygen (O1s), zirconium (Zr3-d) and silicon (Si2p) peaks.

4.4 Tensile bond strength (TBS) testing

Composite resin filled plexiglas tubes were bonded with Panavia F 2.0 (PF 2.0) or Panavia 21 (P21) (Kuraray, Osaka, Japan) to the zirconia ceramic specimens using an alignment apparatus⁷⁵⁾ under a load of 750 g according to the manufacturer's instructions. The specimens bonded with PF 2.0 were light-cured for 20 s from two opposite sides with a dental curing light (Optilux 500, Kerr, Danbury, USA), and the specimens bonded with P21 were placed into 37 °C in cubator for 20 min. Then the bonded specimens were placed for 10 min at room temperature, and stored in 37 °C water for 3 days or 150 days with 37,500 thermal cycles from 5 °C and 55 °C. After the different storage conditions, tensile bond strength (TBS) was tested with a universal testing apparatus (Zwick Z010/TN2A, Germany) at a crosshead speed of 2

mm/min. Statistical analyses were performed using the Kruskal-Wallis test followed by multiple pair-wise comparisons of groups (Mann-Whitney-Test) at $\alpha = 5\%$.

4.5 SEM examination

A scanning electron microscope (SEM, XL 30 CP, Philips, Kassel, Germany) operating at 10 to 25 KV was used to observe the failure modes of the debonded ceramic specimens after tensile testing. Failure modes were classified into one of the following modes: A: Adhesive failure at ceramic surface; C: Cohesive failure in the luting composite resin (PF 2.0 or P21) or in the tube filling composite resin. Failure areas of each mode were calculated and expressed as a percentage of the total bonding surface area for each test group.

4.6 XPS results

Table 4.1 Mean ratios of carbon (C), oxygen (O) and silicon (Si) elements in experimental groups.

Groups	C/O	O/Zr	C/Zr	Si/Zr
After airborne-particle abrasion, no contamination (CAA)	0.3	7.1	2.3	0
Only after saliva immersion (SA)	1.6	16.4	25.5	0
Airborne-particle abrasion cleaning (AA)	0.2	8.1	1.8	0
Phosphoric acid cleaning ⁷⁴⁾	0.3	9.0	2.5	0.4
Acetone cleaning (AC)	2.0	15.8	30.9	0
Tap water cleaning (TW)	1.3	21.7	27.7	1.9

The peak intensity ratios of C/O, O/C and C/Zr in test groups are shown in Table 4.1. After saliva contamination, the C/Zr and O/Zr ratios drastically increased indicating that the ceramic surface was covered with an organic coating, mainly composed of carbon (C) and oxygen (O) compared to control group. However, after try-in simulation, Si was also found on the ceramic surface in addition to increased C/Zr and O/Zr ratios. After cleaning with phosphoric acid or airborne-particle abrasion, ratios for O/Zr and C/Zr were reduced, comparable to those of the uncontaminated control. However, the Si contamination on the surface was only partially removed after phosphoric acid cleaning, in contrast to the complete removal of Si by airborne-particle abrasion. After acetone cleaning, although the concentrations of C and O decreased compared to those of the only water cleaning, the amount of C and O at

the surface was still considerably higher than in the control group. However, Si seemed to be removed completely by acetone cleaning.

4.7 TBS results

Table 4.2 Tensile bond strength to zirconia ceramic after contamination and different cleaning methods. Means, standard deviations (SD) and medians in MPa (n = 8) of experimental groups: CAA (after airborne-particle abrasion, no contamination), AA (airborne-particle abrasion cleaning), HP (phosphoric acid cleaning), AC (acetone cleaning), TW (tap water cleaning).

Groups	Panavia F 2.0				Panavia 21			
	3-d		150-d / 37,500TC		3-d		150-d / 37,500TC	
	Means (SD)	Medians	Means (SD)	Medians	Means (SD)	Medians	Means (SD)	Medians
CAA	44.7 (8.1)	47.0 ^A _α	38.3 (13.6)	41.9 ^A _α	40.4 (19.2)	38.6 ^A _α	38.3 (12.0)	39.0 ^A _α
AA	40.4 (3.6)	40.6 ^A _α	35.3 (9.2)	35.2 ^A _α	36.0 (24.2)	35.9 ^A _α	38.0 (25.3)	39.5 ^A _α
HP	33.6 (5.5)	33.5 ^B _α	7.1 (23.5)	6.8 ^B _γ	34.1 (3.4)	34.7 ^A _α	20.4 (7.6)	18.0 ^B _β
AC	13.1 (21.0)	12.7 ^C _α	0 *	0 * ^C _β	10.1 (2.9)	10.9 ^B _α	0 *	0 * ^C _β
TW	11.6 (26.5)	11.6 ^C _α	0 *	0 * ^C _β	10.6 (2.0)	10.8 ^B _α	0 *	0 * ^C _β

* All specimens in this group debonded spontaneously during water storage with thermal cycling. TC = thermal cycles. Within the same column, medians with the same superscript letter are not statistically different ($p > 0.05$). Within the same row, medians with the same Greek subscript letter are not statistically different ($p > 0.05$).

Medians, means and standard deviations of TBS in MPa of the tested groups are shown in Table 4.2. For both adhesive resins, water cleaning showed significantly lower initial TBS than the control ($p \leq 0.01$), and during storage with thermal cycling all specimens debonded spontaneously. For both adhesive resins, cleaning with airborne-particle abrasion resulted in relatively high initial TBS, which remained statistically stable over 150 days water storage with thermal cycling compared to the control. Acetone cleaning did not increase TBS significantly for both adhesive resins as compared to only water cleaning ($p > 0.05$). For most test conditions there was no statistical difference of TBS between the adhesive resins PF 2.0 and P21 ($p > 0.05$). For both adhesive resins, initial TBS after phosphoric acid cleaning were statistically

higher than after water or acetone cleaning ($p \leq 0.05$), but statistically lower than after air-abrasion or in the control group ($p \leq 0.05$). After 150 days with thermal cycling TBS decreased statistically for both adhesive resins, but TBS of P21 was statistically higher than TBS of PF 2.0.

4.8 SEM observation and fractographic analysis

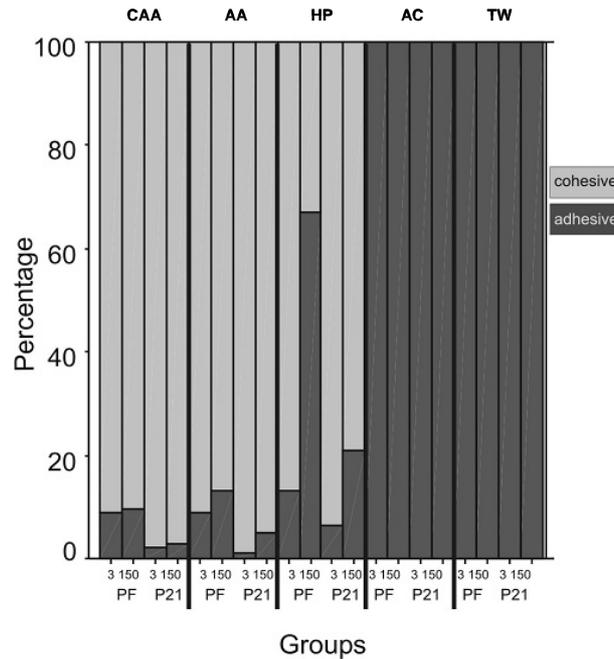


Figure 4.2 Percentages of areas assigned to the failure modes observed in test groups after tensile bond strength testing. A: Adhesive failure at ceramic surface; C: Cohesive failure in luting composite resins (Panavia F 2.0 or Panavia 21) or tube filling composite resin. Mean (SD) percentage of adhesive failure after 3 days and 150 days are: for PF 2.0, CAA (after airborne-particle abrasion, no contamination): 9% (2%), 9.4% (0.5%); AA (airborne-particle abrasion cleaning): 9% (1%), 87% (3%); HP (phosphoric acid cleaning): 87% (4%), 33% (6%); AC (acetone cleaning): 100% (0%), 100% (0%); TW (tap water cleaning): 100% (0%), 100% (0%). For P21, CAA: 2% (0%), 3% (0.2%); AA: 1% (0%), 5% (1%); HP: 6.5% (1%), 79% (2%); AC: 100% (0%), 100% (0%); TW: 100% (0%), 100% (0%).

Mean percentages of areas assigned to the failure modes observed in the bonding groups after tensile bond strength testing are shown in Fig. 4.2.

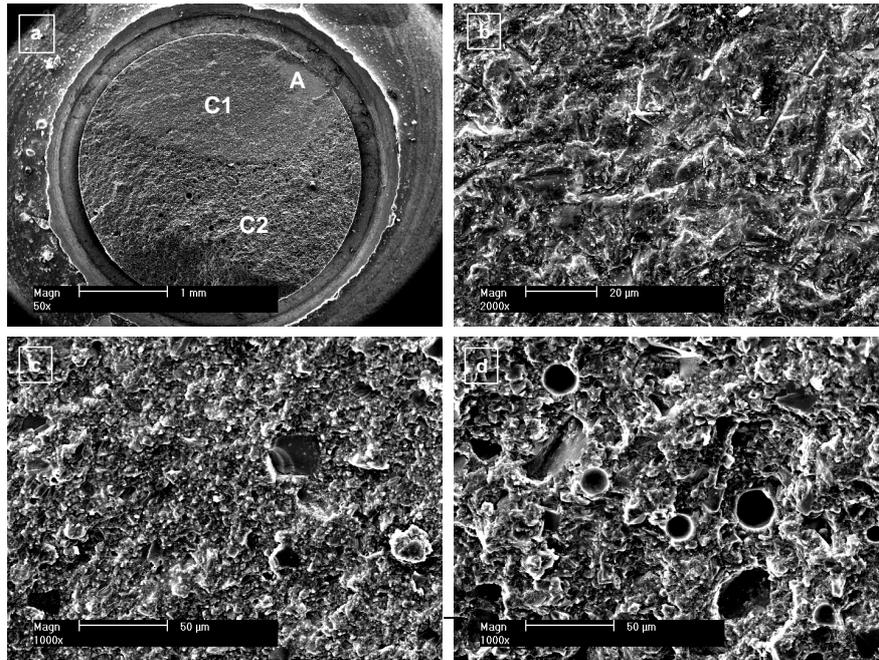


Figure 4.3 (a) Low magnification SEM micrograph showing representative mixed failure modes mostly with cohesive failure in groups CAA and AA; (b) High magnification SEM micrograph of A in (a) showing adhesive failure at the zirconia ceramic surface; (c) C1 in (b) showing cohesive failure in composite resins (Panavia F 2.0 or Panavia 21); (d) C2 in (b) showing cohesive failure in tube filling composite resin (Clearfil FII).

In the control group and after cleaning with air-abrasion (Figure 4.3), failures were found to be mostly cohesive in the luting composite resins (PF 2.0 or P21) (Figure 4.3 c) or in the tube filling composite resin (Clearfil FII) (Figure 4.3 d).

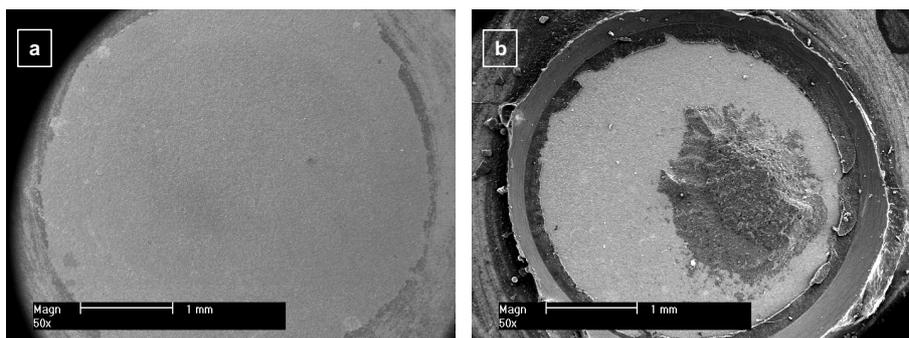


Figure 4.4 (a) Low magnification SEM micrograph showing representative adhesive failure mode in group AC and TW. (b) Low magnification SEM micrograph showing representative cohesive failure mode in group HP.

In contrast, after Acetone or water cleaning the failure mode was completely adhesive at the zirconia ceramic surface without any composite resin residue (Fig. 4.4 a). After phosphoric acid cleaning, the failure mode was mostly cohesive for both

adhesive resins with a high initial TBS. However, after 150 days, for group PF 2.0 there was a significant increase of adhesive failure area accompanied with lower TBS than that of group P21, while the cohesive failure portion in the PF 2.0 adhesive resin increased (Fig. 4.4 b).

4.9 Influence of contamination on zirconia ceramic bonding.

Factors influencing resin bonding to zirconia ceramic include the wettability of ceramic by adhesive resins, the roughness of ceramic surface, the composition of adhesive resins, the handling performance of adhesive resins and possible contaminations during bonding procedures. After saliva immersion, salivary proteins adsorption occurs not only to the tooth surface ⁷⁶⁾, but also on the restorative materials ^{77, 78)}. In this study, the hydrophilic ceramic surface showed a roughed “activated” surface after airborne-particle abrasion ⁷⁵⁾. Non-covalent adsorption of salivary proteins easily occurred on this surface during saliva immersion, which could not be removed by water rinsing as showed by XPS.

Silicone contamination is a well-known problem in material science. The main component of silicone disclosing agent is poly(dimethylsiloxane) containing a Si-O backbone. Organic groups (CH₃) can attach via Si-C bonds to this backbone, which may occur during contaminations in bonding applications. In this study, the presence of Si on ceramic surfaces after try-in simulation proved silicone residue on ceramic surface after the bulk silicone indicator was peeled off ceramic surfaces.

Our TBS results show that for both MDP-containing adhesive resins it was impossible to achieve a stable bond to ceramic after try-in simulation, while a long-term stable bond to clean zirconia ceramic was achieved in the uncontaminated control group confirming previous results ^{32, 33, 41)}. XPS generally detects photoelectrons approximately 2 - 10 nm at the top specimen surfaces ⁷⁹⁾. Therefore, there was an ultra-thin layer (less than 10 nm) of salivary and silicone contaminants covering the ceramic surface since Zr signal originating from the ceramic substrate was still detectable.

Among the tested cleaning methods, airborne-particle abrasion was the most effective method to remove contaminants, as shown by XPS and TBS results. These results further confirm that airborne-particle abrasion not only removed contaminants from ceramic surface ^{35, 80)}, but also exposed a fresh bonding surface by mechanical removal of superficial ceramic, contributing to a strong durable ceramic bonding with MDP-containing composite resins.

In a recent study ⁷²⁾ after saliva immersion and application of silicone disclosing medium, TBS after etching with phosphoric acid (36%) for 30 s two times was

statistically higher than that after etching with phosphoric acid for 60s one time only. Therefore, etching with phosphoric acid two times was used in this study. As shown by XPS, phosphoric acid cleaning seems to be an effective method to remove salivary contamination as airborne-particle abrasion (Table 4.1). However, this cleaning obviously did not completely remove silicone residue from ceramic surface, indicated by the decreased long-term TBS for both adhesive resins (Table 4.2). In addition, the phosphoric acid and water spray might decrease the surface energy of activated ceramic surface, leading to reduced TBS.

Generally the activated ceramic surface is sensitive to the environment and will partially lose its wettability because of air contamination ⁸¹⁾. Airborne-particle abrasion produced an activated rough ceramic surface, which might have made complete air-drying difficult, probably leading to the moisture contamination of the ceramic surface during water rinsing.

Regarding the composition of P21 and PF 2.0, although the basic components are similar, PF 2.0 contains additional photo-initiators and a fluoride compound. The matrix monomer of PF 2.0 has been modified to maintain its mechanical properties after releasing fluoride ions (personal communication with Dr. Kazumitsu Nakatsuka, Kuraray, Osaka, Japan). However, in this study, after phosphoric acid cleaning long-term TBS of PF 2.0, was significantly lower than that of P21. These results indicate that PF 2.0 is probably not as stable as P21, or the photo-initiators in PF 2.0 might be more sensitive to moisture resulting from water spray than the chemical initiators in P21, agreeing with one recent report ⁸²⁾.

Acetone cleaning seems to be effective to remove silicone contamination, but was not effective to remove salivary contaminants as shown by XPS results and low TBS (Tables 4.1 and 4.2). This fact indicates that TBS might be more affected by C and O remains from saliva than Si remains, which were greatly influenced by different cleaning methods. The combination of chemical identification with XPS and long-term TBS is an effective method to determine the effects of contaminations and cleaning methods on zirconia ceramic bonding.

4.10 Summary and Outlook

To remove the contaminations prior to bonding ceramics is very important to realize a long-term durable resin bond clinically. This study tested if there are contaminations on the zirconia ceramic surface left after try-in simulation, and if there are influences of contamination and cleaning methods on zirconia ceramic bonding durability with 10-methacryloyloxy-decyl dihydrogenphosphate-containing composite resins. After saliva immersion and using a silicone disclosing agent, airborne-particle

abraded ceramic specimens were cleaned with acetone, 36% phosphoric acid, additional airborne-particle abrasion, or only water spray. Chemical analyses of specimen surfaces were done using x-ray photoelectron spectroscopy. The influences of contamination and cleaning methods on ceramic bond durability were examined by tensile testing after 3 days or 150 days water storage with 37,500 thermal cycles. Contamination, existing after try-in simulation as confirmed by chemical analysis, significantly reduced zirconia ceramic-resin bonds. Airborne-particle abrasion may be the most effective cleaning method.

However mechanical treatments of zirconia might be done with caution because sandblasting, and grinding may negatively influence its mechanical properties of ceramics. It was supposed that the effect on the fracture resistance of zirconia depended on the time the specimens were subjected to sandblasting. This is probably because sandblasting treatment and/or grinding can induce compressive stresses and/or phase transformation on the surface, which increases the strength; at the same time, they also induce flaws and other defects which induce the strength. Therefore, to find the best possible technique of improving bonding durability, more studies are needed to determine the effects of surface treatment on the bond strength and mechanical properties of zirconia ceramics.

4.11 Author's Related Publications

- [1]. Bin Yang, Michael Scharnberg, Stefan Wolfart, Klaus Ludwig, Rainer Adlung, Matthias Kern. Influence of contamination on zirconia ceramic bonding. *J Dent Res* 2007;86:749-753,
- [2]. Bin Yang, Michael Scharnberg, Stefan Wolfart, Anna C. Quaas, Klaus Ludwig, Rainer Adlung, Matthias Kern. Influence of contamination on bonding to zirconia ceramic. *J Biomed Mater Res B Appl Biomater.* 2007;81:283-90
- [3]. Bin Yang, H. C. Lange-Jansen, Michael Scharnberg, Stefan Wolfart, Klaus Ludwig, Rainer Adlung, Matthias Kern. Influence of saliva contamination on zirconia ceramic bonding. *Dent mater* 2008;24:508-13

Part II. Adhesion of adhesive resin cements to human dentin

5 Background introduction

5.1 Dentin-resin bonding

Adhesive resins are increasingly used for luting all-ceramic, metal or composite indirect restorations due to advantages such as excellent mechanical properties, better bond strengths and improved aesthetics when compared to conventional cements⁸³⁾. However, compared to the bonding of new composite adhesive resins to conditioned indirect restorations, dentin bonding of adhesive resins still remains problematic, such as lower bonding strength and possible post-operative sensitivity⁸⁴⁾. With the growing understanding of dentin and its smear layer, it is now recognized that the smear layer should be removed or modified and the underlying dentin should be demineralized to produce a two-dimensional collagen network which could be infiltrated by adhesive resin monomers^{85, 86)}. Then, during polymerization, a hybrid layer (HL) is formed and an effective bond and seal between the restorations and dentin might be formed.

Dentin is a hydrated composite material composed of the collagen-based organic matrix and mineral reinforcement, varying with the anatomical location⁸⁷⁾. The structural anisotropy in regional dentin responds differently to etching and priming or self-etching priming during dentin bonding procedures, and consequently, the conditioned collagen fibrils show a varying permeability to adhesive resins and varying bond strengths⁸⁸⁾. In general, bond strengths are higher in superficial dentin than in deep dentin^{89, 90)}. Burrow⁹¹⁾ investigated the relation between dentin depth and bonding agents with an acid pretreatment system and suggested that the bond strength was more related to the quality of the HL than to the dentin depth. However, self-etching primers may yield different results⁹²⁾. The infiltration into cervical dentin plays an important role in sealing the restorations under clinical conditions. However, the bonding to cervical dentin was less predictable due to the oblique orientation of the dentin tubules⁹³⁾ and the relatively low density of the tubules⁹⁴⁾.

In 1982 Nakabayashi proposed that the mechanism responsible for resin adhesion to dentin involved creation of a HL resulting from infiltration of 4-META/MMA-TBB resin into acid-etched dentin⁹⁵⁾. In order to simplify

application procedures, and to prevent the collapse of the collagen fibril network of demineralized dentin, and to avoid wet bonding variables, two-step self-etching primer systems have been developed in recent years. However, the literature has reported conflicting results on bond strengths of self-etching systems to dentin⁹⁶). Some recent studies suggested that combining the primer and adhesive resins into a single application step might reduce the quality of hybridization of dentin^{97, 98}). Little information is available about the bond strength of self-etching adhesive resins to different regions of dentin and their bonding mechanism. Previous studies reported that the regional location could influence the tensile-bond strength of resin bonding agents to dentin⁹⁰⁻⁹²). However, few investigations are available about the bonding durability of adhesive resins to regional dentin.

An ideal adhesive resin would provide a long-term reliable bond to the indirect restoration and tooth structure. However, dentin bonding strengths seem to decrease over time although initial tensile bond strengths are rather high⁸⁶). Therefore, understanding the degradation mechanism of dentin bonding is of significant importance for improving the long-term dentin bonding of adhesive resins, which influences the reinforcement of brittle restorations and so the longevity of bonded restorations^{12, 84}).

The hybrid layer is the result of molecular-level intertwining of the resin within the demineralized dentin collagen fibril network⁸⁶). The structural intactness and mechanical properties of collagen fibrils play an important role in the determination of bond strength and its durability^{86, 99}). Human dentin collagen fibrils are mostly composed of type I collagen molecules in hierarchical synthesis. The characteristic organization of collagen molecules on the surface of fibrils results in periodicity banding of about 67 nm along collagen fibrils^{100, 101}). The presence of periodicity banding could be thought as the intactness of the tertiary structure of collagen fibrils^{102, 103}). However, the natural intact collagen fibrils might lose their original structure and become denatured because of the cutting preparation, demineralization conditions and eventual hydrolysis or enzyme degradation (bacterial enzymes or host-derived matrix metalloproteinases) over time¹⁰⁴). This structural alteration of collagen fibrils will decrease their mechanical properties and impair the durability of dentin bond strength⁸⁶). Up to now, no information has been published on the effect of structural changes of the collagen fibrils on the durability of adhesive resin-dentin bonding.

Atomic force microscope (AFM) has been widely used to observe microstructural changes of dentin etched with acidic solutions^{87, 105-107}). Compared to

SEM and TEM, AFM offers high-resolution 3-D images of various dentin states. The measurement of collagen fibrils by AFM has an accuracy of 10 nm¹⁰⁸⁾, with the advantages of little sample preparation or fixation and the potential to operate in air or solution^{105, 109)}. In the present study, tapping mode AFM was used to observe the structural changes of collagen fibrils in the intact dentin conditioned by acidic solution used in a total etching system and a self-etching primer used in a self-etching system.

Several in vitro investigations have recently attempted to evaluate the durability of resin-dentin bonds¹¹⁰⁻¹¹⁴⁾. However, artificial aging methods such as long-term water immersion of bonded specimens and thermal cycling are needed to be developed to evaluate the long-term degradation of bond strengths which is not seen when using water storage only for a short time.

6 Micro-tensile bond strength of three resin cements to human regional dentin

6.1 Introduction

Resin cements are increasingly used for luting all-ceramic, metal or composite indirect restorations due to their excellent mechanical properties, better bond strengths and improved aesthetics when compared to conventional cements⁸³⁾. After dental preparation, smear layer composed of dentin debris is left on the dentin surface. In dentin bonding, this smear layer should be removed or modified and the underlying dentin should be demineralised to expose collagen network and infiltrated by adhesive resin to form a hybrid layer (HL) at resin-dentin interface. Dentin is a hydrated composite material composed of the collagen-based organic matrix with mineral reinforcement, varying with anatomical location⁸⁷⁾. The structural anisotropy in regional dentin responds differently to etching and priming or self-etching primers/adhesives during dentin bonding procedures, and consequently, the conditioned dentin shows varying permeability to resin cements and hence, varying bond strengths⁸⁸⁾. In general, bond strengths are higher in superficial dentin than in deep dentin^{115, 116)}. Burrow⁹¹⁾ suggested that bond strength was more related to the quality of the HL than to the depth of dentin etching. However, resin bonding of the cervical margin was less predictable due to the oblique tubule orientation⁹³⁾ and the lower density of tubules than in deep dentin⁹⁴⁾.

In order to simplify application procedures, and to prevent the collapse of the collagen fibril network of demineralized dentin, two-step self-etching primer systems and one-step self-etching adhesive systems have been developed in recent years. However, the literature has reported conflicting results on bond strengths of self-etching systems to dentin⁹⁶⁾, and some recent studies suggested that combining the primer and adhesive resins into a single application step may reduce the quality of hybridization of dentin^{97, 98)}. Little information is available about the bond strength of self-etching resin cements to different regions of dentin and their bonding mechanism.

Recently, the micro-tensile bond strength test (μ TBS)^{117, 118)} has become popular for testing adhesion to dentin because this technique presumably provides better stress distribution at the adhesive interface due to the small bonding area with fewer defects than in standard tensile tests. Also, this technique can be used to detect regional difference in resin-dentin bond

strengths due to its use of small bonding areas ¹¹⁶⁾. The aim of the present study was to evaluate SEM and TEM ultrastructures and μ TBS of three resin cements used in their self-curing modes to different regions of dentin.

6.2 Tooth preparation

Intact caries-free human molars extracted from individuals 18-45 yrs old were stored in 0.5% chloramine T solution for two weeks, then in distilled water at 4°C prior to preparation. The teeth were used within three months after extraction. In this study, the age difference among the collected teeth was ignored since a previous study showed that age did not greatly influence the dentin bond strength ⁹¹⁾. Dentin disks (about 1.5 mm thick) were prepared by cutting occlusal enamel and dentin perpendicular to the tooth axis 1 mm below the dentino-enamel junction ¹¹⁹⁾ (s: superficial dentin), 1mm above the pulp horn (d: deep dentin), or parallel to the tooth axis, 0.5 mm above the cemento-enamel junction (CEJ) and 0.5 mm below the DEJ (c: cervical dentin) using a slow-speed saw with a diamond-coated disk (Isomet, Buehler, Lake Bluff, IL, USA) under water cooling (Fig. 6.1 a). From each molar, 2 to 4 superficial dentin disks and 2 cervical dentin disks, or 2 to 4 deep dentin disks could be obtained. Then dentin specimens were wet polished with 600 grit SiC paper and stored in distilled water at 4°C. The dentin specimens from each regional location were randomly divided into the test groups for bonding.

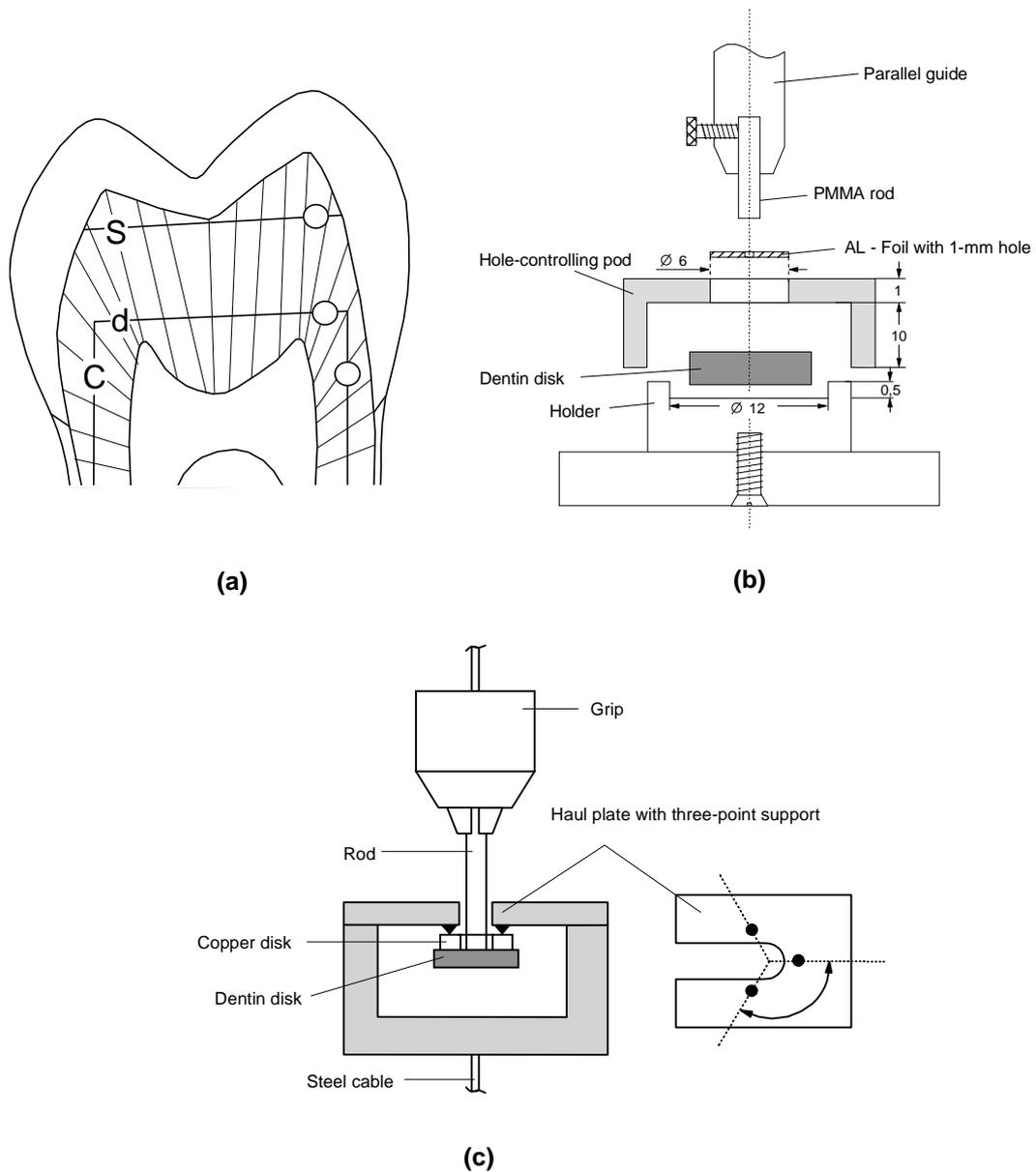


Figure 6.1 (a) Diagram of tested dentin location. s: superficial dentin (1 mm below DEJ); d: deep dentin (1 mm above the pulp horn); c: cervical dentin (0.5 mm below DEJ, 0.5 mm above CEJ); O: tested dentin location. (b) Alignment apparatus. A 10 μ m-thick aluminum foil with a 1-mm-diameter hole was attached to dentin surface. The hole was located at the centre of the bonding area using an alignment jig to control the shape and size of bonding area. (c) Schematic drawing of μ TBS testing. The rod was gripped by a pin-vice of universal testing machine, and then a haul plate with three point support was put on the dentin surface. The μ TBS was measured only by tensile force.

6.3 Micro-tensile bond strength (μ TBS) testing

Super-Bond C&B unfilled resin cement (SB; Sun Medical, Shiga, Japan), Panavia F 2.0 composite resin cement combined with ED self-etching primer 2.0 (PF; Kuraray Medical, Osaka, Japan), and RelyX Unicem self-etching adhesive resin cement (RU; 3M Espe AG, Seefeld, Germany) were used for bonding. The resin cements were used in the self-curing mode according to manufacturers' instructions (Table 6.1).

Table 6.1 Composition and application of the test resin cements (batch number in parenthesis).

Adhesive luting resin	Components	Etching	Priming	Bonding procedures	Storage condition
Super-Bond C&B (SB) Self-curing unfilled luting resin Sun Medical Co. Ltd., Shiga, Japan	Green activator (EM 1) Monomer (FG 2) Polymer L-type radiopaque (FE 2) CatalystS (EM 12)	Etch dentin with green activator for 10 s, rinse and air dry gently	Prewet dentin with 4META/MMA-TBB	Mix liquid and powder with brush-on technique. Apply to dentin surface. Bond the PMMA rod to dentin surface. Place the bonded specimen at room temperature for 6 min	24 h in 37 ° C water
Self-etching primer (PF) Kuraray Medical Inc., Osaka, Japan Panavia F 2.0 (PF) Two-step self-etching luting resin Kuraray Medical nc., Osaka, Japan	ED Primer 2.0 A (00161A) ED Primer 2.0 B (00044) A paste (0001A) B paste (00001A)	Treat dentin with self-etching ED primer 2.0 for 30s, air dry gently		Mix Panavia F 2.0, apply to the composite rod, then bonded to treated dentin. After removal of excess resin, Oxyguard II 2.0 applied to the luting margins. Placed into 37° C incubator for 20 min	24 h in 37 ° C water
RelyX Unicem (RU) One-step self-etching luting resin 3M ESPE AG Seefeld, Germany	Aplicap Self-adhesive universal resin cement (152009)	None	None	Mix RelyX Unicem, apply to the composite rod, then bond to dentin without treating dentin at room temperature for 30 min	72 h in 100% RH at 37 ° C *

* Recommended by 3M ESPE company, 72 h in 100% RH at 37 °C was used for the complete curing of RelyX Unicem resin cement in self-curing mode.

A 10 μ m-thick aluminum foil with a 1-mm-diameter hole was attached to each conditioned or non-conditioned dentin surface. The hole was located at the centre of the bonding area using an alignment jig (Fig. 6.1 b). In order to obtain a reliable bond between the handling rod with a diameter of 2 mm and resin cement, PMMA rods for SB or composite rods made of Clearfil FII composite resin (Kuraray Medical, Osaka, Japan) for PF and RU were bonded perpendicularly with the resin cements on the exposed dentin surface under a load of 7.5 N. After 37 °C water storage for 24 h (groups SB and PF) or 37 °C at 100% relative humidity (RH) for 72 h (group RU), μ TBS testing were performed with a universal testing machine (Zwick Z010/024, Zwick, Germany) at a cross-head speed of 1 mm/min. The PMMA or composite rods were gripped in a pin-vice (Fig. 6.1 c). Based on the resin cements and dentin regions, the test groups with 12

specimens each were classified into: SB-s, SB-d, SB-c; PF-s, PF-d, PF-c; RU-s, RU-d, RU-c. In each group, eight bonded specimens were used for μ TBS testing, and four specimens for TEM examination. The data of μ TBS of the three resin cements to regional dentin were statistically analyzed with a two-way ANOVA (materials vs. region) and Fisher's PLSD test at a confidence level of 95%. The failure mode results were compared for each luting material using the Mann-Whitney U-test.

6.4 SEM examination and Fractographic analysis

Dentin specimens acid-etched using SB green activator (10% citric acid with 3% ferric chloride: 10-3 solution) for 10 s or self-etching ED primer 2.0 for 30 s, were fixed with 2% glutaraldehyde in phosphate buffer for 8 hours, then dehydrated in an ascending ethanol series (50%, 60%, 70%, 80%, 90%, 96% and 100%) for 1 hour each. After the critical point drying procedure (K850 Critical Point Dryer, Emitech Ltd., UK), the specimens were gold-sputtered and examined by a scanning electron microscope (SEM, Philips XL 30 CP, Philips, Germany) operating at 10 to 25 KV.

After μ TBS testing, the debonded dentin specimens were air-dried for 24 hours, gold-sputtered and observed by SEM to evaluate the failure modes. Failure modes were classified into one of the following modes: A: Adhesive failure along dentin surface; B: Mixed failure: adhesive failure with a thin layer of resin cement remaining on the dentin surface; C: Cohesive failure in resin cement. The fractured area of each failure mode on the dentin surfaces was determined from the SEM micrographs with scale paper and expressed as a percentage of the total bonding surface area for each test group.

6.5 TEM examination

After 24 (SB and PF) or 72 h (RU) of water storage, bonded and debonded dentin specimens were immediately immersed into 2.5% glutaraldehyde in phosphate buffer solution for 4 hours. After fixation, the specimens were demineralized in 4% EDTA buffered to pH 7 for 7 days, postfixed with 1% osmium tetroxide for 2 hours, and then dehydrated in an ascending ethanol series (30%, 40%, 50%, 60%, 70%, 80%, 90%, 96% and 100%) twice in each solution for 10 min each time. Finally, the dehydrated specimens were embedded in pure epoxy resin (Araldite CY212, 13824, Serva, Germany) in a 60°C oven for 48 hours. Semithin sections of about 70 nm thick were prepared with an ultramicrotome (Reichert Ultracut E, Leica, Austria) and stained with saturated uranyl acetate for

10 min and lead citrate for 5 min, and examined with a transmission electron microscope (TEM 201, Phillips, The Netherlands).

6.6 μ TBS of the test groups to human regional dentin

Means and standard deviations of μ TBS of the various dentin regions of the three resin cements are shown in Table 6.2. Two-way ANOVA revealed that both tested factors (resin cement and regional location) and their interaction had significant influences on μ TBS. Fisher's PLSD multiple comparison tests further showed that for all three resin cements, the mean μ TBS to superficial dentin were significantly higher than those to deep or cervical dentin ($p \leq 0.05$). There were no significant differences in μ TBS between deep dentin and cervical dentin groups. The μ TBS of SB-s and PF-s groups were significantly higher than that of group RU-s ($p \leq 0.05$), whereas no difference was detected between SB-s and PF-s. In deep and cervical dentin the μ TBS of SB were significantly higher than those of PF and RU with the lowest μ TBS seen in group RU ($p \leq 0.01$). The μ TBS of specimens luted with RU were significantly lower in all regions than those of the other two resin cements ($p \leq 0.01$). No premature bond failures occurred during the μ TBS testing in any of groups.

Table 6.2 Micro-tensile bond strength (μ TBS) of the test groups to human regional dentin. Means (standard deviation) in MPa.

Groups	Super Bond C&B	Panavia F 2.0	RelyX Unicem
Superficial dentin	31.9 (7.2) ^A _a	29.1(8.4) ^A _a	8.2 (2.5) ^A _b
Deep dentin	18.6 (4.3) ^B _a	10.4 (1.9) ^B _b	5.7 (2.0) ^B _c
Cervical dentin	24.2 (6.5) ^B _a	10.2 (3.6) ^B _b	5.5 (2,0) ^B _c

Within the same column, means with the same upper case superscript letter are not statistically different ($p > 0.05$). Within the same row, means with the same lower case subscript letter are not statistically different ($p > 0.05$). Two-way ANOVA followed by Fisher's PLSD multiple comparison tests results at a confidence level of 95%. N=8.

The failure modes of the three resin cements during μ TBS testing are shown in Fig. 6.3. For group SB-s, failures were mostly cohesive (68%) in the resin cement. In deep and cervical dentin, most of the failures were observed to be adhesive failures along the dentin surface for SB-d (74%) and SB-c (45%). For groups PF, 46% of failures occurred cohesively in resin cement in superficial dentin while failures in deep dentin were mostly adhesive in nature (76%). In contrast, for groups RU, most of the failures to regional dentin were found to be adhesive failure along the dentin surface or partially adhesive failures with a thin layer of cohesively fractured resin cement. No adhesive failures were seen between PMMA rod-cement or composite rod-cement interfaces and no cohesive failures in the demineralized dentin under the HL were observed in any of μ TBS test specimens.

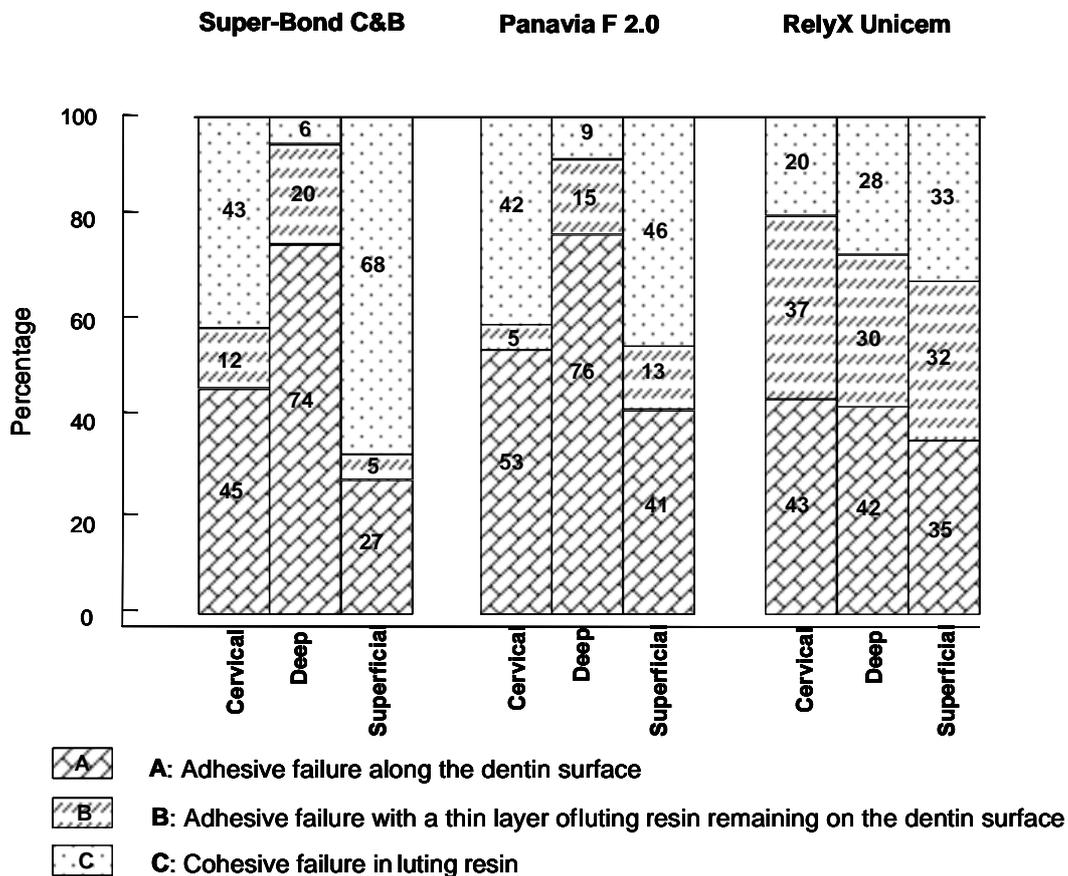


Figure 6.2 Failure modes of Super-Bond C&B, Panavia F 2.0 and RelyX Unicem to dentin regions during the tensile bonding strength test.

The SEM observations of the etched treated dentin in specimens from the SB and PF groups are shown in Fig. 6.3 a and b. After the dentin was etched with 10-3 solution⁴³⁾, the smear plugs appeared to be removed and the tubule orifices were completely exposed (Fig. 6.3 a). Some residual smear layer material was seen around tubule orifices. Circumferentially oriented collagen fibrils around the tubule wall were exposed. After the dentin was treated with self-etching ED primer 2.0 (Fig. 6.3 b), the smear layer appeared to be demineralized exposing collagen fibrils on the intertubular dentin surface. Some smear plugs were only partially removed leaving some smear debris in the tubules. Some peritubular dentin remained in PF specimens. The polished and untreated dentin used in the RU group was covered with a smear layer (Fig. 6.3 c).

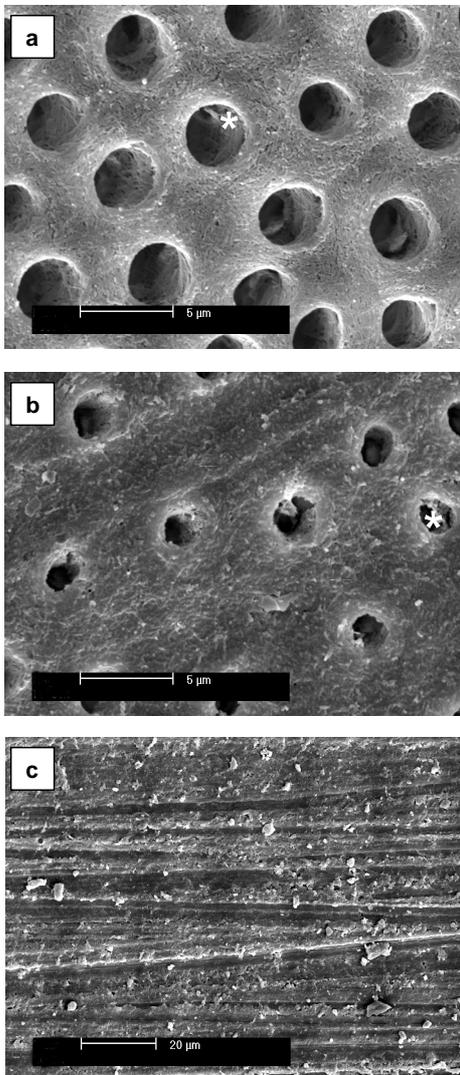


Figure 6.3 SEM micrographs of conditioned and unconditioned dentin surfaces, as the bonding substrates in the three groups. (a) SEM micrograph illustrating the dentin surface etched with 10% citric acid with 3% ferric chloride (group Super-Bond C&B). The smear plugs appeared to be removed and the tubule orifices were exposed completely by removal of peritubular dentin. Some residual smear layer material was seen around tubule orifices. The circumferentially oriented collagen fibrils (asterisk) around the tubular wall are exposed. (b) SEM micrograph illustrating the dentin surface treated with self-etching ED primer 2.0 (group Panavia F 2.0). The dentin surface exhibited demineralized collagen fibrils. The tubule orifices were exposed with some smear debris (asterisk) remaining in the tubules. (c) SEM micrograph of polished and unconditioned dentin surface covered by a smear layer (group RelyX Unicem).

Figures 6.4-6.6 present examples of the interface and fractured surfaces of dentin bonded with three resin cements using SEM and TEM. In group SB specimens, a HL with a width of approximately 4 μm was formed (Fig. 6.4 a) between the SB resin cement and superficial dentin. Adhesive failure occurred along the top of HL on deep dentin surfaces with cohesive failure within the resin tags (Figs. 6.4 b and c). The hybrid layer on the deep intertubular dentin surface extended into the tubule walls surrounding the resin tags, occluding the tubule openings (Fig. 6.4 d).

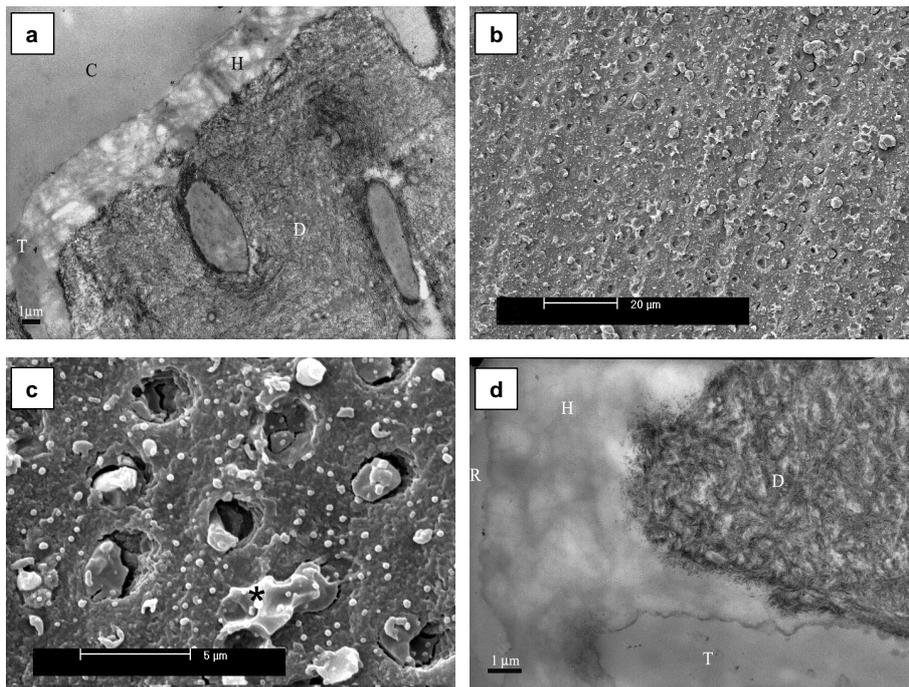


Figure 6.4 Interface and Fractographic analysis of group SB (Super-Bond C&B). (a) TEM photomicrograph at 3000 magnification illustrating an overview of the interface between SB resin cement and superficial dentin. The hybrid layer is approximately 4 μm thick. (b) SEM micrograph at 600 magnification of a debonded deep dentin specimen where adhesive failures occurred on the dentin surface. (c) SEM micrograph at 3600 magnification of the same specimen as in Fig. 4b. Adhesive failure occurred along the top of the hybrid layer and cohesive failures occurred in the resin tags (asterisk). (d) TEM micrograph at 6000 magnification of a resin tag in deep dentin. The hybrid layer on the intertubular dentin surface extended into the tubule walls surrounding the resin tag, occluding the tubule opening. C: Resin cement; H: Hybrid layer; T: Resin tag; D: Demineralized dentin in the preparation of TEM; R: Embedding resin.

In group PF specimens, the HL between PF resin cement and superficial dentin was approximately 1.5 - 2 μm thick, consisting of a 0.5 μm hybridized smear layer and a 1-1.5 μm thick authentic HL (Fig. 6.5 a). Adhesive failure was found at the top of HL on deep dentin with cohesively fractured resin tags occluding the tubules (Figs. 6.5 b and c). A tubule cut obliquely revealed the presence of a lining membrane within the tubule orifice (Fig. 6.5 d).

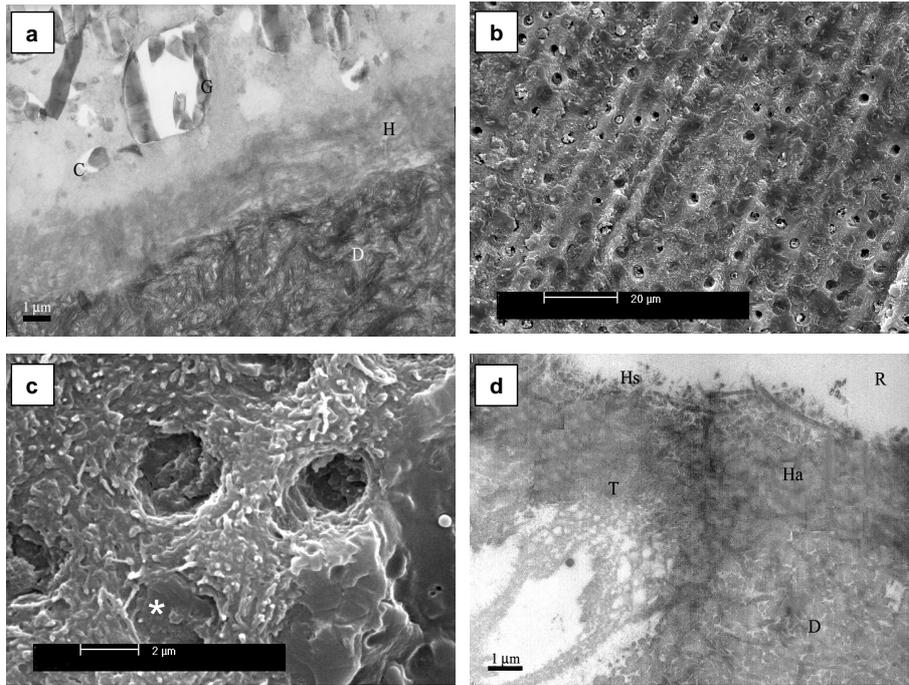


Figure 6.5 Interface and Fractographic analysis of group PF (Panavia F 2.0). (a) TEM photomicrograph at 4000 magnification illustrating an overview of the interface between PF resin cement and superficial dentin. The hybrid layer is approximately 1.5 - 2 μm thick. (b) SEM micrograph at 600 magnification of adhesive failure from the deep dentin surface. (c) SEM micrograph at 4500 magnification of the same specimen as in Fig. 5b. The failure occurred at the top of hybrid layer with cohesively fractured resin tags occluding the tubules (asterisk). (d) TEM photomicrograph at 5000 magnification illustrating the failure within the hybridized smear layer and smear plug in deep dentin. C: Resin cement; H: Hybrid layer; Ha: Authentic hybridized dentin; Hs: Hybridized smear layer; T: Resin tag; G: Glass filler particle; D: Demineralized dentin in the preparation of TEM; R: Embedding resin.

In group RU specimens, no obvious HL was observed (Fig. 6.6 a). Adhesive failure occurred at the top of demineralized deep dentin surface with cohesively fractured resin tags occluding the tubules (Figs. 6.6 b and c). Loose collagen fibrils on the dentin surface of an adhesively debonded cervical dentin specimen do not seem to be enveloped by the resin cement (Fig. 6.6 d).

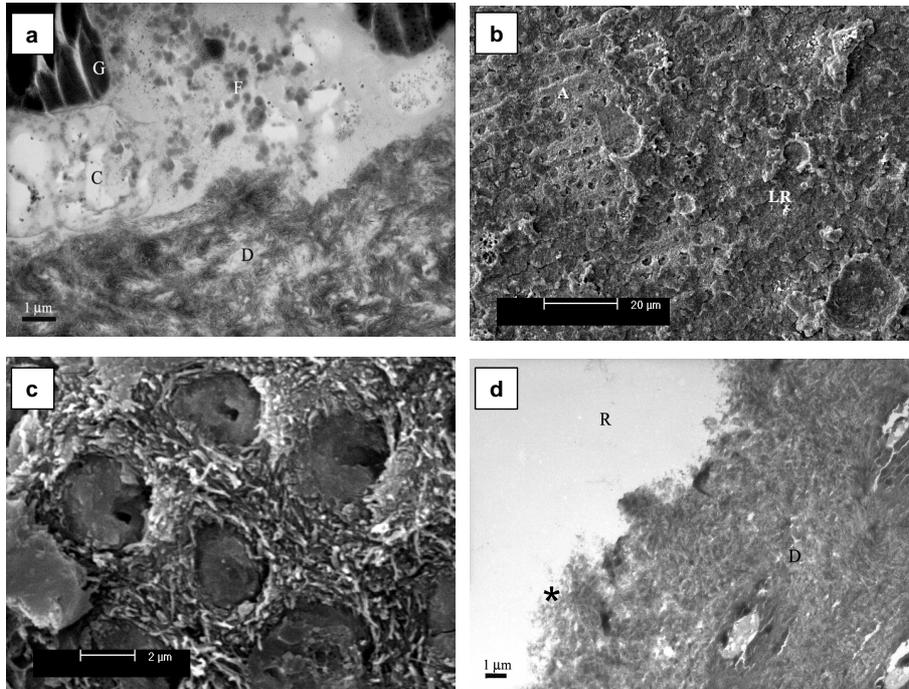


Figure 6.6 Interface and Fractographic analysis of a specimen in group RU (RelyX Unicem). (a) TEM photomicrograph at 5000 magnification illustrating an overview of the interface between RU resin cement and superficial dentin. The smear layer appears to be completely dissolved, but no obvious hybrid layer is observed. (b) SEM micrograph at 600 magnification of a debonded deep dentin specimen that adhesively failed at the top of dentin surface with a thin layer of resin cement ¹²⁰⁾ remaining on the dentin surface. (c) SEM micrograph at 4500 magnification of adhesive failure at “A” in the same specimen as in Fig. 6b. The loose collagen fibrils in the intertubular dentin do not seem to be adequately enveloped by resin cement. (d) TEM photomicrograph at 3000 magnification illustrating the adhesive failure from the demineralized cervical dentin surface. The collagen fibrils along the fractured surface appear to be stretched into loose microfibrils (asterisk) without resin infiltration. C: Resin cement; D: Demineralized dentin in the preparation of TEM; G: Glass filler particle; F: Nanofiller R: Embedding resin.

6.7 Micro-tensile bond strength of three resin cements to human regional dentin

In the present study, μ TBS to superficial dentin was significantly higher than those to deep dentin and cervical dentin for all resin cements, which is in good agreement with previous studies ¹¹⁶). In superficial dentin there is more intertubular dentin area rich in collagen fibrils than in deep and cervical dentin. Therefore, the μ TBS was significantly higher in superficial dentin due to the opportunity for more micromechanical adhesion to collagen fibrils in the HL ^{86, 88}).

For group PF-s, the mean μ TBS of 29.1 MPa and 46% of cohesive failure in resin cement also demonstrated that the bonded interface was stronger compared to the cohesive strength of the resin cement. This shows that the ED primer 2.0 successfully etched through the smear layer to partially demineralize the underlying dentin and improved the permeability of dentin to resin monomers (Fig. 6.5). Therefore, the smear layer and partially demineralized dentin could be incorporated into a hybridized complex by infiltration and polymerization of resin monomers. However, the top of the hybridized smear layer appears to be a potential weak link as the smear layer is weaker than sound dentin ⁸⁶), since there was a high percentage of adhesive failure at the top of HL (Fig. 6.5).

In the present study, the μ TBS of RU to different dentin regions was significantly lower than those of the other two resin cements, although its μ TBS to superficial dentin was statistically higher than to deep and cervical dentin. Theoretically, the acidic polymerizable methacrylate-based monomers in RelyX Unicem, a bis-GMA/TEDGMA based resin, typically have at least two phosphoric acid groups and a minimum of two C=C double bond units per molecule. With the presence of water, these monomers should demineralize the smear layer and the underlying dentin and simultaneously infiltrate the porous dentin surface due to their hydrophilic properties ¹²¹). However, TEM micrograph showed that no obvious HL was formed at resin-dentin bonding interface (Fig. 6). Resin infiltration is proportional to the applied concentration, viscosity of the solution, molecular weight or size, the affinity of monomers for the substrate and the time allowed for penetration ⁸⁸). RelyX Unicem is a heavily filled (72 wt% reactive glass fillers) (Technical Product Profile. 3M ESPE AG, Germany) and highly viscous resin cement. The smear layer and underlying dentin have been regarded as solid buffers that probably rapidly buffer the acidity of viscous solutions, thereby limiting the etching ability of acidic monomers (David H Pashley, personal communication). The inability of RU to penetrate demineralized dentin is supported by SEM observation of insufficient infiltration of resin into the collagen network (Fig. 6.6). Since the HL was very thin to nonexistent, the μ TBS of RU to regional dentin sites was relatively low, even in superficial dentin (Fig. 6.6 a).

Theoretically, in deep and cervical dentin the decreased amount of intertubular dentin available limits the contribution of the HL to the μ TBS, while the increased number and diameter of the tubules increases the cross-sectional area and volume of the resin tags. Therefore, the cohesive strength of the resin tags and the hybridization of resin tags to tubular walls play an important role in determining the bond strength in deep dentin ¹²². For specimens in the SB group, after the peritubular dentin was etched with 10-3 solution, the circumferentially oriented collagen fibrils that line the tubule walls were completely exposed (Fig. 6.3 a). This allowed adhesive resin to infiltrate into the adjacent intertubular dentin and form hybridized resin tags with many branches. Partially oxidized tri-N-butylborane (TBB), as the polymerization initiator in Super-Bond C&B resin cement system, utilizes oxygen and water to initiate radical polymerization of the resin monomers ¹²³. Therefore, when using SB for bonding to deep water-rich dentin, polymerization should be enhanced, at the interface of hydrated dentin with resin and continue outward into the resin cement. This moisture tolerance and interfacial polymerization of SB results in thorough polymerization and improvement of regional bond strength near the pulp ¹²⁴. This proposition is supported in the current study by the high μ TBS to deep and cervical dentin and TEM observation of the extension of hybridized resin tags into the tubules (Fig. 6.4). It might be concluded that well-hybridized resin tags contribute to the total micromechanical retention and bonding strength in dentin bonded with SB, especially in deep or cervical dentin ¹²².

However, this mechanism of adhesion might not be directly applied to self-etching systems. In the present study, the mean μ TBS of PF to deep dentin and cervical dentin were significantly lower than that of superficial dentin. It was discovered that ED primer 2.0 did not completely remove smear plugs (Fig. 6.3 b). Therefore, PF resin cement probably penetrated into the residual smear plug to the partially demineralized collagen network around the tubular walls to form a thin bonding interface (Fig. 6.5 d). However, this thin bonding of PF to the walls of tubules was strong enough to make the hybridized smear plugs and resin tags fracture at the tubule orifice during μ TBS testing instead of being pulled out from the tubules (Fig. 6.5 c). It can be concluded that the top of the hybridized smear layer became the weak link during μ TBS testing, supported the conclusions of others ^{125, 126}. In the current study, since PF cured in its self-curing mode, water may have time to diffuse from the tubules through the self-etching primed smear plugs to form water droplets at bonding interface between dentin surface and resin cement during the curing time. These water droplets might function as sites of stress concentration when specimens were stressed to failure.

Water is an important ingredient for self-etching systems to ionize the acid and dissolve the minerals of the smear layers and dental hard tissues. However, if any residual water is not sufficiently removed during the bonding procedures of self-etching systems, water

would compete with the monomers infiltrating into the demineralized zone to occupy the space on the demineralized collagen. Such an “overwet” condition might result in a dilution of the monomer concentration and interfering with the polymerization degree of the resin ¹²⁷). This is perhaps one reason for the lower μ TBS of the two self-etching systems to deep and cervical dentin than to superficial dentin.

Compared to groups SB and PF, a rather high percentage of partial adhesive failures that left a thin layer of cohesively fractured resin cement was found in all RU groups, indicating that the adhesion of resin cement to dentin was rather weak. The possible reason is that the self-curing polymerization of RU is not complete, although a prolonged storage time was used, which is supported by the low degree of conversion (26%) reported for self-cured RU ¹²⁸). Therefore, even if RU is a heavily filled composite resin, its strength is not high if it is not completely polymerised, which might be also one reason for the low μ TBS in groups RU.

6.8 Summary and Outlook

The aim of the present study was to evaluate the μ TBS of three resin cements used in their self-curing modes to different regions of dentin, and to investigate the resin-dentin bonding with SEM and TEM. ANOVA results showed that μ TBS to superficial dentin was significantly higher than to deep or cervical dentin for all three resin cements. For groups SB and PF, with the highest μ TBS to superficial dentin, failed primarily cohesively in resin cement. μ TBS of SB to deep and cervical dentin were significantly higher than those of PF and RU. RU, with the lowest regional μ TBS, failed mostly within demineralized dentin. SEM and TEM showed that adhesive failures in SB and PF occurred at the top of hybrid layer, but no obvious hybrid layer was observed in RU.

One possible reason for the lower μ TBS of the two self-etching systems (PF and RU) to deep and cervical dentin than to superficial dentin is that there is much more water in deep dentin and cervical dentin than superficial dentin. Water is an important ingredient for self-etching systems to ionize the acid and dissolve the minerals of the smear layers and dental hard tissues. However, if any residual water is not sufficiently removed during the bonding procedures of self-etching systems, water would compete with the monomers infiltrating into the demineralized zone to occupy the space on the demineralized collagen. Such an “overwet” condition might result in a dilution of the monomer concentration and interfering with the polymerization degree of PF and RU.

In contrast, the special polymerization initiator in Super-Bond C&B resin cement system, is able to utilize oxygen and water to initiate radical polymerization of the resin monomers. Therefore, when using SB for bonding to deep water-rich dentin, polymerization could be enhanced at the interface of hydrated dentin with resin and continuous outward into the

resin cement. This moisture tolerance and interfacial polymerization of SB results in thorough polymerization and improvement of regional bond strength near the pulp.

In conclusion, resin cements with different chemical formulations and application techniques yield morphologically different interfacial microstructures and regional dentin bond strengths.

Hybrid layer formation, the basic mechanism of resin-dentin bonding, is the result of molecular-level intertwining of resin within the demineralized dentin collagen fibril network. The structural integrity and mechanical properties of collagen fibrils play an important role in the determination of bond strength and its durability. However, natural collagen fibrils might lose their original structure and become denatured during cavity preparation and acidic conditioning. Such structural alterations of collagen fibrils will decrease the mechanical properties and impair the durability of resin-dentin bonds.

Several in vitro and in vivo investigations have recently attempted to evaluate the durability of resin-dentin bonds and recent studies have provided morphologic evidence of hydrolytic degradation or enzyme degradation of collagen fibrils over time. In these studies, one important fact that has not been properly reported is the structural intactness of the collagen fibrils during acidic conditioning. And what is the influence of structural changes of collagen fibrils on dentin bonding durability. Therefore, it is worth investigating if there is structural changes of collagen fibrils during acidic conditioning and after bonding, and how about the effect of structural changes of collagen fibrils in hybrid layer on the durability of dentin bonding.

6.9 Author's Related Publications

[1]. Bin Yang, Klaus Ludwig, Rainer Adlung, and Matthias Kern. Micro-tensile bond strength of the resin cements to human regional dentin. *Dental Materials*. 2006 ;22:45-56

7 Effect of structural change of collagen fibrils on the durability of dentin bonding

7.1 Introduction

Improving the bonding durability of resin cements to dentin is of significant importance for the reinforcement of brittle restorations and the longevity of bonded restorations in Prosthodontics¹²⁾. It is generally thought that hybrid layer (HL) formation, the basic mechanism of resin-dentin bonding, is the result of molecular-level intertwining of resin within the demineralized dentin collagen fibril network⁸⁶⁾. The structural integrity and mechanical properties of collagen fibrils play an important role in the determination of bond strength and its durability⁸⁶⁾. Human dentin collagen fibrils are mostly composed of type I collagen molecules in a hierarchical organization. The characteristic organization of collagen molecules on the surface of fibrils results in a periodicity in cross-banding of about 67 nm along collagen fibrils^{100, 101)}. The presence of period banding is thought to indicate the intactness of the tertiary structure of collagen fibrils^{102, 103)}. However, natural collagen fibrils might lose their original structure and become denatured during cavity preparation and acidic conditioning. Such structural alterations of collagen fibrils will decrease the mechanical properties and impair the durability of resin-dentin bonds⁸⁶⁾.

Acidic conditioners are used to demineralize the smear layer and the underlying intact dentin to create a microporous surface rich in collagen fibrils for the formation of the HL. Several studies demonstrated that the disorganized collagen fibrils in the smear layer denatured during the acidic treatment^{129, 130)}. However, there is some controversy regarding whether or not the collagen fibrils in intact dentin underlying the smear layer are denatured during acidic conditioning^{102, 103)}. Some studies reported that acids do not grossly denature collagen fibrils in the intact dentin^{103, 131)}, while EL Feninat et al.¹⁰²⁾ found that the characteristic periodicity of collagen fibrils was absent in dentin treated by 17% phosphoric acid. Self-etching adhesive systems that combine the conditioning and priming steps are thought to overcome the shortcomings of early total etch systems, such as incomplete infiltration of the demineralized dentin¹³²⁾. There is some concern that the self-etching primer might denature the dentin collagen fibrils during conditioning, further impairing the durability of bonds.

Several in vitro and in vivo investigations have recently attempted to evaluate the durability of resin-dentin bonds¹³³⁻¹³⁶⁾ and recent studies have provided morphologic

evidence of hydrolytic degradation or enzyme degradation (bacterial enzymes or host-derived matrix metalloproteinases)^{104, 137)} of collagen fibrils over time. In these studies, one important fact that has not been properly reported is the structural intactness of the collagen fibrils after acidic conditioning. Therefore, the first purpose of this study was to determine whether the intact collagen fibrils of the dentin surface underlying the smear layer will lose their structural integrity and denature at the molecular level during acidic conditioning. The second purpose was to investigate the effect of structural changes in collagen fibrils at the resin-dentin bonding interface on the durability of dentin bonding. In this study, one total etch resin cement system (Super-Bond C&B: SB) and one self-etching composite resin cement system (Panavia F 2.0: PF) were investigated. Thermal cycling as an aging model was used to accelerate the degradation of resin-dentin bonds in this study.

7.2 Tooth preparation

Tooth preparation is the same as tooth preparation in chapter 6 (see 6.2.)

7.3 Tapping mode AFM study

An atomic force microscope (AFM, AUTOPROBE CP, Thermo Microscopes, Sunnyvale, CA, USA) in tapping mode was used to observe demineralized intact collagen fibrils on intertubular dentin surfaces, treated by green activator (10% citric acid with 3% ferric chloride: 10-3 solution) or self-etching ED primer 2.0 (Table 1). The smear layer produced by 600 grit SiC paper was imaged by the AFM as a control group. To create a flat intact dentin surface without a smear layer, the dentin disk was sequentially wet ground on 600-, 800-, 1000-, 2000-, 2500-, 4000-grit SiC polishing paper, and ultrasonic cleaned in de-ionized water for 30 min.

Then the highly polished dentin disks were cut into two equal halves, and the halves were randomly divided into two test groups, to minimize the variability between different dentin disks. The test group specimens were then demineralized with 10-3 solution for 10 s⁴³⁾, rinsed and gently air-dried. Specimens treated with the self-etching ED primer 2.0 for 30 s (PF) were not rinsed but were gently air-dried. In order to reduce the influence of self-etching primer monomer on the AFM images, the conditioned specimens in the PF group were rinsed with 100% ethanol for 5 min to remove the ED primer monomer, and then soaked in distilled water for another 5 min to reverse the shrinkage effect of the ethanol on the collagen fibril network [17]. Then the conditioned dentin specimens from both SB and PF groups were further treated with an aqueous solution of 3 vol% sodium hypochlorite (NaOCl_{aq}) as deproteinizing agent for 100 to 120 s to remove non-collagenous proteins from the extracellular

organic matrix and reveal the collagen fibril network. In preliminary testing, 3 vol% NaOCl was found to be more effective at exposing collagen fibril periodicity than 6 vol% which was used in a previous study [5]. After extensive rinsing with water, the specimens were immediately observed with tapping-mode AFM in air with high-aspect-ratio non-contact ultralevers (ULNC-AUMT-AB, Thermo Microscopes, Sunnyvale, CA, USA) with a radius of approximately 10 nm, at a resonance frequency of 32.5 kHz. The scan rate was typically 0.5 Hz with a scan size of 1×1 μm and a resolution of 512×512 pixels per image. The measurements of cross-banding periodicity along the fibrils and their diameters were performed using section analysis software (Thermo Microscopes ProScan Software, Thermo Microscopes, Sunnyvale, CA, USA).

7.4 Micro-tensile bond strength (μTBS) testing

Two self-curing resin cements were used for bonding according to the manufacturers' instructions (see 6.3 in chapter 6). Briefly, after bonding, the specimens in the subgroups were stored in 37 °C water for 1 d, 90 d, or 90 d with additional 15,000 thermal cycles (TC) from 5 °C to 55 °C with dwell time of 30 sec. Thermal cycling was used in order to accelerate the degradation of resin-dentin bonds, as a form of artificial aging. The μTBS was measured after the different storage conditions with a universal testing machine (Zwick BZ 010/TNZA, Zwick, Ulm, Germany) at a cross-head speed of 1 mm/min (Fig. 1c). Based on the resin cements, dentin depth (superficial: s; or deep: d), and storage conditions, the following test groups with 12 specimens each were obtained: Super-Bond C&B: SB-s 1d, SB-d 1d; SB-s 90d, SB-d 90d.; SB-s 90d-TC, SB-d 90d-TC. Panavia F 2.0: PF-s 1d, PF-d 1d; PF-s 90d, PF-d 90d; PF-s 90d-TC, PF-d 90d-TC. In each group, eight bonded specimens were used for μTBS testing and SEM examination, and four specimens for TEM examination.

The μTBS of the two resin cements to superficial or deep dentin after different storage conditions were statistically analyzed using a three-way ANOVA (resin cement vs dentin depth vs storage condition) and Fisher's PLSD test at a confidence level of 95%.

7.5 SEM and TEM examination

The protocols of SEM and TEM preparations and examinations are the same as in chapter 6 (see 6.4 and 6.5).

7.6 Tapping mode AFM result

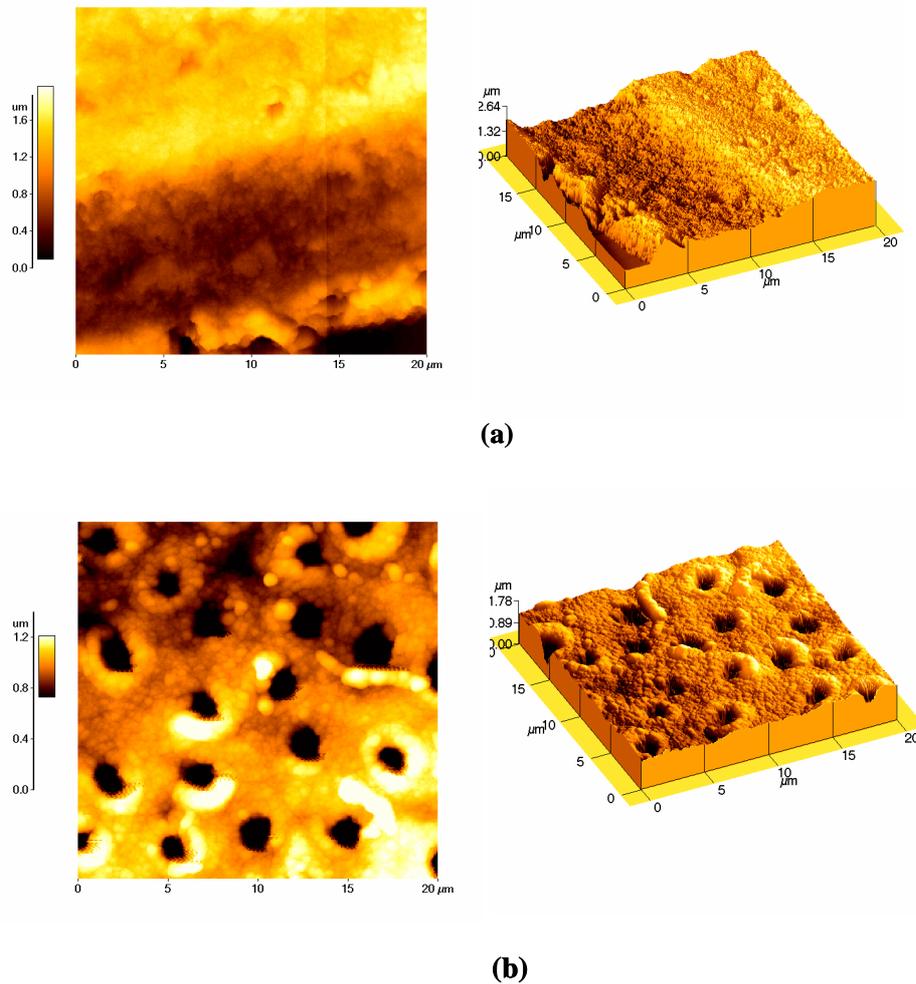


Figure 7.1 AFM images (flat and 3-d) of dentin surface polished by 600-grit SiC paper. (a) The dentin surface was covered with smear layer. (b) AFM image (flat and 3-d) of intact dentin surface polished by 4000-grit SiC paper. With the removal of smear layer and smear plugs, the tubules, the peritubular dentin and intact intertubular dentin were completely exposed.

After polishing with 600 grit SiC paper, the dentin surfaces were covered by a smear layer and the tubules were occluded by smear plugs (Fig. 7.1 a). Sequential polishing from 600 grit to 4000 grit abrasive paper and ultrasonic cleaning resulted in the complete exposure of tubule openings, peritubular dentin and intact intertubular dentin (Fig. 7.1 b), confirming the removal of the smear layer and smear plugs.

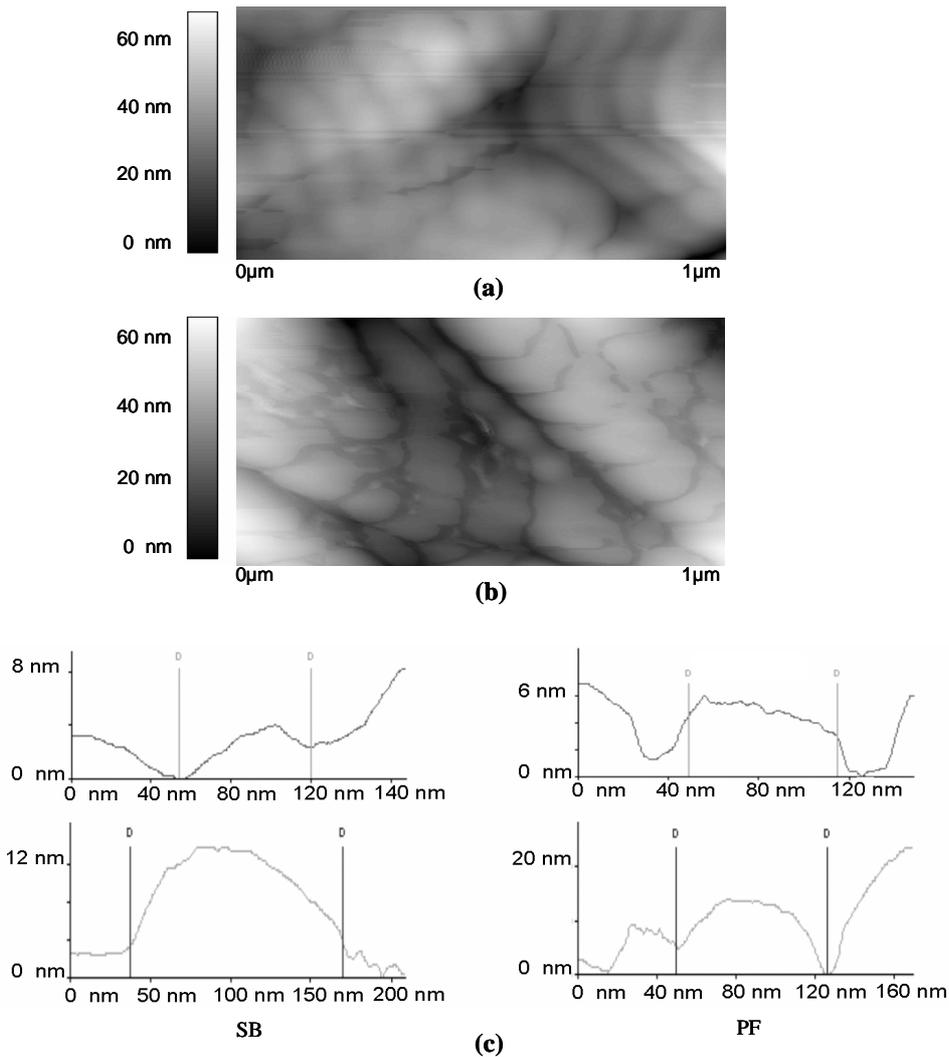


Figure 7.2 High magnification tapping mode AFM image of the dentin collagen fibrils on the intact intertubular dentin surface conditioned with 10% citric acid with 3% ferric chloride (10-3 solution) in group SB (a) or self-etching ED Primer 2.0 in group PF (b). (c) Section analysis revealed the collagen fibrils with an axial periodicity banding of about 67 nm and diameter of 90-120 nm.

Figure 7.2 shows $1 \times 1 \mu\text{m}$ tapping mode AFM images of collagen fibrils on the intact intertubular dentin (Figure 7.2) after acidic conditioning and bleaching with NaOCl. The specimens from both SB (Figure 7.2 a) and PF (Figure 7.2 b) groups, exhibited the characteristic axial periodicity banding of type I collagen fibrils. The gap zone and over gap zone on collagen fibrils were observed clearly. Section analyses along the axis of fibrils and across the fibrils exhibited the axial periodicity banding of about 67 nm and fibril diameters between 90-120 nm (Figure 7.2 c).

7.7 Structural change of intact collagen fibrils during acidic condition

In general, the periodicity of collagen fibrils can be observed using TEM. However, the length of the periodicity may change when demineralized dentin is dehydrated physically or chemically during processing for TEM¹⁰³⁾. Compared to TEM, AFM offers high resolution 3-D images of microstructural changes on etched dentin surface in various states^{103, 105, 108, 138)} with little sample preparation or fixation. The measurement of collagen fibrils by AFM has an accuracy of 10 nm¹⁰⁸⁾. In the present study, tapping mode AFM was used to avoid damaging collagen fibrils due to the adhesion and friction of a contact mode tip on the soft collagen fibril network¹³⁹⁾.

Initial attempts to image the periodicity of conditioned fibrils on 600-grit polished dentin surface were unsuccessful, confirming the need to remove surface contaminants with a highly polished process and a brief treatment with diluted NaOCl¹⁰³⁾. Presumably, the surface contaminants include residual denatured smear layer materials and non-collagenous proteins. Once the surface contaminants were removed, the structure of collagen fibrils on the intact intertubular dentin could be imaged by AFM. The period banding of about 67 nm along collagen fibrils and their diameters of 90-120 nm were revealed by high-magnification AFM observations of groups SB and PF (Fig. 7.2). This normal periodicity in the type I collagen fibrils indicates that the collagen fibrils did not lose their tertiary structure and were not denatured during short acidic conditionings in both groups SB and PF. This result is in good agreement with previous reports that collagen fibrils were known to resist swelling and solubilization in acids¹⁴⁰⁾. Therefore, the conditioned collagen fibrils kept their intact structure, which permits that the collagen fibril network within the HL to resist tensile loading¹⁴¹⁾.

After acidic conditioning, the exposed intact collagen fibrils were infiltrated by adhesive resin and polymerized in situ to form a hybrid layer. When the bonded interface is subjected to stress, it is thought that the load is simultaneously borne by both the resin and the collagen fibrils in a manner that is analogous to the mineral phase and collagen fibril matrix in the dentin as natural composite materials⁸⁶⁾. Previous studies^{86, 142)} reported that the micro-tensile strength of mineralized dentin was 106 MPa, and resin-infiltrated demineralized dentin had micro-tensile strength values of 103 to 122 MPa. This indicates that the resin-infiltrated collagen fibrils may be as strong as the original apatite-collagen compound, at least in tension over short time. In this study, few cohesive failures could be found in hybrid layer for either SB-1d or PF-1d groups, which also indicates that the weak link in the adhesive-hybrid layer-dentin substrate might not be the hybrid layer in the short-term.

7.8 Micro-tensile bond strength (μ TBS) testing

Table 7.1 Micro-tensile bond strength (μ TBS) of tested groups to human dentin after different storage condition (N=8). Means (standard deviations) in MPa.

Groups	Super-Bond C&B			Panavia F 2.0		
	1d	90d	90d-TC	1d	90d	90d-TC
Superficial dentin	31.9 (7.2) ^{A_α}	25.8 (9.7) ^{A_α}	13.1 (5.1) ^{A_β}	29.1(8.4) ^{A_α}	25.8 (8.8) ^{A_α}	16.3 (4.6) ^{A_β}
Deep dentin	18.6 (4.3) ^{B_α}	16.6 (5.1) ^{B_α}	8.0 (1.7) ^{B_β}	10.4 (1.9) ^{B_α}	7.3 (1.1) ^{B_β}	5.6 (1.7) ^{B_γ}

Mean μ TBS are presented in Table 7.1. Three-way ANOVA revealed that there were no significant interactions between the three factors 'resin cement', 'dentin depth' and 'storage condition' ($p = 0.743$). However, significant interactions on the μ TBS were detected between 'resin cement' and 'dentin depth' ($p = 0.005$), and between 'dentin depth' and 'storage condition' ($p = 0.017$). Therefore, two way ANOVAs were done for each resin cement separately. Although there is no significant interaction between 'location' and 'storage condition' for both resin cements, Fisher's PLSD multiple comparison tests further showed that for both resin cements, the μ TBS of superficial dentin was significantly higher than those of deep dentin at every storage condition. The μ TBS of groups 90 d-TC decreased significantly ($p < 0.05$) compared to groups 1 d and 90 d, while μ TBS of groups 1 d were not different from those of groups 90 d except for PF-d 90d. No premature bond failure occurred during specimen preparation for μ TBS testing and there were no cohesive failures in mineralized dentin.

Failure modes of the test groups are shown in Figure 7.3. For groups SB, a substantial percentage of cohesive failure in adhesive resin cement (failure mode C) occurred in groups 1d and 90d for superficial dentin and cervical dentin, while for deep dentin most of failures were found to be adhesive failure at the dentin surface (failure mode A). Cohesive failure in demineralized dentin under the HL (failure mode D) was not detected in groups 1d, but appeared in a low percentage in groups 90d. In contrast, there was an increase of partial adhesive failure with a thin layer of adhesive resin cement remaining on the dentin surface (failure modes B) in groups 90d-TC for each regional location.

7.9 SEM and TEM results

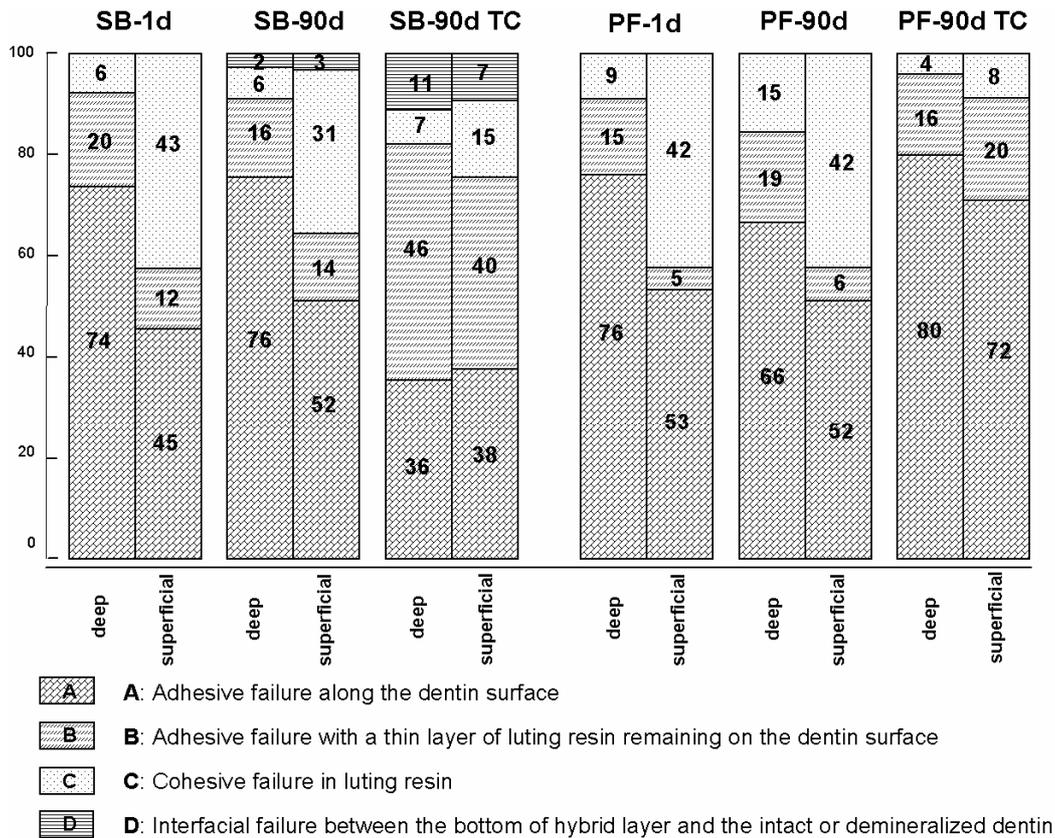


Figure 7.3 Failure modes of Super-Bond C&B and Panavia F 2.0 to human regional dentin during the micro-tensile bond strength test after different storage condition. A: Adhesive failure along the top of dentin surface; B: Mixed failure: Adhesive failure with a thin layer of adhesive resin cement remaining on the dentin surface; C: Cohesive failure in the adhesive resin cement; D: Interfacial failure between the bottom of hybrid layer and the intact or demineralized dentin.

For groups PF, a substantial percentage of cohesive failure in adhesive resin cement (failure mode C) was found in groups 1d and 90d for superficial dentin and cervical dentin, while adhesive failure mostly occurred for deep dentin. Compared to group 1d, an increased percentage of partial adhesive failure with a thin layer of adhesive resin cement remaining on the dentin surface (failure mode B) was found in 90d and 90d-TC groups. In groups 90d-TC, almost all debonded specimens showed adhesive failure from dentin surface (failure mode A) or partial adhesive failure with a thin layer of adhesive resin cement remaining on the dentin surface (failure mode B) for each regional location. For this adhesive resin cement, failure mode D (cohesive failure in demineralized dentin) was not detected in any of the specimens.

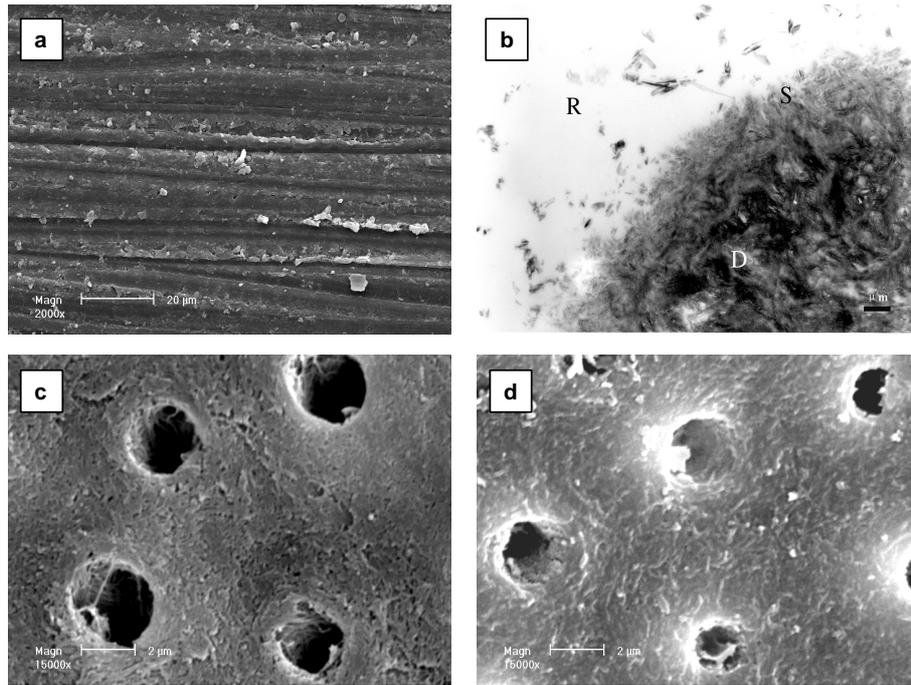


Figure 7.4 SEM and TEM photomicrograph of polished dentin surfaces and conditioned dentin surfaces. **(a)** SEM photomicrograph illustrating the smear layer on the dentin surface polished with 600- grit SiC paper. **(b)** TEM photomicrograph illustrating the smear layer on the dentin surface polished with 600- grit SiC paper. Approximately 0.5 μm of smear layer was formed on the underlying dentin surface. Smear layer seems to be contiguous with the underlying intact dentin. S: Smear layer; D: Demineralized dentin in TEM preparation; R: Embedding resin. **(c)** SEM photomicrograph illustrating the etched dentin surface with 10% citric acid with 3% ferric chloride (Super-Bond C&B). After the dentin was etched, the smear layer appeared to be removed and the tubule orifices were exposed completely. The circumferentially oriented collagen fibers around the tubular wall are exposed. **(d)** SEM photomicrograph illustrating the treated dentin surface with self-etching ED Primer 2.0 (Panavia F 2.0). The smear layer appears to be dissolved with loose collagen network standing on the intertubular dentin surface. Many smear plugs are partially removed with smear debris remaining in the tubules or a thin smear layer loosely attaching to the tubular walls. The circumferentially oriented collagen fibers around the tubular walls are not exposed completely.

Figure 7.4 a and b show the smear layer on the dentin surface polished with 600 grit SiC paper as observed by SEM and TEM. Approximately 0.5 μm of smear layer was formed on the underlying dentin surface. Smear layer seems to be contiguous with the underlying intact dentin. After the dentin was etched with 10% citric acid with 3% ferric chloride⁴³⁾, the smear layer appeared to be removed and the tubule orifices were exposed completely (Figure 7.4 c). The circumferentially oriented collagen fibrils around the tubular wall are exposed. After the dentin was treated with self-etching ED Primer 2.0 (Figure 7.4 d), the smear layer appeared to be dissolved with loose collagen network standing on the intertubular dentin surface. Many smear

plugs are partially removed with smear debris remaining in the tubules. Some peritubular dentin remained in PF specimens.

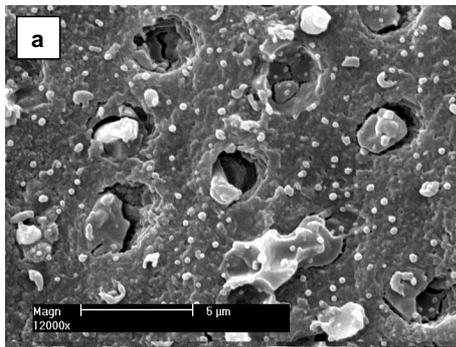
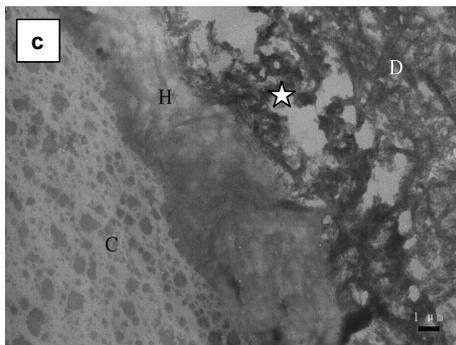
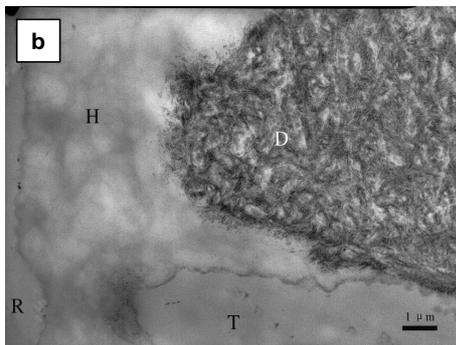


Figure 7.5 Fractographic analysis of group Super-Bond C&B⁴³. (a) SEM micrograph of a debonded dentin specimen in group 1 d. Adhesive failure occurred on the top of the hybrid layer (HL) and cohesive failure within the resin tags. (b) TEM photomicrograph illustrating the adhesive failure occurring at the top of HL. A HL with a width of approximately 4 μm was formed. (c) TEM micrograph of cohesive failure occurring in demineralized dentin below the HL (group 90 d-TC). Under the bottom of HL was loose fractured demineralized collagen fibrils (star). The collagen fibril network in this area appears to be inadequately enveloped by resin cement and took up more heavy metal stain than other areas. H: hybrid layer; D: demineralized dentin in preparation of TEM; C: resin cement; P: radiopaque particle. Bar=1μm.



Figures 7.5-7.6 present examples of the Fractographic analysis using SEM and TEM. In group SB-1d specimens, adhesive failure occurred along the top of HL with cohesive failure within the resin tags (Fig. 7.5 a), which were confirmed by TEM observation (Fig. 7.5 b). A HL with a depth of approximately 4 μm was found which extended into the tubule walls surrounding the resin tags (Fig. 7.5 b). After 90 d and 15,000 thermal cycles, cohesive failure in the demineralized dentin under the HL was found (Fig. 7.5 c). The collagen fibrils in this area appear to be inadequately enveloped by resin cement and took up more heavy metal stain than other areas.

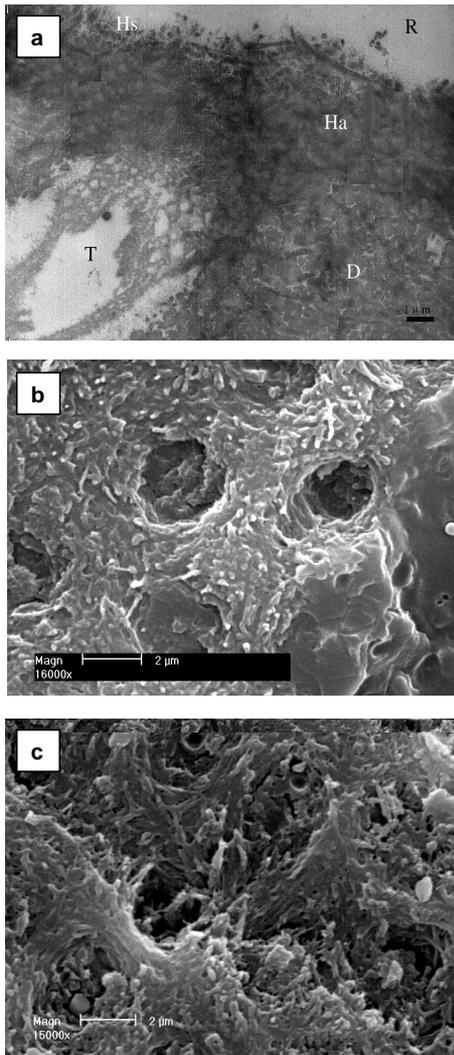


Figure 7.6 Fractographic analysis of group Panavia F 2.0 (PF). (a) TEM photomicrograph illustrating the cohesive failure within the hybridized smear layer - the top of hybrid layer (HL) (group 1d). The HL was approximately 2 μm , consisting of a hybridized smear layer (ca. 0.5 μm) and a 1-1.5 μm authentic HL. (b) High-magnification SEM micrograph of a debonded dentin specimen in group 1 d that failed at the top of the HL and cohesively fractured resin tags occluded the tubules. (c) High-magnification SEM micrograph of a debonded dentin specimen in group 90 d-TC that failed in the HL. Resin in inter-fibrillar spaces between collagen fibrils was partially lost. The collagen fibrils exhibited odd shapes and bulbous ends that are characteristics of plastically deformed and broken fibrils. C: resin cement; Ha: hybrid authentic dentin; Hs: hybridized smear layer; D: demineralized dentin in preparation of TEM; T: resin tag; R: embedding resin. Bar=1 μm .

In group PF-1d specimens, the HL was approximately 2 μm thick, and consisted of a hybridized smear layer (ca. 0.5 μm) and a 1-1.5 μm authentic HL (Fig. 7.6 a). In one debonded dentin specimen of group 1d, adhesive failure occurred at the top of hybrid layer (hybridized smear layer) with cohesively fractured resin tags sealing the tubules (Fig. 7.6 b). After 90 d and 15,000 thermal cycles, cohesive failure within HL was found in the deep dentin group (Fig. 7.6 c). Resin in inter-fibrillar spaces between collagen fibrils was partially lost. Some of the collagen fibrils exhibited odd shapes and bulbous ends that are characteristics of plastically deformed and broken fibrils.

7.10 Effect of thermal cycling on the durability of μTBS

Thermocycling is a commonly used thermal fatigue loading method in bond strength studies. Although it cannot simulate the chemical attack from the water into the bond interface, thermocycling is still an adjunct to assess the effect of thermal stresses and prolonged water exposure on the bond strength. Since the effect of

thermal cycling on the dentin bond strength is strongly related with the bonding systems, C-factor, dentin substrate, surface preparation, smear layer and storage time^{39, 143, 144}), conflicting results have been often reported. The bond strength generally decreased in total-etch adhesives with thermal stress, while no significant difference were observed after 30,000 thermal cycles¹⁴³) or 37,500 thermal cycles after 150 days water storage for self-etching primer systems. In the current study, we speculate that the 1-mm-diameter bonding area contributes to more rapid water diffusion from the storage media into the bond interface after 90 days water storage and that it accelerated water degradation of the bond interface compared to the 3-mm-diameter bond areas used in conventional tensile tests^{39, 143, 144}). The fact that the 15,000 thermal cycles used in this study significantly decreased μ TBS indicates that 15,000 cycles was an appropriate thermal challenge to small diameter specimens after 90 days water storage.

In the present study, although there may have been some uninfiltreated demineralized collagen fibrils, no cohesive failure was found below the bottom of the HL during TBS testing in group SB-1d. Even in group SB-90d, the μ TBS and failure modes were not significantly different from those of group SB 1d. The reason might be that 90 days of water storage is not long enough to cause degradation of the collagen fibrils to an extent that could significantly compromise their mechanical properties. However, after 90 days storage and thermal cycling, μ TBS of SB decreased significantly with an increase in cohesive failures within the demineralized dentin collagen fibrils at the bottom of the HL (Fig. 7.5 c). This demonstrated that the exposed collagen fibrils might be less resistant to thermal fatigue testing than the resin-infiltrated collagen fibrils in the HL. Therefore the resistance of the collagen fibrils to tensile loading decreased over time, leading to the decrease of μ TBS and failure in the demineralized collagen fibrils at the bottom of HL¹⁴⁵).

In native collagen fibrils, the collagen molecules are highly oriented and packed in crystal-like aggregates. Thermal denaturation of collagen fibrils corresponds to the melting (or unfolding) of the crystalline organisation of collagen molecules caused by the increased temperature¹⁴⁶). It has been reported that triple helices of type I collagen fibrils in human unfold (denature) at body temperature¹⁴⁷). This phenomena was shown with pure reconstituted collagen that had not yet developed any cross-linking. However, human dentin collagen molecules have developed the extensive cross-linking that thermally stabilizes collagen fibrils. A recent study reported that demineralized dentin matrix has been shown to have a thermal denaturation temperature of 67 °C¹⁴⁸). Thus, the highest temperature of thermal stressing (55 °C) used in the current study would not denature the collagen fibrils. However, it may have

accelerated the hydrolytic activity of endogenous collagenase in dentin, thereby accelerating aging of the bonded interfaces.

7.11 Effect of denatured collagen fibrils in the smear layer on the durability of μ TBS

Recent micro-Raman spectroscopic analysis results indicate that the disorganized collagen fibrils within the smear layer are not removed by acid etching and rinsing, but are denatured by acid treatment¹³⁰⁾. Therefore, in the SB groups, it is likely that a layer of disorganized denatured collagen fibrils remained on the conditioned surface that has been termed a “collagen smear layer”⁸⁸⁾. For specimens in the PF groups, the smear layer was hybridized by resin infiltration into the underlying authentic hybrid layer. In comparison with the subjacent, intact collagen fibrils of the hybrid layer, the denatured collagen fibrils from the smear layer lost not only their intact structure but also their mechanical strength. Therefore, compared to the authentic hybrid layer composed of resin and intact collagen fibrils, the top of HL for SB, or hybridized smear layer for PF seems to be a potential weak link in the bonding interface (Fig. 7.5 a, Fig. 7.6 a). This became obvious over time due to the degradation of the hybridized smear layer, confirmed by an increasingly substantial percentage of adhesive failure along the top of hybrid layer after 90 d and thermocycling for both resin cements (Fig. 7.4). This is in agreement with previous findings^{149, 150)}.

7.12 Effect of structural changes of intact collagen fibrils on the durability of μ TBS

In the HL, adhesive resin has a protective function around well-infiltrated collagen fibrils. However, such a protective function of the resin may eventually be altered by water sorption and hydrolytic degradation of the hydrophilic resin components in self-etching bonding systems^{125, 141)}. In the present study, ANOVA results showed that the μ TBS of PF was more sensitive to deep dentin than to superficial dentin, and a significant difference was found in μ TBS of PF to deep dentin among the different experimental periods with the increase of adhesive failure over time. One possible reason is that the “overwet” condition in deep dentin with too much water in the tubules may result in phase changes or in dilution of monomer concentration and interfering with the polymerization degree of the resin¹²⁷⁾. If this resulted in unpolymerized monomers or low-molecular-weight oligomers among the collagen fibrils within the HL, they may have been gradually extracted over time.

AFM images in this study have shown that the collagen fibrils in authentic hybridized dentin were not denatured during acidic conditioning. However, any uninfiltated

collagen fibrils, would be subject to the entire load, deform plastically and finally catastrophically fracture during μ TBS testing (Fig. 7.6 c). This assumption is also supported by Hashimoto's TEM results¹³⁵⁾ of micromorphological changes (resin elution and alteration of the collagen fibrils), which seem to be responsible for the bond degradation after 1 year of water storage reported in that study. In this study, the repetitive thermal changes might have accelerated water movement between the bonded interface and the exterior storage media, thereby accelerating the release of unpolymerized monomers and water degradation of the HL. This might explain the differences of the μ TBS and failure modes between group PF-90d TC and group PF-90d.

7.13 Schematic drawing of bonding procedures and fractographic analysis during tensile testing – Investigation of resin-dentin bonding mechanism

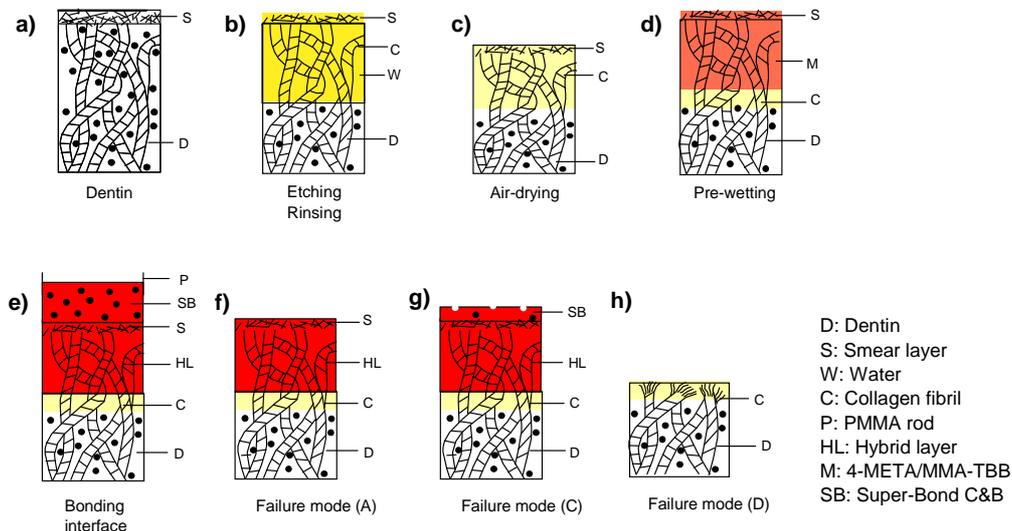


Figure 7.7 Schematic drawing of bonding procedures and failure modes during tensile testing (Super-Bond C&B). **(a)** Normal dentin with smear layer. **(b)** The dentin surface was etched with 10% citric acid with 3% ferric chloride and rinsed. **(c)** The acid-etched dentin surface was air-dried. **(d)** The treated dentin was pre-wet with 4META/MMA-TBB. **(e)** The bonding interface of PMMA rod-SB-hybrid layer-dentin with a HL of 4 μ m thickness. **(f)** Failure mode A - adhesive failure at the surface of the hybrid layer (HL). **(g)** Failure mode C - cohesive failure within the adhesive resin cement. **(h)** Failure mode D - cohesive failure in the demineralized collagen fibril network at the bottom of the HL.

A schematic drawing of SB bonding procedure and failure modes during tensile testing in this study is presented in Figure 7.7. The dentin specimens were wet polished with 600-grit SiC paper, with a smear layer remaining on the dentin surface (Figure 7.7 a). After the dentin surface was etched with 10% citric acid with 3% ferric chloride (10-3 solution, green activator) for 10 s, and rinsed for 15 s (Figure 7.7 b),

the smear layer was partially removed with denatured collagen fibril debris remaining on the dentin surface. The intact dentin underlying the smear layer was demineralized and infiltrated by water. After gentle air-drying (Figure 7.7 c), the demineralized collagen fibril network collapsed due to the dehydration. Prior to bonding with SB adhesive resin cement, the treated dentin surface was pre-wet with 4META/ MMA-TBB liquid to promote the resin infiltration (Figure 7.7 d). However, the demineralization depth might be deeper than the infiltration depth of adhesive resin cement. After bonding with SB adhesive resin cement, the bonding interface of PMMA rod-SB-hybrid layer-dentin with a HL of 4 μm thickness was formed (Figure 7.7 e).

During the tensile testing, the top of HL seems to be a weak link due to the denatured collagen fibril debris in the smear layer remaining on the etched dentin surface, resulting in adhesive failure on the dentin surface (failure mode A) (Figure 7.7 f). After water storage with thermal cycling, the radiopaque particles were missing at the resin matrix, leaving a defective zone in resin cement, which caused cohesive failure within the adhesive resin cement (failure mode C) (Figure 7.7 g). Due to an incomplete resin infiltration into the demineralized collagen fibrils network under the HL, the collagen fibrils network fractured cohesively during tensile testing (failure mode D) (Figure 7.7 h).

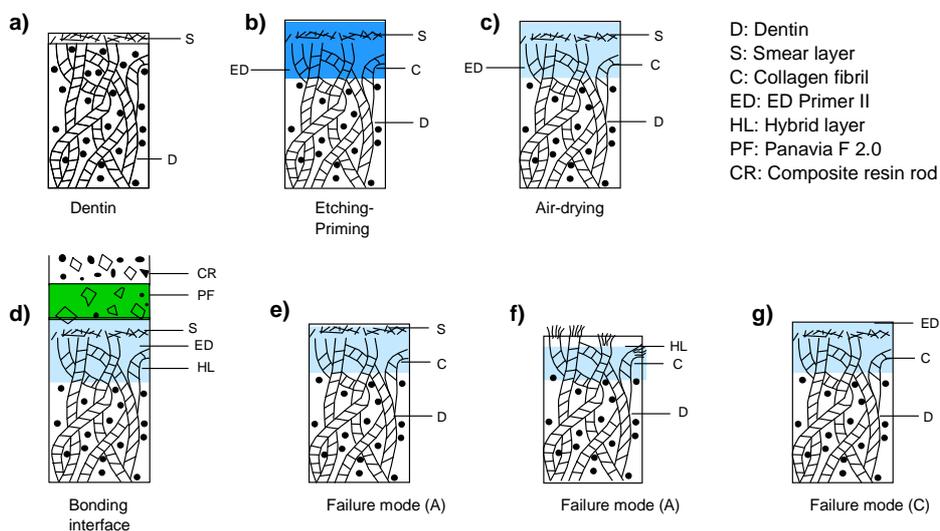


Figure 7.8 Schematic drawing of bonding procedures and failure modes during tensile testing (Panavia F 2.0). **(a)** Normal dentin with smear layer. **(b)** The dentin surface was self-etched and primed simultaneously. **(c)** The treated dentin surface was air-dried. **(d)** The bonding interface of composite rod-PF-HL-dentin with a HL of 2 μm thickness. **(e)** Failure mode A - adhesive failure at the surface of the hybrid layer (HL) or hybridized smear layer. The hybridized smear layer seems to be a weak link due to the denaturation and disorganization of the collagen fibrils in smear layer although

the smear layer was hybridized by resin into one complex with the underlying intact dentin. **(f)** Failure mode A - adhesive failure within the top of HL. After the adhesive resin cement was distracted from the HL, the tensile load was transferred directly to the collagen fibril network in hybridized intact dentin, resulting in the plastic fracture and cohesive failure within the top of the HL. **(g)** Failure mode C - cohesive failure in the adhesive resin - cured self-etching ED Primer.

A schematic drawing of PF bonding procedure and failure modes during tensile testing in this study is presented in Figure 7.8. The dentin specimens were wet polished with 600-grit SiC paper, with a smear layer remaining on the dentin surface (Figure 7.8 a). The dentin surface was self-etched and primed simultaneously with the self-etching ED Primer for 30 s (Figure 7.8 b), and air-dried gently (Figure 7.8 c). The smear layer and the underlying intact dentin were partially demineralized, with smear layer remaining on the treated dentin surface. The demineralization depth is equal to the infiltration depth of self-etching ED Primer. After the bonding with PF adhesive resin cement, the composite rod-PF-HL-dentin bonding interface with a HL of 2 μm thickness was formed (Figure 7.8 d), which was composed of the hybridized smear layer and hybrid layer.

During the tensile testing, the hybridized smear layer seems to be a weak link due to the denaturation and disorganization of the collagen fibrils in smear layer, leading to the adhesive failure at the surface of the hybrid layer (HL) or hybridized smear layer (failure mode A) (Figure 7.8 e). After water storage with thermal cycling, the adhesive resin cement was distracted from the HL, consequently the tensile load was transferred directly to the collagen fibril network in HL without the resin protection, resulting in the plastic fracture and cohesive failure within the top of HL (failure mode A) (Figure 7.8 f). The interface between the cured self-etching primer 2.0 and the hydrophobic PF luting composite resin the interface became the weak link during the tensile testing, which resulted in cohesive failure in the adhesive resin - cured self-etching ED Primer II (failure mode C) (Figure 7.8 g).

7.14 Summary and outlook

In this study a total etching bonding system (SB) and a self-etching bonding system (PF) were utilised to evaluate the micro-tensile bond strength (μTBS) to regional dentin, to further identify the difference in their bonding mechanisms and the influence of the structural changes of dentin collagen fibrils on the durability of dentin bonding.

The periodicity banding of about 67 nm on collagen fibrils conditioned with both bonding systems was observed in AFM images. For both adhesive resin cements,

μ TBS to superficial dentin (13.1-31.9 MPa) was significantly higher than those to deep and to cervical dentin after applying the different storage conditions (5.6-24.2 MPa) ($p < 0.001$, ANOVA). However the difference between μ TBS to deep dentin and to cervical dentin was not significant except that μ TBS of PF to deep dentin was significantly lower than that of PF to cervical dentin after 90d water storage without thermal cycling. After 90 d water storage with 15,000 thermal cycles, μ TBS decreased significantly, while the decrease after 90d storage without thermal cycling was not significant with the exception of group PF bonded to deep dentin.

Fractographic analysis revealed that there was a primary increase of adhesive failure at the top of the hybrid layer (HL) for both adhesive resin cements, accompanied by an increasing cohesive failure in demineralized dentin at the bottom of the HL or within the HL (PF) after 90 d storage with 15,000 thermal cycles. The possible reason for the weak link at the top of the HL is that the top of the HL contains disorganized collagen fibrils from the smear layer that degrade over time. Although the demineralized collagen fibrils underlying the smear layer were not denatured during acidic conditioning, they may be structurally unstable due to poor infiltration by resin ⁴³⁾ or loss of resin protection within the HL (PF) over time, decreasing the long-term μ TBS, which was accelerated by prolonged thermal cycling.

Within the limitations of this study, the following conclusions can be drawn: The presence of the periodicity banding along collagen fibrils indicates that the short-term application of the acidic conditioners used in the two bonding systems do not denature the intact dentin collagen fibrils. The μ TBS of the two bonding systems vary with the regional location in human dentin. The different chemical formulations and applications of total etching system and self-etching system result in a different morphological appearances of the bonding interface and bonding mechanisms. After water storage with thermal cycling, the μ TBS of both adhesive resin cements decreased significantly. The top and the bottom of the HL were the weak links in the bonding interface due to the structural instability of the dentin collagen fibrils over time, resulting in the deterioration of bonding durability. Artificial aging using water storage with thermal cycling accelerates the degradation of adhesive resin cement-dentin bonding and therefore serves as aging model.

Type I collagen plays an important role in the determination of resin-dentin bonding durability. Recently, our results and in vitro and in vivo studies demonstrated that the hydrolytic degradation of dentin collagen fibrils in and under resin-dentin bonding interfaces significantly decreases the bonding durability. It is well accepted that the degradation of the dentinal collagen matrix is caused by Matrix Metalloproteinases (MMPs) - a family of zinc-dependent host-derived proteolytic enzymes, which are present in dentinal and can be activated by modern self-etch and etch-and-rinse

adhesives. Inhibition of MMPs by a suitable chelator agent for zinc may slow down or prevent the degradation of dentinal collagen. And it is very urgent to incorporate MMP-inhibitory functionality into dentin adhesives to inhibit the activation of MMPs during bonding procedure. Therefore, in a multidisciplinary approach, we propose that a novel bio-functional macromonomer, as a biocompatible component in adhesives, possesses durable MMPs-inhibitory property and can inhibit collagen degradation in resin bonding to dentin. And it may promote the remineralization of decalcified dentin, allowing for natural healing of caries lesions. This new concept will significantly contribute to improving durability of resin-dentin bonds.

7.15 Author's Related Publications

[1] Bin Yang, Rainer Adelung, Klaus Ludwig, Klaus Brößmann, David H Pashley and Matthias Kern. Effect of structural change of collagen fibrils on the durability of dentin bonding. *Biomaterials*. 2005;26:5021-5031

8 General Conclusions and Outlook

In this work, the long-term bond strengths of adhesive resin cements to zirconia ceramic and human dentin were evaluated and resin-ceramic and resin-dentin bonding mechanisms were investigated.

In chapter 3, the influence of surface pretreatment on the bonding durability of the resin cements to zirconia ceramic was studied. Most importantly, the influence of chemical reactions of functional monomers in primer on the resin-ceramic bonding were investigated. Within the limitation of this study, priming pretreatment with primers can increase the bonding durability of three resin cements to airborne-particle abraded zirconia ceramic. Only silane is important for the initial resin-ceramic bonding, but are not able to produce a strong durable resin-ceramic bonding. The pretreatment with MDP or 4-META-containing primers make SB and CEC to produce a durable bond to airborne-particle abraded zirconia ceramic. Due to the decomposition of CH resin cement, the bonding durability of CH without pretreatment and with pretreatment with MS and MZP are not testable due to the spontaneous debond during storage. However the pretreatment with PLM and CCP help CH produce a low bonding strength after long-term water storage and thermal cycling. Without surface priming pretreatment, only SB showed acceptable long-term bond strength to airborne-particle abraded zirconia ceramic. These conclusions can be supported by the combination of XPS, TBS and SEM results.

In clinical try-in procedures of zirconia ceramic restorations, to remove contaminations prior to bonding is very important to realize a long-term durable resin bond clinically. In chapter 4, XPS and TBS were combined together to investigate whether there are contaminations on the zirconia ceramic surface left after try-in simulation, and the influences of contamination and cleaning methods on zirconia ceramic bonding durability with MDP-containing resin cements. After saliva immersion and using a silicone disclosing agent, airborne-particle abraded ceramic specimens were cleaned with acetone, 36% phosphoric acid, additional airborne-particle abrasion, or only water spray. Chemical analyses of specimen surfaces were done using XPS. The influences of contamination and cleaning methods on resin-ceramic bond durability were examined by tensile testing after 3 days or 150 days water storage with 37,500 thermal cycles. Our results showed that contamination, existing after try-in simulation as confirmed by chemical analysis with XPS, significantly reduced resin -ceramic bonds. Airborne-particle abrasion was the most effective method to remove contaminants and to create a clean zirconia ceramic surface suitable for long-term durable resin bonding. The combination of chemical surface characterization with XPS and long-term TBS performance was very useful

to determine the effects of the contamination and cleaning methods on ceramic bonding.

In our study and most of previous studies dealing with zirconia specimens, mechanical treatments such as sandblasting or tribochemical silica coating followed by silanization were used. However mechanical treatments of zirconia might be done with caution because sandblasting, and grinding may negatively influence its mechanical properties of ceramics. It was supposed that the effect on the fracture resistance of zirconia depended on the time the specimens were subjected to sandblasting. This is probably because sandblasting treatment and/or grinding can induce compressive stresses and/or phase transformation on the surface, which increases the strength; at the same time, they also induce flaws and other defects which induce the strength. Therefore, to find the best possible technique of improving resin-zirconia ceramic bonding durability, more studies are needed to determine the effects of surface pretreatment on the bond strength and mechanical properties of zirconia ceramics.

Understanding the degradation mechanism of dentin bonding is of significant importance for improving the long-term dentin bonding of adhesive resin cements and the longevity of bonded zirconia ceramic restorations.

In chapter 6, μ TBS was used to evaluate the bonds of three resin cements (SB, PF, and RU) to different regions of dentin, SEM and TEM were used to investigate the resin-dentin bonding interface and fractographic analysis after μ TBS testing. ANOVA results showed that μ TBS to superficial dentin was significantly higher than to deep or cervical dentin for all three resin cements. For groups SB and PF, with the highest μ TBS to superficial dentin, failed primarily cohesively in resin cement. μ TBS of SB to deep and cervical dentin were significantly higher than those of PF and RU. RU, with the lowest regional μ TBS, failed mostly within demineralized dentin. SEM and TEM showed that adhesive failures in SB and PF occurred at the top of hybrid layer, but no obvious hybrid layer was observed in RU.

One possible reason for the lower μ TBS of the two self-etching systems (PF and RU) to deep and cervical dentin than to superficial dentin is that there is much more water in deep dentin and cervical dentin than superficial dentin. Such an "overwet" condition might result in a dilution of the monomer concentration and interfering with the polymerization degree of PF and RU. In contrast, due to the special polymerization initiator in SB, this moisture tolerance and interfacial polymerization of SB results in thorough polymerization and improvement of regional bond strength near the pulp (in deep dentin and cervical dentin). In conclusion, three resin cements with different

chemical formulations and application techniques yield morphologically different interfacial microstructures and regional dentin bond strength.

In chapter 7, the effect of structural changes of collagen fibrils on the bonding durability of a total etch resin cement (SB) and a self-etching resin cement (PF) to dentin was investigated. AFM was used to observe structural changes of intact dentin collagen fibrils after acidic conditionings of two bonding systems. After 90 d water storage and 15,000 thermal cycles (TC) as artificial aging, μ TBS was utilized to evaluate the bonding durability of the two bonding systems to dentin. μ TBS after 1 d or 90 d water storage without TC were separately measured in control groups.

A cross-banding periodicity of about 67 nm along collagen fibrils was seen on demineralized intertubular dentin surfaces in AFM images. For both resin cements, thermal cycling decreased ($p < 0.05$) μ TBS of 1 d and 90 d, compared to controls. Scanning electron microscope and transmission electron microscopic examinations revealed that the top and bottom of HL were weak links in the bonding interface over time. The results suggest that the top of HL contains disorganized collagen fibrils from the smear layer which degrade over time. AFM results indicate that the demineralized intact collagen fibrils beneath the smear layer were not denatured during acidic conditioning. However, these collagen fibrils may be structurally unstable due to poor-infiltration by resin or loss of resin protection within the HL over time, reducing the long-term μ TBS. Artificial aging using water storage with thermal cycling accelerates the degradation of adhesive resin cement-dentin bonding and therefore serves as aging model. This study is very important to provide the evidence that the decomposition of dentin collagen fibrils in the resin-dentin bonding interface over time, although the short-term application of the acidic conditioners used in the two bonding systems do not denature the intact dentin collagen fibrils, is one main factor decreasing the dentin bonding.

Recent *in vitro* and *in vivo* studies also demonstrated that the hydrolytic degradation of dentin collagen fibrils in and under resin-dentin bonding interfaces significantly decreases the bonding durability. Furthermore, recent studies revealed endogenous collagenolytic and gelatinolytic activities derived from acid etched dentin result in degradation of hybrid layers in dentin bonding interface. The degradation of incompletely infiltrated zones by host-derived proteinases (MMPs) within the dentin matrix proceeded in the absence of bacterial enzymes. This discovery suggested the use of enzyme inhibitors in primers to block the adverse effects of enzymes at the resin/dentin interface in order to slow or prevent the destruction of bonded dentin matrices.

Inhibition of MMPs by a suitable chelator agent for zinc may slow down or prevent the degradation of dentin collagen. Therefore, it is very urgent to incorporate MMP-inhibitory functionality into dentin adhesives to inhibit the activation of MMPs during bonding procedure. In a multidisciplinary approach, we propose that a novel bio-functional macromonomer, as a biocompatible component in adhesives, possesses durable MMPs-inhibitory property and can inhibit collagen degradation in resin bonding to dentin. And it may promote the remineralization of decalcified dentin, allowing for natural healing of caries lesions. This new concept will significantly contribute to improving durability of resin-dentin bonds.

Bibliography

- 1) H. M. Clearfield, D. K. McNamara and G. D. Davis, Eds., "Adherent surface preparation for structural adhesive bonding, in : Adhesive Bonding (L. H. Lee, ed.)," Plenum Press, New York, 1991.
- 2) M. P. Walker, Y. Wang, J. Swafford, A. Evans and P. Spencer, *J Prosthodont*, **9**, 77-81 (2000).
- 3) C.W.Jennings, *Journal of adhesion*, **4**, 25-34 (1972).
- 4) A. J. Kinloch, Ed. "Adhesion and Adhesives, Science and Technology," Chapman and Hall, London, 1987.
- 5) E. P. Plueddemann (1991) Adhesion through silane coupling agents, in Fundamentals of Adhesion New York, Plenum Press.
- 6) O. M. el-Mowafy, A. H. Fenton, N. Forrester and M. Milenkovic, *J Prosthet Dent*, **76**, 524-9 (1996).
- 7) J. A. Sorensen and E. C. Munksgaard, *Eur J Oral Sci*, **103**, 116-20 (1995).
- 8) A. Attia and M. Kern, *J Prosthet Dent*, **91**, 247-52 (2004).
- 9) M. A. Latta and W. W. Barkmeier, *Compend Contin Educ Dent*, **21**, 635-9, 642-4; quiz 646 (2000).
- 10) K. Kamada, K. Yoshida and M. Atsuta, *J Prosthet Dent*, **79**, 508-13 (1998).
- 11) M. Rosentritt, M. Behr, R. Lang and G. Handel, *Dent Mater*, **16**, 159-65 (2000).
- 12) M. B. Blatz, A. Sadan and M. Kern, *J Prosthet Dent*, **89**, 268-74 (2003).
- 13) R. Strang, C. J. Whitters, D. Brown, R. L. Clarke, R. V. Curtis, P. V. Hatton, A. J. Ireland, C. H. Lloyd, J. F. McCabe, J. W. Nicholson, S. N. Scrimgeour, J. C. Setcos, M. Sherriff, R. van Noort, D. C. Watts and D. Woods, *J Dent*, **26**, 273-91 (1998).
- 14) N. Kramer, U. Lohbauer and R. Frankenberger, *Am J Dent*, **13**, 60D-76D (2000).
- 15) J. C. Chang, T. Nguyen, J. H. Duong and G. D. Ladd, *J Prosthet Dent*, **79**, 503-7 (1998).
- 16) H. Kato, H. Matsumura and M. Atsuta, *J Oral Rehabil*, **27**, 103-10 (2000).
- 17) K. B. Frazier and D. C. Sarrett, *Am J Dent*, **8**, 161-4 (1995).
- 18) D. Williams, *Med Device Technol*, **8**, 6-8 (1997).
- 19) C. Piconi and G. Maccauro, *Biomaterials*, **20**, 1-25 (1999).
- 20) A. Devigus and G. Lombardi, *Int J Comput Dent*, **7**, 379-88 (2004).
- 21) F. J. Burke, G. J. Fleming, D. Nathanson and P. M. Marquis, *J Adhes Dent*, **4**, 7-22 (2002).
- 22) P. A. Brunton, P. Cattell, F. J. Burke and N. H. Wilson, *J Prosthet Dent*, **82**, 167-71 (1999).
- 23) M. Fuzzi, G. Carnevale and M. P. Tonelli, *J Esthet Dent*, **7**, 235-43 (1995).
- 24) J. F. Roulet, *J Dent*, **25**, 459-73 (1997).
- 25) M. Kern and J. R. Strub, *J Dent*, **26**, 245-9 (1998).
- 26) M. Kern and S. M. Wegner, *Dent Mater*, **14**, 64-71 (1998).
- 27) W. Awliya, A. Oden, P. Yaman, J. B. Dennison and M. E. Razzoog, *Acta Odontol Scand*, **56**, 9-13 (1998).

- 28) B. Yang, M. Scharnberg, S. Wolfart, A. C. Quaas, K. Ludwig, R. Adelung and M. Kern, *J Biomed Mater Res B Appl Biomater*, **81**, 283-90 (2007).
- 29) A. Della Bona, C. Shen and K. J. Anusavice, *Dent Mater*, **20**, 338-44 (2004).
- 30) L. F. Valandro, A. Della Bona, M. Antonio Bottino and M. P. Neisser, *J Prosthet Dent*, **93**, 253-9 (2005).
- 31) A. Della Bona, K. J. Anusavice and J. A. Hood, *Int J Prosthodont*, **15**, 248-53 (2002).
- 32) M. Kern, *Int J Prosthodont*, **13**, 350 (2000).
- 33) S. M. Wegner, W. Gerdes and M. Kern, *Int J Prosthodont*, **15**, 267-72 (2002).
- 34) A. C. Quaas, B. Yang and M. Kern, *Dent Mater*, **23**, 506-12 (2007).
- 35) M. Kern and V. P. Thompson, *J Prosthet Dent*, **71**, 453-61 (1994).
- 36) M. Kern and V. P. Thompson, *J Prosthet Dent*, **73**, 240-9 (1995).
- 37) M. Guazzato, M. Albakry, M. V. Swain and J. Ironside, *Int J Prosthodont*, **15**, 339-46 (2002).
- 38) M. Blixt, E. Adamczak, L. A. Linden, A. Oden and K. Arvidson, *Int J Prosthodont*, **13**, 221-6 (2000).
- 39) R. B. Price, T. Derand, P. Andreou and D. Murphy, *Biomaterials*, **24**, 1013-21 (2003).
- 40) J. Perdigao, R. Frankenberger, B. T. Rosa and L. Breschi, *Am J Dent*, **13**, 25D-30D (2000).
- 41) S. M. Wegner and M. Kern, *J Adhes Dent*, **2**, 139-47 (2000).
- 42) B. Yang, S. Wolfart, M. Scharnberg, K. Ludwig, R. Adelung and M. Kern, *J Dent Res*, **86**, 749-53 (2007).
- 43) R. Hanemaaijer, H. Visser, P. Koolwijk, T. Sorsa, T. Salo, L. M. Golub and V. W. van Hinsbergh, *Adv Dent Res*, **12**, 114-8 (1998).
- 44) M. Ozcan, S. Kerkdijk and L. F. Valandro, *Clin Oral Investig* (2007).
- 45) B. Bott and M. Hannig, *Dent Mater*, **19**, 264-9 (2003).
- 46) B. Yang, H. C. Lange-Jansen, M. Scharnberg, S. Wolfart, K. Ludwig, R. Adelung and M. Kern, *Dent Mater* (2007).
- 47) J. F. Roulet, K. J. Soderholm and J. Longmate, *J Dent Res*, **74**, 381-7 (1995).
- 48) J. Pisani-Proenca, M. C. Erhardt, L. F. Valandro, G. Gutierrez-Aceves, M. V. Bolanos-Carmona, R. Del Castillo-Salmeron and M. A. Bottino, *J Prosthet Dent*, **96**, 412-7 (2006).
- 49) W. S. Oh and C. Shen, *J Prosthet Dent*, **90**, 241-6 (2003).
- 50) A. B. M. KERN, and B. YANG,, Long-term Bond Strength to Zirconia Ceramic after Different Surface Conditioning, AADR 37th Annual Meeting and Exhibition Dallas, Texas, USA, 2008.
- 51) J. Wahlgren, T. Salo, O. Teronen, H. Luoto, T. Sorsa and L. Tjaderhane, *Int Endod J*, **35**, 897-904 (2002).
- 52) S. S. Atsu, M. A. Kilicarlan, H. C. Kucukesmen and P. S. Aka, *J Prosthet Dent*, **95**, 430-6 (2006).
- 53) Y. Tsuchimoto, Y. Yoshida, A. Mine, M. Nakamura, N. Nishiyama, B. Van Meerbeek, K. Suzuki and T. Kuboki, *Dent Mater J*, **25**, 120-4 (2006).
- 54) M. Madani, F. C. Chu, A. V. McDonald and R. J. Smales, *J Prosthet Dent*, **83**, 644-7 (2000).

- 55) J. D. Miller and H. Ishida, Eds., "Adhesive-adherend interface and inter-phase through silane coupling agents. in Fundamentals of adhesion (L. H. Lee, ed.)," Plenum Press, New York, 1991.
- 56) D. L. Allara, F. M. Fowkes, J. Noolandi, G. W. Rubloff and M. V. Tirrell, *Materials science & Engineering*, **83**, 213-226 (1986).
- 57) A. J. Kinloch, *Journal of Adhesion*, **10**, 193-219 (1979).
- 58) R. A. Gledhill, A. J. Kinloch and S. J. Shaw, *Journal of Adhesion*, **11**, 3-5 (1980).
- 59) J. W. Thurmond, W. W. Barkmeier and T. M. Wilwerding, *J Prosthet Dent*, **72**, 355-9 (1994).
- 60) M. F. Burrow, S. Inokoshi and J. Tagami, *Am J Dent*, **12**, 295-8 (1999).
- 61) R. L. Bowen, P. S. Bennett, R. J. Groh, M. Farahani and F. C. Eichmiller, *J Dent Res*, **75**, 606-10 (1996).
- 62) M. P. Patel, M. B. Johnstone, F. J. Hughes and M. Braden, *Biomaterials*, **22**, 81-6 (2001).
- 63) J. H. van Schalkwyk, F. S. Botha, P. J. van der Vyver, F. A. de Wet and S. J. Botha, *Sadj*, **58**, 143-7 (2003).
- 64) Y. E. Aboush, *J Prosthet Dent*, **80**, 649-53 (1998).
- 65) S. E. Bishara, C. Oonsombat, R. Ajlouni and G. Denehy, *Angle Orthod*, **72**, 554-7 (2002).
- 66) V. Cacciafesta, M. F. Sfondrini, L. Baluga, A. Scribante and C. Klersy, *Am J Orthod Dentofacial Orthop*, **124**, 420-6 (2003).
- 67) S. O. Eiriksson, P. N. Pereira, E. J. Swift, Jr., H. O. Heymann and A. Sigurdsson, *Dent Mater*, **20**, 37-44 (2004).
- 68) L. M. Rosenstiel SF, Fujimoto J., "Contemporary Fixed Prosthodontics.," Mosby, St. Louis, ed. 2nd ed., 1995.
- 69) S. Szep, C. Schmid, P. Weigl, L. Hahn and D. Heidemann, *J Prosthet Dent*, **89**, 60-5 (2003).
- 70) P. L. Millstein, J. C. Ho, W. Naim and D. Nathanson, *J Prosthet Dent*, **62**, 510-1 (1989).
- 71) K. K. Sheth, M. Staninec, A. V. Sarma and D. Fried, *Lasers Surg Med*, **35**, 245-53 (2004).
- 72) A. C. Quaas, B. Yang and M. Kern, *Dent Mater*.
- 73) B. D. Ratner and D. G. Castner (1997) *Electron Spectroscopy for Chemical Analysis*, ed. J. C. Vickerman. Chichester, John Wiley & Sons, pp. 43-96.
- 74) P. Chpindel and M. Cristou, *Pract Periodontics Aesthet Dent*, **6**, 19-28; quiz 30 (1994).
- 75) M. Hummel and M. Kern, *Dent Mater*, **20**, 498-508 (2004).
- 76) R. E. Baier, *Oper Dent*, **Suppl 5**, 1-9 (1992).
- 77) A. Carlen, K. Nikdel, A. Wennerberg, K. Holmberg and J. Olsson, *Biomaterials*, **22**, 481-7 (2001).
- 78) M. Hannig and R. Schmeiser, *Quintessence Int*, **28**, 79-83 (1997).
- 79) J. F. Moulder, W. F. Stickle, P. E. Sobol and K. D. Bomben, "Handbook of X-ray photoelectron spectroscopy," Perkin-Elmer Corporation, Minnesota, 1992.
- 80) M. Kern and V. P. Thompson, *Dent Mater*, **9**, 151-61 (1993).

- 81) (2001) Surface preparation for improved adhesion, March Plasma Systems, Inc.
- 82) H. Lüthy, O. Loeffel and C. H. F. Hammerle, *Dent Mater*, **22**, 195-200 (2006).
- 83) J. F. McCabe and A. W. G. Walls (1998) Applied dental materials. Malden, MA, USA, Blackwell Science Ltd.,.
- 84) A. M. Diaz-Arnold, M. A. Vargas and D. R. Haselton, *J Prosthet Dent*, **81**, 135-41 (1999).
- 85) D. H. Pashley, H. Sano, B. Ciucchi, M. Yoshiyama and R. M. Carvalho, *Dent Mater*, **11**, 117-25 (1995).
- 86) N. Nakabayashi and D. H. Pashley, Eds., "Hybridization of dental hard tissues," Quintessence, Tokyo, Japan, 1998.
- 87) G. W. Marshall, Jr., S. J. Marshall, J. H. Kinney and M. Balooch, *J Dent*, **25**, 441-58 (1997).
- 88) D. H. Pashley and R. M. Carvalho, *J Dent*, **25**, 355-72 (1997).
- 89) Y. Shono, M. Terashita, J. Shimada, Y. Kozono, R. M. Carvalho, C. M. Russell and D. H. Pashley, *J Adhes Dent*, **1**, 211-8 (1999).
- 90) A. Takahashi, Y. Sato, S. Uno, P. N. Pereira and H. Sano, *Dent Mater*, **18**, 263-8 (2002).
- 91) M. F. Burrow, H. Takakura, M. Nakajima, N. Inai, J. Tagami and T. Takatsu, *Dent Mater*, **10**, 241-6 (1994).
- 92) N. Konishi, L. G. Watanabe, J. F. Hilton, G. W. Marshall, S. J. Marshall and M. Staninec, *Dent Mater*, **18**, 516-20 (2002).
- 93) J. M. Mixson, P. Spencer, D. L. Moore, R. P. Chappell and S. Adams, *Am J Dent*, **8**, 5-9 (1995).
- 94) M. Ferrari, M. C. Cagidiaco, A. Vichi, F. Mannocci, P. N. Mason and I. A. Mjor, *Dent Mater*, **17**, 156-64 (2001).
- 95) N. Nakabayashi, *Oper Dent*, **Suppl 5**, 125-30 (1992).
- 96) E. J. Swift, Jr., *J Esthet Restor Dent*, **15**, 71 (2003).
- 97) B. Van Meerbeek, Y. Yoshida, J. Snauwaert, L. Hellemans, P. Lambrechts, G. Vanherle, K. Wakasa and D. H. Pashley, *J Adhes Dent*, **1**, 7-23 (1999).
- 98) S. Bouillaguet, P. Gysi, J. C. Wataha, B. Ciucchi, M. Cattani, C. Godin and J. M. Meyer, *J Dent*, **29**, 55-61 (2001).
- 99) F. R. Tay, S. M. Kwong, A. Itthagarun, N. M. King, H. K. Yip, K. M. Moulding and D. H. Pashley, *J Adhes Dent*, **2**, 9-28 (2000).
- 100) E. Baer, J. J. Cassidy and A. Hiltner, Eds., "Hierarchical structure of collagen and its relationship to the physical properties of tendon. In: Nimni, M.E. (Ed.), Collagen: vol. II, Biochemistry and Biomechanics.," CRC Press, Boca Raton, FL, 1988.
- 101) D. R. Baselt, J. P. Revel and J. D. Baldeschwieler, *Biophys J*, **65**, 2644-55 (1993).
- 102) F. El Feninat, T. H. Ellis, E. Sacher and I. Stangel, *J Biomed Mater Res*, **42**, 549-53 (1998).
- 103) S. Habelitz, M. Balooch, S. J. Marshall, G. Balooch and G. W. Marshall, Jr., *J Struct Biol*, **138**, 227-36 (2002).

- 104) D. H. Pashley, F. R. Tay, C. Yiu, M. Hashimoto, L. Breschi, R. M. Carvalho and S. Ito, *J Dent Res*, **83**, 216-21 (2004).
- 105) G. W. Marshall, Jr., M. Balooch, R. J. Tench, J. H. Kinney and S. J. Marshall, *Dent Mater*, **9**, 265-8 (1993).
- 106) G. W. Marshall, Jr., *Quintessence Int*, **24**, 606-17 (1993).
- 107) N. Silikas, D. C. Watts, K. E. England and K. D. Jandt, *J Dent*, **27**, 137-44 (1999).
- 108) S. S. Oliveira, S. J. Marshall, J. F. Hilton and G. W. Marshall, *Biomaterials*, **23**, 4105-12 (2002).
- 109) N. Silikas, *Microscop. Analys.*, **3**, 19-21 (2001).
- 110) J. A. Gwinnett, F. R. Tay, K. M. Pang and S. H. Wei, *J Prosthet Dent*, **74**, 575-85 (1995).
- 111) M. F. Burrow, H. Sano, M. Nakajima, N. Harada and J. Tagami, *Am J Dent*, **9**, 223-9 (1996).
- 112) P. N. Pereira, T. Yamada, S. Inokoshi, M. F. Burrow, H. Sano and J. Tagami, *J Dent*, **26**, 479-85 (1998).
- 113) J. De Munck, B. Van Meerbeek, I. Satoshi, M. Vargas, Y. Yoshida, S. Armstrong, P. Lambrechts and G. Vanherle, *Am J Dent*, **16**, 414-20 (2003).
- 114) M. Hashimoto, H. Ohno, H. Sano, M. Kaga and H. Oguchi, *J Biomed Mater Res B Appl Biomater*, **66**, 324-30 (2003).
- 115) A. Takahashi, S. Inoue, C. Kawamoto, R. Ominato, T. Tanaka, Y. Sato, P. N. Pereira and H. Sano, *J Adhes Dent*, **4**, 151-9 (2002).
- 116) Y. Shono, T. Ogawa, M. Terashita, R. M. Carvalho, E. L. Pashley and D. H. Pashley, *J Dent Res*, **78**, 699-705 (1999).
- 117) H. Sano, T. Shono, H. Sonoda, T. Takatsu, B. Ciucchi, R. Carvalho and D. H. Pashley, *Dent Mater*, **10**, 236-40 (1994).
- 118) D. H. Pashley, R. M. Carvalho, H. Sano, M. Nakajima, M. Yoshiyama, Y. Shono, C. A. Fernandes and F. Tay, *J Adhes Dent*, **1**, 299-309 (1999).
- 119) H. Tassery, P. de Donato, O. Barres and J. Dejou, *J Adhes Dent*, **3**, 247-55 (2001).
- 120) J. W. van Dijken, L. Hasselrot, A. Ormin and A. L. Olofsson, *Eur J Oral Sci*, **109**, 222-9 (2001).
- 121) H. Ohno, M. Kimura and M. Fuchigamis Oguri (1998.) Dental composition. , vol. No. 5,739,177. United States
- 122) D. H. Pashley, B. Ciucchi, H. Sano, R. M. Carvalho and C. M. Russell, *Arch Oral Biol*, **40**, 1109-18 (1995).
- 123) T. K. Okamoto Y, Saeki K., *Chemistry letter, The Chemical Society of Japan* 1247-8 (1998).
- 124) A. N. Ozturk, S. Belli and G. Eskitascioglu, *J Prosthet Dent*, **91**, 253-7 (2004).
- 125) R. M. Carvalho, T. A. Pegoraro, F. R. Tay, L. F. Pegoraro, N. R. Silva and D. H. Pashley, *J Dent*, **32**, 55-65 (2004).
- 126) P. R. Jayasooriya, P. N. Pereira, T. Nikaido, M. F. Burrow and J. Tagami, *Oper Dent*, **28**, 28-35 (2003).
- 127) P. N. Pereira, M. Okuda, H. Sano, T. Yoshikawa, M. F. Burrow and J. Tagami, *Dent Mater*, **15**, 46-53 (1999).

- 128) O. Kumbuloglu, L. V. Lassila, A. User and P. K. Vallittu, *Int J Prosthodont*, **17**, 357-63 (2004).
- 129) E. Asmussen and E. C. Munksgaard, *Int Dent J*, **38**, 97-104 (1988).
- 130) Y. Wang and P. Spencer, *J Biomed Mater Res*, **60**, 300-8 (2002).
- 131) B. Van Meerbeek, L. J. Conn, Jr., E. S. Duke, J. D. Eick, S. J. Robinson and D. Guerrero, *J Dent Res*, **75**, 879-88 (1996).
- 132) H. Koibuchi, N. Yasuda and N. Nakabayashi, *Dent Mater*, **17**, 122-6 (2001).
- 133) H. Sano, T. Yoshikawa, P. N. Pereira, N. Kanemura, M. Morigami, J. Tagami and D. H. Pashley, *J Dent Res*, **78**, 906-11 (1999).
- 134) Y. Kitasako, M. F. Burrow, N. Katahira, T. Nikaido and J. Tagami, *J Dent*, **29**, 139-44 (2001).
- 135) M. Hashimoto, H. Ohno, H. Sano, M. Kaga and H. Oguchi, *Biomaterials*, **24**, 3795-803 (2003).
- 136) J. De Munck, B. Van Meerbeek, Y. Yoshida, S. Inoue, M. Vargas, K. Suzuki, P. Lambrechts and G. Vanherle, *J Dent Res*, **82**, 136-40 (2003).
- 137) M. Ferrari, P. N. Mason, C. Goracci, D. H. Pashley and F. R. Tay, *J Dent Res*, **83**, 414-9 (2004).
- 138) G. W. Marshall, K. Saeki, S. A. Gansky and S. J. Marshall, *Am J Dent*, **12**, 271-6 (1999).
- 139) G. Eliades, G. Vougiouklakis and G. Palaghias, *Dent Mater*, **15**, 310-7 (1999).
- 140) A. Veis and R. J. Schlueter, *Biochemistry*, **3**, 1650-7 (1964).
- 141) F. R. Tay, R. M. Carvalho, C. K. Yiu, N. M. King, Y. Zhang, K. Agee, S. Bouillaguet and D. H. Pashley, *J Adhes Dent*, **2**, 175-92 (2000).
- 142) H. Sano, T. Takatsu, B. Ciucchi, C. M. Russell and D. H. Pashley, *J Dent Res*, **74**, 1093-102 (1995).
- 143) M. Miyazaki, M. Sato, H. Onose and B. K. Moore, *Am J Dent*, **11**, 118-22 (1998).
- 144) T. Nikaido, K. H. Kunzelmann, H. Chen, M. Ogata, N. Harada, S. Yamaguchi, C. F. Cox, R. Hickel and J. Tagami, *Dent Mater*, **18**, 269-75 (2002).
- 145) Y. Kitasako, M. F. Burrow, T. Nikaido and J. Tagami, *Dent Mater*, **18**, 276-80 (2002).
- 146) C. A. Miles and A. J. Bailey, *J Mol Biol*, **337**, 917-31 (2004).
- 147) E. Leikina, M. V. Merts, N. Kuznetsova and S. Leikin, *Proc Natl Acad Sci U S A*, **99**, 1314-8 (2002).
- 148) S. R. Armstrong, J. L. Jessop, E. Winn, F. R. Tay and D. H. Pashley, *J Endod*, **32**, 638-41 (2006).
- 149) H. Sano, T. Takatsu, B. Ciucchi, J. A. Horner, W. G. Matthews and D. H. Pashley, *Oper Dent*, **20**, 18-25 (1995).
- 150) S. J. Paul, D. A. Welter, M. Ghazi and D. Pashley, *Oper Dent*, **24**, 181-8 (1999).

List of Figures

- Figure 2.1 Angle of contact of a drop of liquid with the surface of a solid object (published by Wikimedia foundation, San Francisco, California, U.S.A.)..... 4
- Figure 3.1 Study design for XPS examination and TBS testing. 13
- Figure 3.2 XPS wide-scan spectra of untreated zirconia ceramic surface, and treated surface with Monobond S (MS), Metal/Zirconia primer (MZP), Porcelain Liner M (PLM) or Clearfil™ ceramic primer (CCP). 16
- Figure 3.3 (a) One representative debonded ceramic surface in group Super-Bond C&B⁴³-control after 3-d showed small area of adhesive failure from ceramic surface (A) and big area of cohesive failure in luting cement (C) at low magnification. (b) Cohesive failure in luting cement (a) at high magnification (b). Adhesive failure at high magnification (c). (d) One representative debonded ceramic surface in group SB after 150d and 37,500 thermal cycling showed big area of cohesive failure with a very thin layer of SB adhesive resin cement remaining on the ceramic surface and small area of cohesive failure in luting cement at low magnification. (e) and (f) Cohesive failure in luting cement (a) at high magnification (b). 17
- Figure 3.4 (a) One representative debonded ceramic surface in group Chemiace II (CH)-control after 3-d showing small area of adhesive failure from ceramic surface (A), cohesive failure in thin layer of adhesive resin cement and big area of cohesive failure in luting cement or filling resin (C) at low magnification. (b) Adhesive failure at ceramic surface at high magnification. (c) One representative debonded ceramic surface in group SB-control after 150d and 37,500 thermal cycling showing completely adhesive failure at ceramic surface at low magnification. (d) Adhesive failure at ceramic surface at high magnification. 19
- Figure 3.5 (a) One representative debonded ceramic surface in group Chemiace II (CH)-Pocelain Liner M (PLM) after 3-d showing primarily cohesive failure in bulk adhesive resin cement or filling composite resin and big area of cohesive failure in luting cement or filling resin at low magnification. (b) Adhesive failure at ceramic surface with PLM primer infiltrating in ceramic surface at high magnification. (c) One representative debonded ceramic surface in group CH-PLM after 150d and 37,500 thermal cycling showing mostly adhesive failure at ceramic surface (A) and small area of adhesive failure at the bonding interface between adhesive resin cement and PLM primer at low magnification. (d) Cohesive failure in adhesive resin cement or adhesive failure at the bonding interface between adhesive resin cement and PLM primer at high magnification. 19
- Figure 3.6 (a) One representative debonded ceramic surface in group Chemiace II (CH)-Clearfil™ ceramic primer (CCP) after 3-d showing primarily cohesive failure in

bulk adhesive resin cement or filling composite resin and big area of cohesive failure in luting cement or filling resin at low magnification. (b) Cohesive failure in bulk adhesive resin cement at high magnification. (c) One representative debonded ceramic surface in group CH-CCP after 150d and 37,500 thermal cycling showing mostly adhesive failure at ceramic surface (A) and small area of cohesive failure in adhesive resin cement at low magnification. (d) Cohesive failure with adhesive resin cement remaining at ceramic surface at high magnification. 20

Figure 3.7 (a) One representative debonded ceramic surface in group Clearfil™ Esthetic cement (CE) - control after 3-d showing completely adhesive failure from ceramic surface (A) at low magnification. (b) Adhesive failure without any adhesive resin cement on ceramic surface at high magnification. (c) One representative debonded ceramic surface in group Clearfil™ Esthetic cement (CE) - control group after 150d and 37,500 thermal cycling showing completely adhesive failure at ceramic surface at low magnification. (d) Adhesive failure without any adhesive resin cement on ceramic surface at high magnification. 22

Figure 3.8 (a) One representative debonded ceramic surface in group Clearfil™ Esthetic cement – Pcelain Liner M (PLM) after 3-d showing primarily cohesive failure in bulk luting cement (C) at low magnification. (b) Adhesive failure with primer on ceramic surface at high magnification. (c) One representative debonded ceramic surface in group Clearfil™ Esthetic cement (CE) - Pcelain Liner M (PLM) after 150d and 37,500 thermal cycling showing primarily cohesive failure in bulk luting cement (C) with increasing adhesive failure at ceramic surface at low magnification. (d) Adhesive failure with primer on ceramic surface at high magnification. 22

Figure 4.1 Study design for XPS examination and TBS testing 30

Figure 4.2 Percentages of areas assigned to the failure modes observed in test groups after tensile bond strength testing. A: Adhesive failure at ceramic surface; C: Cohesive failure in luting composite resins (Panavia F 2.0 or Panavia 21) or tube filling composite resin. Mean (SD) percentage of adhesive failure after 3 days and 150 days are: for PF 2.0, CAA (after airborne-particle abrasion, no contamination): 9% (2%), 9.4% (0.5%); AA (airborne-particle abrasion cleaning): 9% (1%), 87% (3%); HP (phosphoric acid cleaning): 87% (4%), 33% (6%); AC (acetone cleaning): 100% (0%), 100% (0%); TW (tap water cleaning): 100% (0%), 100% (0%). For P21, CAA: 2% (0%), 3% (0.2%); AA: 1% (0%), 5% (1%); HP: 6.5% (1%), 79% (2%); AC: 100% (0%), 100% (0%); TW: 100% (0%), 100% (0%). 34

Figure 4.3 (a) Low magnification SEM micrograph showing representative mixed failure modes mostly with cohesive failure in groups CAA and AA; (b) High magnification SEM micrograph of A in (a) showing adhesive failure at the zirconia ceramic surface; (c) C1 in (b) showing cohesive failure in composite resins (Panavia F 2.0 or

- Panavia 21); (d) C2 in (b) showing cohesive failure in tube filling composite resin (Clearfil FII). 35
- Figure 4.4 (a) Low magnification SEM micrograph showing representative adhesive failure mode in group AC and TW. (b) Low magnification SEM micrograph showing representative cohesive failure mode in group HP. 35
- Figure 6.1 (a) Diagram of tested dentin location. s: superficial dentin (1 mm below DEJ); d: deep dentin (1 mm above the pulp horn); c: cervical dentin (0.5 mm below DEJ, 0.5 above CEJ); O: tested dentin location. (b) Alignment apparatus. A 10 μm -thick aluminum foil with a 1-mm-diameter hole was attached to dentin surface. The hole was located at the centre of the bonding area using an alignment jig to control the shape and size of bonding area. (c) Schematic drawing of μTBS testing. The rod was gripped by a pin-vice of universal testing machine, and then a haul plate with three point support was put on the dentin surface. The μTBS was measured only by tensile force. 44
- Figure 6.2 Failure modes of Super-Bond C&B, Panavia F 2.0 and RelyX Unicem to dentin regions during the tensile bonding strength test. 48
- Figure 6.3 SEM micrographs of conditioned and unconditioned dentin surfaces, as the bonding substrates in the three groups. (a) SEM micrograph illustrating the dentin surface etched with 10% citric acid with 3% ferric chloride (group Super-Bond C&B). The smear plugs appeared to be removed and the tubule orifices were exposed completely by removal of peritubular dentin. Some residual smear layer material was seen around tubule orifices. The circumferentially oriented collagen fibrils (asterisk) around the tubular wall are exposed. (b) SEM micrograph illustrating the dentin surface treated with self-etching ED primer 2.0 (group Panavia F 2.0). The dentin surface exhibited demineralized collagen fibrils. The tubule orifices were exposed with some smear debris (asterisk) remaining in the tubules. (c) SEM micrograph of polished and unconditioned dentin surface covered by a smear layer (group RelyX Unicem). 49
- Figure 6.4 Interface and Fractographic analysis of group SB (Super-Bond C&B). (a) TEM photomicrograph at 3000 magnification illustrating an overview of the interface between SB resin cement and superficial dentin. The hybrid layer is approximately 4 μm thick. (b) SEM micrograph at 600 magnification of a debonded deep dentin specimen where adhesive failures occurred on the dentin surface. (c) SEM micrograph at 3600 magnification of the same specimen as in Fig. 4b. Adhesive failure occurred along the top of the hybrid layer and cohesive failures occurred in the resin tags (asterisk). (d) TEM micrograph at 6000 magnification of a resin tag in deep dentin. The hybrid layer on the intertubular dentin surface extended into the tubule walls surrounding the resin tag, occluding the tubule

opening. C: Resin cement; H: Hybrid layer; T: Resin tag; D: Demineralized dentin in the preparation of TEM; R: Embedding resin..... 50

Figure 6.5 Interface and Fractographic analysis of group PF (Panavia F 2.0). (a) TEM photomicrograph at 4000 magnification illustrating an overview of the interface between PF resin cement and superficial dentin. The hybrid layer is approximately 1.5 - 2 μm thick. (b) SEM micrograph at 600 magnification of adhesive failure from the deep dentin surface. (c) SEM micrograph at 4500 magnification of the same specimen as in Fig. 5b. The failure occurred at the top of hybrid layer with cohesively fractured resin tags occluding the tubules (asterisk). (d) TEM photomicrograph at 5000 magnification illustrating the failure within the hybridized smear layer and smear plug in deep dentin. C: Resin cement; H: Hybrid layer; Ha: Authentic hybridized dentin; Hs: Hybridized smear layer; T: Resin tag; G: Glass filler particle; D: Demineralized dentin in the preparation of TEM; R: Embedding resin. 51

Figure 6.6 Interface and Fractographic analysis of a specimen in group RU (RelyX Unicem). (a) TEM photomicrograph at 5000 magnification illustrating an overview of the interface between RU resin cement and superficial dentin. The smear layer appears to be completely dissolved, but no obvious hybrid layer is observed. (b) SEM micrograph at 600 magnification of a debonded deep dentin specimen that adhesively failed at the top of dentin surface with a thin layer of resin cement ¹²⁰⁾ remaining on the dentin surface. (c) SEM micrograph at 4500 magnification of adhesive failure at "A" in the same specimen as in Fig. 6b. The loose collagen fibrils in the intertubular dentin do not seem to be adequately enveloped by resin cement. (d) TEM photomicrograph at 3000 magnification illustrating the adhesive failure from the demineralized cervical dentin surface. The collagen fibrils along the fractured surface appear to be stretched into loose microfibrils (asterisk) without resin infiltration. C: Resin cement; D: Demineralized dentin in the preparation of TEM; G: Glass filler particle; F: Nanofiller R: Embedding resin..... 52

Figure 7.1 AFM images (flat and 3-d) of dentin surface polished by 600-grit SiC paper. (a) The dentin surface was covered with smear layer. (b) AFM image (flat and 3-d) of intact dentin surface polished by 4000-grit SiC paper. With the removal of smear layer and smear plugs, the tubules, the peritubular dentin and intact intertubular dentin were completely exposed. 60

Figure 7.2 High magnification tapping mode AFM image of the dentin collagen fibrils on the intact intertubular dentin surface conditioned with 10% citric acid with 3% ferric chloride (10-3 solution) in group SB (a) or self-etching ED Primer 2.0 in group PF (b). (c) Section analysis revealed the collagen fibrils with an axial periodicity banding of about 67 nm and diameter of 90-120 nm..... 61

Figure 7.3 Failure modes of Super-Bond C&B and Panavia F 2.0 to human regional dentin during the micro-tensile bond strength test after different storage condition. A: Adhesive failure along the top of dentin surface; B: Mixed failure: Adhesive failure with a thin layer of adhesive resin cement remaining on the dentin surface; C: Cohesive failure in the adhesive resin cement; D: Interfacial failure between the bottom of hybrid layer and the intact or demineralized dentin. 64

Figure 7.4 SEM and TEM photomicrograph of polished dentin surfaces and conditioned dentin surfaces. **(a)** SEM photomicrograph illustrating the smear layer on the dentin surface polished with 600- grit SiC paper. **(b)** TEM photomicrograph illustrating the smear layer on the dentin surface polished with 600- grit SiC paper. Approximately 0.5 μm of smear layer was formed on the underlying dentin surface. Smear layer seems to be contiguous with the underlying intact dentin. S: Smear layer; D: Demineralized dentin in TEM preparation; R: Embedding resin. **(c)** SEM photomicrograph illustrating the etched dentin surface with 10% citric acid with 3% ferric chloride (Super-Bond C&B). After the dentin was etched, the smear layer appeared to be removed and the tubule orifices were exposed completely. The circumferentially oriented collagen fibers around the tubular wall are exposed. **(d)** SEM photomicrograph illustrating the treated dentin surface with self-etching ED Primer 2.0 (Panavia F 2.0). The smear layer appears to be dissolved with loose collagen network standing on the intertubular dentin surface. Many smear plugs are partially removed with smear debris remaining in the tubules or a thin smear layer loosely attaching to the tubular walls. The circumferentially oriented collagen fibers around the tubular walls are not exposed completely. 65

Figure 7.5 Fractographic analysis of group Super-Bond C&B⁴³. **(a)** SEM micrograph of a debonded dentin specimen in group 1 d. Adhesive failure occurred on the top of the hybrid layer (HL) and cohesive failure within the resin tags. **(b)** TEM photomicrograph illustrating the adhesive failure occurring at the top of HL. A HL with a width of approximately 4 μm was formed. **(c)** TEM micrograph of cohesive failure occurring in demineralized dentin below the HL (group 90 d-TC). Under the bottom of HL was loose fractured demineralized collagen fibrils (star). The collagen fibril network in this area appears to be inadequately enveloped by resin cement and took up more heavy metal stain than other areas. H: hybrid layer; D: demineralized dentin in preparation of TEM; C: resin cement; P: radiopaque particle. Bar=1 μm . 66

Figure 7.6 Fractographic analysis of group Panavia F 2.0 (PF). **(a)** TEM photomicrograph illustrating the cohesive failure within the hybridized smear layer - the top of hybrid layer (HL) (group 1d). The HL was approximately 2 μm , consisting of a hybridized smear layer (ca. 0.5 μm) and a 1-1.5 μm authentic HL. **(b)** High-magnification SEM micrograph of a debonded dentin specimen in group 1 d that failed at the top of the HL and cohesively fractured resin tags occluded the

tubules. (c) High-magnification SEM micrograph of a debonded dentin specimen in group 90 d-TC that failed in the HL. Resin in interfibrillar spaces between collagen fibrils was partially lost. The collagen fibrils exhibited odd shapes and bulbus ends that are characteristics of plastically deformed and broken fibrils. C: resin cement; Ha: hybrid authentic dentin; Hs: hybridized smear layer; D: demineralized dentin in preparation of TEM; T: resin tag; R: embedding resin. Bar=1 μ m..... 67

Figure 7.7 Schematic drawing of bonding procedures and failure modes during tensile testing (Super-Bond C&B). (a) Normal dentin with smear layer. (b) The dentin surface was etched with 10% citric acid with 3% ferric chloride and rinsed. (c) The acid-etched dentin surface was air-dried. (d) The treated dentin was pre-wet with 4META/MMA-TBB. (e) The bonding interface of PMMA rod-SB-hybrid layer-dentin with a HL of 4 μ m thickness. (f) Failure mode A - adhesive failure at the surface of the hybrid layer (HL). (g) Failure mode C - cohesive failure within the adhesive resin cement. (h) Failure mode D - cohesive failure in the demineralized collagen fibril network at the bottom of the HL..... 70

Figure 7.8 Schematic drawing of bonding procedures and failure modes during tensile testing (Panavia F 2.0). (a) Normal dentin with smear layer. (b) The dentin surface was self-etched and primed simultaneously. (c) The treated dentin surface was air-dried. (d) The bonding interface of composite rod-PF-HL-dentin with a HL of 2 μ m thickness. (e) Failure mode A - adhesive failure at the surface of the hybrid layer (HL) or hybridized smear layer. The hybridized smear layer seems to be a weak link due to the denaturation and disorganization of the collagen fibrils in smear layer although the smear layer was hybridized by resin into one complex with the underlying intact dentin. (f) Failure mode A - adhesive failure within the top of HL. After the adhesive resin cement was distracted from the HL, the tensile load was transferred directly to the collagen fibril network in hybridized intact dentin, resulting in the plastic fracture and cohesive failure within the top of the HL. (g) Failure mode C - cohesive failure in the adhesive resin - cured self-etching ED Primer..... 71

List of Tables

Table 3.1 Compositions and application of the test adhesive resin cements and primers.	13
Table 3.2 Tensile bond strength and the percentage of failure mode for Super Bond C&B to zirconia ceramic after different surface pretreatment. Means, standard deviations (SD) and medians in MPa (n = 8).	16
Table 3.3 Tensile bond strength and the percentage of failure mode for Chemiac II to zirconia ceramic after different surface treatment. Means, standard deviations (SD) and medians in MPa (n = 8).	18
Table 3.4 Tensile bond strength and the percentage of failure mode for Clearfil™ Esthetic cement to zirconia ceramic after different surface treatment. Means, standard deviations (SD) and medians in MPa (n = 8).	21
Table 4.1 Mean ratios of carbon (C), oxygen (O) and silicon (Si) elements in experimental groups.	32
Table 4.2 Tensile bond strength to zirconia ceramic after contamination and different cleaning methods. Means, standard deviations (SD) and medians in MPa (n = 8) of experimental groups: CAA (after airborne-particle abrasion, no contamination), AA (airborne-particle abrasion cleaning), HP (phosphoric acid cleaning), AC (acetone cleaning), TW (tap water cleaning).	33
Table 6.1 Composition and application of the test resin cements (batch number in parenthesis).....	45
Table 6.2 Micro-tensile bond strength (μ TBS) of the test groups to human regional dentin. Means (standard deviation) in MPa.	47
Table 7.1 Micro-tensile bond strength (μ TBS) of tested groups to human dentin after different storage condition (N=8). Means (standard deviations) in MPa.....	63

Acknowledgments

This study was carried out as an interdisciplinary collaboration project between Department of Prosthodontics, Propaedeutics and Dental Materials, and Multicomponent Materials Faculty of Engineering, Christian-Albrechts University at Kiel from 2003 to 2007.

First and foremost I would like to thank Prof. Dr. Franz Faupel, and Prof. Dr. Rainer Adelung. The former gave me the opportunity to perform my PhD program as a joint project at his chair. I thank the latter one for the interesting topics, the scientific guidance and technical direction throughout this study and careful correction of this thesis. Especially I greatly appreciate Prof. Dr. Rainer Adelung for his key orientation in the development of my professional career. I will bear in mind all the pleasant and impressive discussions with him.

Many thanks should be given to Prof. Dr. Matthias Kern and Prof. Dr. K. Ludwig for their scientific suggestions, original technical guidance in completing this study and careful correction of part of this thesis.

Thanks a lot to Dipl.-Ing. Mithael Scharnberg for his important technical support and help in XPS study. Many thanks should be given to Prof. D. H. Pashley (School of Dentistry, Medical College of Georgia, USA), Prof. H. Sano (Graduate School of Dental Medicine, Hokkaido University, Japan) Dr. S. Habelitz (Department of Preventive and Restorative Dental Sciences, University of California, USA), for their very useful discussions about SEM, TEM and AFM results in this study.

I am grateful to Ms. Marquardt, Mr. F. Lehmann, Mr. Möller, Ms. Galsterer, and Mr. Gostomsky for their technical support in TEM and SEM studies. Colleagues of the two departments ever gave me a lot of understanding, help and pleasure in my studying and living in Kiel. They are also appreciated.

Finally, I sincerely thank my daughter, my husband and my parents, for their understanding and constant support during my studying in Kiel.

Curriculum Vitae

Name: Bin Yang

Address: Niemannsweg 152, 24105 Kiel

Born: 22.Mai 1971 in Xinjiang, P. R.China

Parents: Mingfa Yang, Guilan Sun

School Education

09/1986 – 07/1989 High school affiliated to He Nan University, P. R.China

Academic Education

09/1989 – 07/1994 Bachelor in Stomatology, Henan Medical University, P. R.China

06/1996 – 01/1998 Post-graduate continuing education, School of Stomatology,
Peking University, P. R. China

08/1998 – 07/2001 Master, School of Stomatology, Peking University, P. R.China

11/2002 – 08/2005 Doc. Dent. Med., Christian-Albrechts-University at Kiel, Germany

02/2003 – Now PhD candidate Christian-Albrechts-University at Kiel, Germany

Occupational History

1994 – 1996 Assistant professor, Zhengzhou University, P. R. China

1998 – 2001 Assistant professor, School of Stomatology, Peking University, P. R. China

2001 – 2002 Lecturer in Restorative Dentistry and Dental Materials, P. R. China

2006 – Now Assistant professor, Christian-Albrechts-University at Kiel